Titre: Title:	Improving the Processability of Polylactide for Film Blowing Application
Auteur: Author:	Sahar Nouri
Date:	2015
Type:	Mémoire ou thèse / Dissertation or Thesis
Référence: Citation:	Nouri, S. (2015). Improving the Processability of Polylactide for Film Blowing Application [Ph.D. thesis, École Polytechnique de Montréal]. PolyPublie. https://publications.polymtl.ca/1693/

UNIVERSITÉ DE MONTRÉAL

IMPROVING THE PROCESSABILITY OF POLYLACTIDE FOR FILM BLOWING APPLICATION

SAHAR NOURI

DÉPARTEMENT DE GÉNIE CHIMIQUE

ÉCOLE POLYTECHNIQUE DE MONTRÉAL

THÈSE PRÉSENTÉE EN VUE DE L'OBTENTION

DU DIPLÔME DE PHILOSOPHIAE DOCTOR

(GÉNIE CHIMIQUE)

FÉVRIER 2015

UNIVERSITÉ DE MONTRÉAL

ÉCOLE POLYTECHNIQUE DE MONTRÉAL

Cette thèse intitulée:

IMPROVING THE PROCESSABILITY OF POLYLACTIDE FOR FILM BLOWING APPLICATION

présentée par : NOURI Sahar

en vue de l'obtention du diplôme de : Philosophiae Doctor

a été dûment acceptée par le jury d'examen constitué de :

M. LEGROS Robert, Ph. D., président

M. LAFLEUR Pierre, Ph. D., membre et directeur de recherche

M. DUBOIS Charles, Ph. D., membre et codirecteur de recherche

Mme HEUZEY Marie-Claude, Ph. D., membre

M. HATZIKIRIAKOS Savvas, Ph. D., membre

DEDICATION

“To my family who always stands by me”

ACKNOWLEDGMENT

I would like to express my sincere gratitude to my supervisor, Prof. Pierre Lafleur, professor and dean of Academic and International Affairs at Polytechnique Montréal, for placing his trust and confidence in my abilities. He always supported me during my graduate study with availability, patience and encouragement and provided me with fundamental advises. Also, I had the honor of working under co-supervision of Prof. Charles Dubois. He has been encouraging since the days I came to Polytechnique. Ever since, Prof. Dubois has supported me not only by providing a research assistantship, but also emotionally through the road to the new life in Canada. Indeed, without his immense knowledge, inspiration and perseverance I was not able to finish this project.

For experimental work, I had a great privilege to benefit from the professional staff and technicians of Chemical engineering department at Polytechnique and CREPEC. My greatest appreciation goes to Mrs. Martine Lamarche and Mr. Gino Robin for providing material and equipment. Also, I would like to thank Mr. Guillaume Lessard, Mrs. Mélina Hamdine, Mr. Richard Silverwood and Mrs. Claire Cerclé for their training, assistance and availability. I could not complete my work without their invaluable friendly assistance.

I owe special thanks to Dr. Babak Esmaili for his helps, sympathy and precious advices during the polymerization step of my experimental work.

For film blowing process and some characterization of this work, I had the advantage of working in different labs and research facilities. I acknowledge great assistance of Mr. Jacques Dufour at National Research Council of Canada in Boucherville, technicians at Polynov, Dr. Cédric Malveau at Chemisty department of Université de Montréal, Prof. Jérome Claverie and his staff at Chemistry department of Université du Québec à Montréal.

I would like to extend my gratitude to my parents and adorable sisters for their unconditional love and enormous support. I hope I have made them proud with this work. Finally, I could not accomplish this work without inspiration and valuable advices of my loving and caring husband, Sajjad.

RÉSUMÉ

Le polylactide (PLA) est l'un des biopolymères les plus importants ayant suscité des intérêts dans de nombreux domaines; non seulement en raison de sa production à partir de ressources renouvelables et compostable, mais aussi parce qu'il a une résistance élevée, un module élastique élevé et possède de bonnes propriétés optiques. Cependant, le PLA souffre des faiblesses qui limitent son développement pour diverses applications. Le manque de groupes latéraux réactifs, une faible cristallinité, une faible résistance à l'impact, une basse température de fléchissement sous charge (HDT), ainsi que des problèmes de mise en œuvre, c'est à dire la sensibilité à la chaleur et à l'humidité et une faible élasticité à l'état fondu sont les défis principaux à surmonter. L'objectif de cette recherche est de faciliter la transformation et la mise en forme de la résine PLA. Plus précisément, sa faible élasticité à l'état fondu limite l'usage du PLA dans les procédés de soufflage de film, de moulage par soufflage, de moussage à faible densité, etc. Il n'y a pas assez d'informations au sujet de ce problème dans la littérature scientifique.

Basé sur notre revue de la littérature et en comparant le PLA avec d'autres polymères linéaires tels que le polyéthylène basse densité linéaire (LLDPE) et le polypropylène (PP) pour qui les améliorations d'élasticité à l'état fondu ont été fait par l'incorporation de polymère ramifié, il a été décidé d'utiliser des analogues ramifiés pour améliorer le comportement d'écoulement du PLA à l'état fondu. En outre, il a été observé que l'incorporation de poly (D-lactide) (PDLA) en poly (L-lactide) (PLLA) résulte en leur co-cristallisation ce qui améliore les propriétés rhéologiques en extension; cependant, ce comportement n'a pas encore été étudié en détail. Par conséquent, les principales approches de cette recherche sont basées sur l'emploi de le PLA ramifié, le stéréocomplexe de PLA et leur combinaison.

Après avoir examiné différentes méthodes de ramification de PLA, la synthèse directe du PLA a été choisie en raison de sa flexibilité pour produire différentes architectures de chaîne, du contrôle sur la masse moléculaire et le potentiel d'augmenter l'élasticité à l'état fondu sans formation de gel. Différentes structures ramifiées ont été synthétisées et caractérisées afin de montrer un comportement rhéologique et une cristallinité plus intéressants que ceux du PLA linéaire. Les PLA branchés avec différentes stéréochimies ont été mélangés avec le PLA linéaire selon différents rapports de mélange pour explorer l'effet de l'architecture de branchage et leur

contenu ainsi que du stéréocomplexe sur la rhéologie de polymère linéaire en cisaillement et en extension. Une viscosité plus élevée, en cisaillement et en extension, et un durcissement par déformation ont été observés par l'application de ces stratégies. Par ailleurs, une étude détaillée a révélé des modifications importantes au comportement de cristallisation suite à l'addition de ramifications. La cinétique de cristallisation en modes isotherme et dynamique a été considérablement améliorée en comparaison avec le PLA linéaire et le rôle de la nucléation des points de branchement a été démontré par des moyens différents. La formation de cristallites de stéréocomplexe entre le PDLA ramifié et le PLLA linéaire ainsi que le rôle de nucléation de cristallites de stéréocomplexe ont été étudiés et différentes morphologies internes de sphérulites de cristallites de stéréocomplexe et d'homocristaux ont été illustrées. En outre, la facilité de mise en œuvre des mélanges modifiés a été examinée dans un procédé de soufflage de film, présentant une large fenêtre de traitement et le taux de production plus élevé en comparaison avec la résine commerciale de référence. En outre, la cristallisation et les propriétés mécaniques et optiques des films produits ont été étudiées, révélant l'effet significatif des modifications de la structure sur les propriétés finales du film.

ABSTRACT

Polylactide (PLA) is among the most important biopolymers that has raised interests in many areas; not only because of its production from renewable resources and compostability, but also because it has high strength, high modulus and good optical properties. However, PLA suffers weaknesses that restrict its development for different applications. Lack of reactive side groups, low crystallization rate, impact resistance and heat deflection temperature (HDT) as well as processability problems, i.e. heat and moisture sensitivity and low melt strength are the main challenges. The objective of this research is to overcome the processability problem of PLA. More specifically, its low melt strength has limited its applications in film blowing, blow molding, low density foaming, etc., and there is not much information regarding this problem in the open literature.

Based on our review and comparing PLA with other linear polymers such as linear low density polyethylene (LLDPE) and polypropylene (PP) for which melt strength improvements were done by incorporation of branched polymer, branched PLA is used for this purpose. Besides, it was observed that incorporation of poly(D-lactide) (PDLA) into poly(L-lactide) (PLLA) results in their co-crystallization that also improves the extensional rheological properties; however, it has not been studied in detail. Therefore, the main approaches in this research were based on employing branched PLA, PLA stereocomplex and their combination.

After reviewing different PLA branching methods, direct synthesis of branched PLA was selected because of the flexibility to produce different chain architectures, more control on molecular weight and its potential to increase melt strength without gel formation. Different branched structures were synthesized and characterized, showing interesting rheological and crystallization behavior compared to linear PLA. Branched PLAs with different stereochemistry were blended with linear PLA at different blending ratios to explore the effect of branch architecture and content as well as stereocomplex structure on shear and elongational rheology of linear polymer. Higher shear and extensional viscosities and strain hardening behavior were observed by applying these strategies. In addition, a detailed study revealed significant changes to crystallization behavior as a consequence of branched chain architecture. Crystallization kinetics in isothermal and dynamic mode was considerably enhanced in comparison with linear PLA and the nucleation role of branching points was demonstrated by different means. Stereocomplex formation between branched PDLAs and linear PLLA as well as the nucleation

role of stereocomplex crystals for homocrystallization were studied and different internal spherulite morphologies for stereocomplex and homocrystal was illustrated. Furthermore, processability of the modified blends was examined through film blowing process, showing a wider processing window and higher production rate in comparison with the reference commercial resin. In addition, mechanical, crystallization and optical properties of the produced films were investigated, revealing the significant effect of structure modification on final film properties.

TABLE OF CONTENTS

LIST OF TABLES

LIST OF FIGURES

LIST OF NOMENCLATURE

Symbols

A_0	Cross-sectional area of the specimen in the solid state
C_∞	Characteristic ratio
dn/dc	Refractive index increment
$\dot{\varepsilon}_H$	Hencky strain rate
G'	Storage modulus
G''	Loss modulus
G_N^0	Plateau modulus
$[I]$	Molar concentration of initiator
K	Flory-Fox equation constant
L	Stretch zone length
l_0^2	Mean square bond length
$[lactide]_0$	Initial concentration of lactide
M_b	Critical value for branch entanglement
m_b	Relative molecular mass per backbone bond
M_c	Critical entanglement molecular weight
M_e	Entanglement molecular weight
M_n	Number average molecular weight
M_v	Viscosity average molecular weights
M_w	Weight verage molecular weights
N_1	First normal stress difference
R	Radius
R	Universal gas constant
Tan (δ)	tangent of phase angle
T_c	Crystallization temperature
T_g	Glass transition temperature
T_g^∞	Glass transition temperature at infinite molecular weight
T_m	Melting temperature

X_c	Crystallinity
α	Crystal type
α_1	Thermal expansion coefficient
δ	Phase angle
ΔH_c	Enthalpies of crystallization
ΔH_{cc}	Heat of cold crystallization
ΔH_m	Heat of fusion
η^*	Complex viscosity
η_0	Zero-shear viscosity
η_E^+	Time dependent extensional viscosity
ρ	Density
ρ_M	Melt density
ρ_S	Solid state density
T	Torque
ω	Oscillation frequency
Ω	Angular speed

Acronyms

5HDON	5-hydroxymethyl-1,4-dioxane- 2-one
BHB	2,2-bis (hydroxymethyl) butyric acid
BUR	Blow up ratio
DDR	Draw down ratio
DSC	Differential scanning calorimetry
FTIR	Fourier transform infrared spectroscopy
HDPE	High-density polyethylene
HDT	Heat deflection temperature
LDPE	Low density polyethylene
LLDPE	Linear low density polyethylene
MA	Maleic anhydride
MD	Machine direction
MFI	Melt flow index
PBAT	Poly(butyleneadipate-co-butyleneterephthalate)

PBSA	Poly(butylene succinate-co-adipate)
PCL	Poly(ε-caprolactone)
PDI	Polydispersity index
PDLA	Poly(D-lactide)
PE	Polyethylene
PET	Polyethylene terephthalate
PGA	Poly (glycolic acid)
PHB	Poly(hydroxibutyrate)
PHBV	Poly(3-hydroxybutyrate-co-3-hydroxyvalerate)
PLA	Polylactide
PLLA	Poly(L-lactide)
POM	Polarizing optical microscopy
PP	Polypropylene
ROP	Ring-opening polymerization
SEC	Size exclusion chromatography
SER	Sentmanat Extensional Rheometer
TD	Transverse direction
TNPP	Tris(nonylphenyl) phosphite
TPS	Thermoplastic starch
TUR	Take-up ratio
XRD	X-ray diffraction

CHAPTER 1. INTRODUCTION

Industrial use of bio-based materials is growing rapidly as a consequence of exceptional advantages accompanying these materials. In parallel, scientific community has boosted significantly the fundamental and applied research to keep up with the evolution in this field, to promote biopolymers consumption by overcoming their inherent deficiencies and to make them cost-performance competitive with conventional commodity polymers.

One of the most promising polymers in the biomaterials family is polylactide or PLA, an aliphatic thermoplastic polyester that can be produced from renewable resources. It is an eco-friendly polymer which has been considered as a potential replacement for petrochemical-based polymers such as polyethylene (PE), polypropylene (PP) and polyethylene terephthalate (PET). PLA is biocompatible, compostable and possesses good mechanical and physical properties such as high strength, high modulus, low permeability and high optical clarity.

Biomedical applications were among the first areas in which biocompatible and biodegradable polymers raised interest. The first synthetic biodegradable polymer was Poly (glycolic acid) (PGA). Subsequently, PLA and its copolymers with PGA were produced. 'Vicryl' suture is a copolymer of PGA and PLA, introduced in USA in 1975 (Gilding and Reed, 1979).

Recent developments in the economical production of the monomers have advanced PLA and its copolymers production as the forefront of the biopolymer industry (Lunt, 1998). Also, more attention of authorities to the environment protection after facing recycling problems has made them to apply higher tax rates for non-degradable polymers consumption; this has oriented the packaging industry to some extent into employing degradable materials such as PLA. However, PLA is not yet able to compete with commodity plastics because of the higher production costs and the adaptation of industrial facilities to polyolefin processing. Thus, total production volume of PLA has remained smaller than commodity plastics (Mehta et al., 2005). For instance, PE production capacity in 2007 was about 79 million tons (Otto G. Piringer 2008) while that of PLA was 390,000 tons in 2008 (Mehta et al., 2005). However, with the fast and steady increase in PLA production capacity that has happened during last decade, it is expected that this fascinating polymer takes a considerable share of the packaging market with a production capacity of over 800,000 tons by 2020 (Carus et al., 2013).

Although many advantages associated to PLA make it one of a kind, some weaknesses have limited its application development. These deficiencies are classified as the final product properties and PLA melt processing problems. The main problems concerning end-use applications are low heat deflection temperature (HDT) that limits PLA service temperature, slow crystallization rate and low crystallinity which affect other properties such as mechanical and barrier characteristics, as well as brittleness that restricts PLA implementation to low impact applications. There are numerous studies regarding these aspects which have been successful to some extent. On the other hand, from the melt processing point of view, degradation and molecular weight reduction during the process and PLA low melt strength and elasticity are the most important concerns. Especially, melt strength is required in many processes to have a high quality and consistent production, such as film blowing, fiber spinning, thermoforming and foam extrusion. Despite that, the melt strength of PLA has been less studied. Additives such as chain extenders or peroxides are added to PLA during its processing to prevent the molecular weight and viscosity reduction, while no study has been reported on a real control of the final polymer structure and properties in those reactive processes. In addition, some works have shown the potential use of PLA stereocomplex to increase melt strength and viscosity of molten polymer; however, melt processing of PLA containing stereocomplex crystals has not been studied intensively.

In this present work, the aim was to overcome the low melt strength problem of PLA for film blowing application. For this purpose changing molecular structure to a branched one through direct synthesis as well as blending stereochemically opposite chains was implemented. Different characterization techniques were used to show the effectiveness of these methods in PLA melt rheology modification as well as their influence on PLA crystallization behavior. Also, blends were examined in a film blowing process to evaluate the processability and final film properties.

The central theme of this thesis is the synthesis of different architecture branched PLAs and study of rheological and crystallization behavior of chemically and physically branched chains in context of their contribution to the challenging PLA film blowing process. A literature review was done on PLA synthesis routes, its thermophysical and rheological properties and film blowing process. Also techniques reported in open literature to produce branched PLA and to increase its melt strength were reviewed. Afterwards, identified problems and objectives of this

study are clarified. Next, the methodology to achieve the specified objectives are explained, including materials, followed procedures and characterization techniques. In Chapter 4, organization of the articles in the thesis and their relation with specified objectives are explained followed by four articles presented in chapters 5 to 8. A general discussion combining the main findings of the articles is given in Chapter 9. Finally, conclusions and recommended work for the future continuation of this study are presented in Chapter 10. All references used in the literature review and articles are integrated at the end of the thesis.

CHAPTER 2. LITERATURE REVIEW

In this part, we take a look at different aspects of PLA in relation to this study, starting from its synthesis, followed by its thermophysical and rheological characterization. Subsequently, different applications and processes are presented; with a particular focus on film blowing process. Finally, prior works that have been done so far to modify PLA for a better processability are presented and discussed.

2.1 PLA Synthesis

Two types of monomer, in cyclic and linear forms, exist for production of PLA, and each implies a specific route of polymerization. These monomers are presented followed by the polymerization methods suitable for them.

2.1.1 Monomer

Lactic acid or 2-hydroxypropionic acid is the PLA's building block. It is a hygroscopic material with melting point of 53 ^{o}C, boiling point of 122 ^{o}C at 15 mmHg and density of 1.2 g/cm^3. It was first isolated in 1780 from sour milk by the Swedish chemist Scheele, and first produced commercially in 1881 (Garlotta, 2001). It is the simplest hydroxy acid with an asymmetric carbon atom which causes the existence of two optically active configurations (see Figure 2.1). The L-isomer is produced in human's body and other mammals, whereas both D and L forms are produced in bacterial systems. L-isomer consists 99.5% of the lactic acid produced from fermentation process (Gupta et al., 2007).

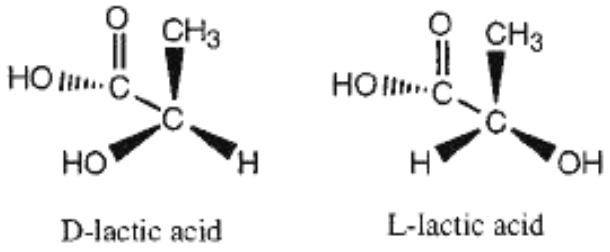

Figure 2.1. Stereochemistry of lactic acid

Recent developments in bacterial genetic modification have led to strains that can produce D-lactic acid efficiently (Mazumdar et al., 2010; Tashiro et al., 2011). This is very important since presence of two monomer types significantly influences different PLA properties which will be discussed later.

Lactide, the cyclic dimer molecule of lactic acid, is also used to produce PLA. The existence of two optically active lactic acid molecules, results in three potential forms of lactide, L-lactide, D-lactide and meso-lactide. L and D-lactide are optically active while the meso form is optically inactive. Lactide is produced via depolymerization of PLA oligomers under reduced pressure. Yield of each isomer depends on the oligomer, temperature, and catalyst (Garlotta, 2001). Chemical structure of different lactide stereoisomers are depicted in Figure 2.2.

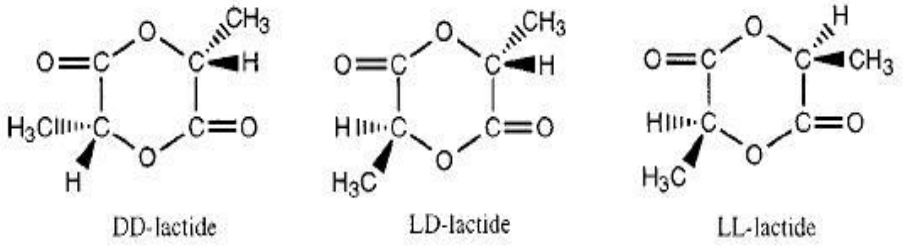

Figure 2.2 Stereoisomers of lactide

2.1.2 Polymerization method

Based on the monomer type for PLA synthesis, i.e. lactic acid or lactide, two completely different polymerization methods are possible. In this section we will explain these synthesis routes by discussing the effect of different parameters on the properties of final product as well as their limitations and advantages.

2.1.2.1 Polycondensation

In polycondensation method, lactic acid is used as the monomer. For the first time in 1932, Carothers (DuPont) produced a low molecular weight PLA (Mehta et al., 2005). Under high vacuum and elevated temperatures, water is removed to let the reaction proceed for high conversions. This can be done in bulk or solution, with or without catalyst. Due to the equilibrium nature of the reaction, removing traces of water at the late stages of the polymerization becomes very difficult which prevents achieving a high molecular weight polymer. Later on, some researchers modified the polycondensation process to produce high

molecular weight PLA (Enomoto, 1994; Ajioka et al., 1995; Moon et al., 2000; Dutkiewicz et al., 2003). Mitsui Toatsu Chemicals has patented an azeotropic distillation process in which a high-boiling point solvent and a Dean-Stark trap were used to remove water in the direct esterification process (Enomoto, 1994). Weight average molecular weights (M_w) up to 184,000 g/mol were achieved by this method. Ajioka et al. (Ajioka et al., 1995) presented kinetic control, efficient water removal and suppression of depolymerization as three key factors to achieve high molecular weight PLA by polycondensation of lactic acid. They showed the polymerization rate during first stage of reaction to be proportional to the boiling point of solvent, and reasoned that water removal is more efficient with higher boiling point solvents. Moreover, they prevented depolymerization by working at high vacuum and relatively low temperatures (~130 ^{o}C). Molecular weights of 100,000 to 240,000 were obtained using different catalysts such as tin compounds and protonic acids. Dutkiewicz et al. (Dutkiewicz et al., 2003) presented o-chlorotoluene as a new potential solvent for this process and achieved a higher polymerization rate at 159 ^{o}C. In another work by Moon et al (Moon et al., 2000), bulk polycondensation of lactic acid was presented. The reason was to avoid complexity of process control and complete solvent removal. It was found that Sn(II) catalysts reduce the reaction time and also prevent racemization and discoloration of the product. In addition, evaporation of lactide formed in equilibrium with PLA was controlled by temperature and pressure to avoid depolymerization. Thus, M_w of 80,000 g/mol was obtained at 180 ^{o}C (slightly above melting point of PLA) and pressure of 10 mmHg.

Although these works show that relatively high molecular weight PLA can be achieved through polycondensation polymerization, long reaction times e.g. 12-24 hours, high level of vacuum and using organic solvents in most of the cases make this route less favorable.

2.1.2.2 Ring-opening polymerization

Ring-opening polymerization (ROP) is another way to produce PLA in which lactide is used as monomer. PLAs produced initially by this method had low molecular weights until lactide purification techniques were improved by DuPont (Garlotta, 2001). Followed by that, Schneider introduced high molecular weight PLA from lactide, which was suitable for film and fiber production (Schneider, 1955). The polymerization method was to heat the purified monomer above its melting point in a closed evacuated vessel, using oxides of polyvalent heavy

metals such as lead, antimony and zinc or their salts for catalyzing the reaction. Best results were obtained with temperatures ranging from 140 to 180 ^{o}C. Today, PLA is produced with different catalysts through cationic, anionic and coordination-insertion polymerization mechanisms in bulk or solution (Stridsberg et al., 2002; Thongchul, 2013). Tin 2-ethylhexanoate or stannous octoate ($Sn(Oct)_2$), with the chemical structure depicted in Figure 2.3, is the most common catalyst used for PLA synthesis (Andreopoulos et al., 1999; Garlotta, 2001; Korhonen et al., 2001; Mehta et al., 2005). It is preferred because of the high reaction rate, low racemization and its approval by the US Food and Drug Administration. In addition, it is easy to work with $Sn(Oct)_2$ due to its solubility in organic solvents and lactide.

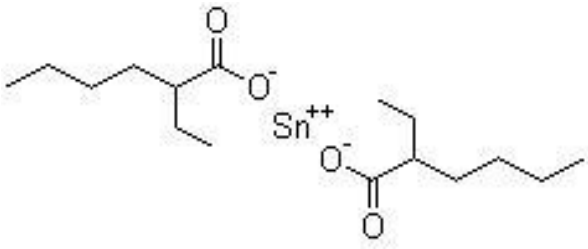

Figure 2.3. Chemical structure of stannous octoate

One of the first studies concerning L-lactide polymerization using stannous octoate was published in 1987 by Eenink et al. (Eenink et al., 1987). They synthesized PLLA at 130 ^{o}C through bulk ring-opening polymerization and showed that $Sn(Oct)_2$ might be connected to chain ends, thus acting as initiator. Different mechanisms have been proposed on the role of $Sn(Oct)_2$ in polymerization (Zhang et al., 1994; Kricheldorf et al., 1995; Kowalski et al., 2000; Kricheldorf et al., 2000). The most popular one suggests that $Sn(Oct)_2$ first reacts with compounds containing hydroxyl groups to form a tin alkoxide, the latter then acts as the actual initiator of the polymerization reaction (Storey and Sherman, 2002). This reaction mechanism is illustrated in Figure 2.4. The use of alcohols increases the reaction rate and provides the opportunity to synthesize PLA in different chain architectures by employing multifunctional molecules. This will be explained in more details in section 2.4.1.3.

Block or random copolymers of PLA with other cyclic esters such as glycolide, caprolactone, etc. can be synthesized by addition of the monomers at different reaction stages (Jung et al., 2013; Contreras et al., 2014; Dalmoro et al., 2014; Jiao et al., 2014). Controlling the polymer's molecular weight is possible by simply adjusting the monomer to initiator ratio in this type of polymerization. Most applications require high molecular weight polymers, and the

preferred route for the synthesis of such PLA is ring-opening polymerization of lactide. In addition, reaction time is much shorter than polycondensation and high vacuum is not necessary, since there is no by-product to prevent molecular weight increase. However, the reaction should take place in an inert atmosphere due to adverse effect of oxygen and moisture on catalyst and PLA degradation.

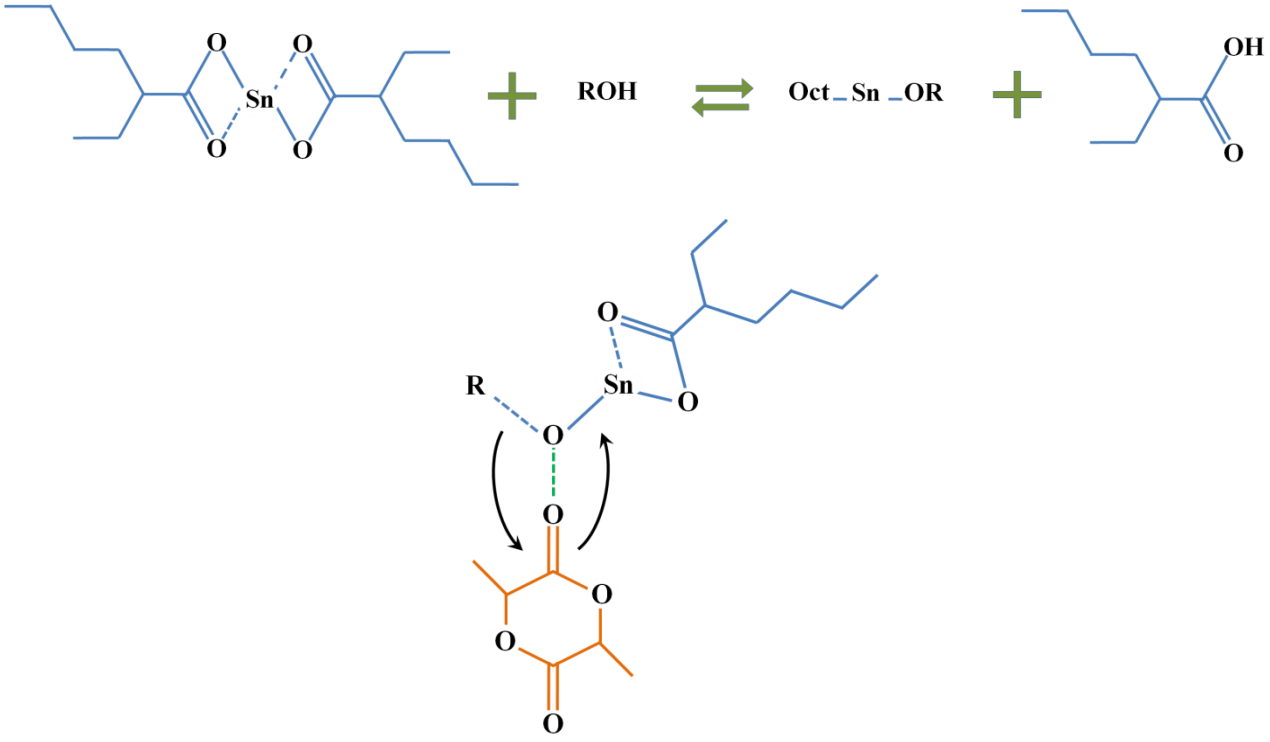

Figure 2.4. Ring-opening polymerization mechanism of lactide by stannous octoate in presence of OH group (tin alkoxide mechanism)

In addition to the type of catalyst, other important parameters affecting the molecular weight of the polymer in ROP of lactide are catalyst to monomer ratio, initiator to monomer ratio, reaction time and temperature. These parameters are explained in the following by providing some examples from the literature.

Effect of catalyst and initiator concentration: Hyon et al. studied the effect of catalyst concentration on molecular weight of PLA (Hyon et al., 1997). PLA was synthesized through polycondensation and ROP. Polycondensation gave weight average molecular weights (M_w) lower than 16,000 g/mol, whereas ring-opening polymerization in bulk using stannous octoate as catalyst in the concentration range from 0.003 to 0.8 wt% produced polylactides with viscosity

average molecular weights (M_v) ranging from 20,000 to 680,000 g/mol. As it is illustrated in Figure 2.5, the monomer conversion and M_v showed a maximum at a catalyst concentration

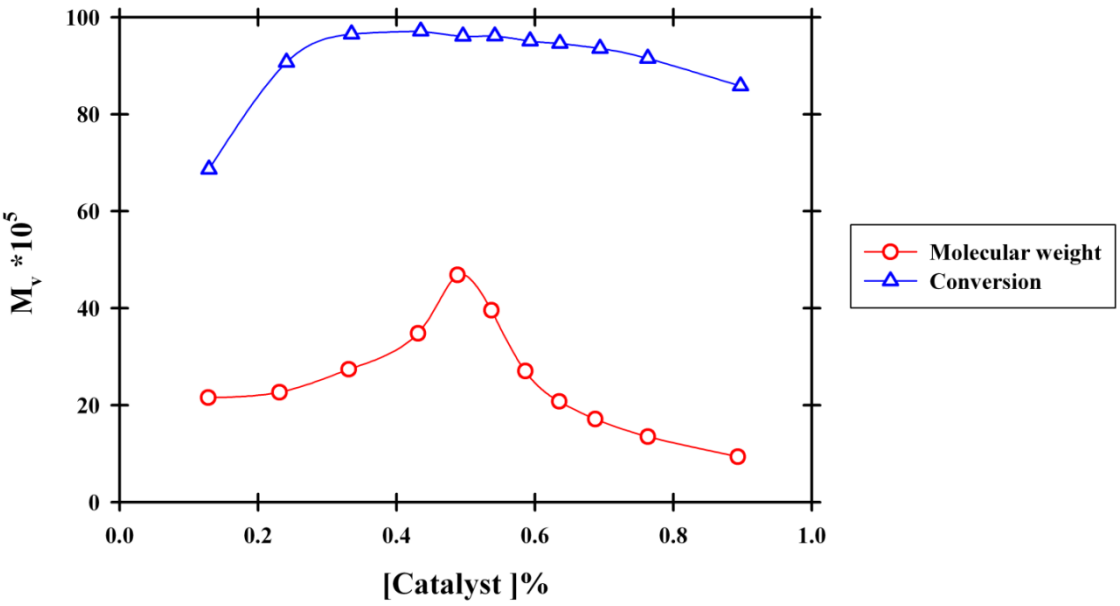

Figure 2.5. Effect of the $Sn(Oct)_2$ concentration on the M_v and monomer conversion adapted from (Hyon et al., 1997)

around 0.05wt%. In another work Kowalski et al. showed that optimum $Sn(Oct)_2$ concentration was about 0.05 mol/L (Kowalski et al., 2000). Zhang et al. (Zhang et al., 1994) investigated the effect of hydroxy substances on lactide polymerization in the presence of stannous octoate and showed that increasing alcohol concentration increased reaction rate while decreased PLLA molecular weight. The time required to reach 90% conversion was two times more when monomer to initiator ratio was increase from 500 to 5000. Recently, Yu et al. developed a kinetic model for lactide polymerization with $Sn(Oct)_2$ and 1-dodecanol in bulk and validated that for a wide range of temperature by experimental results (Yu et al., 2009). Data confirmed the direct relation of OH concentration with polymerization rate and its inverse effect on final molecular weight. Korhonen et al. (Korhonen et al., 2001) studied the role of alcohol initiators with different number of functional groups and showed that polymerization rate and molecular weight increased with increasing the functionality of initiator. Achieving higher molecular weights with increased number of OH group was a consequence of higher number of initiation sites for a single molecule from which polymer chains propagate in a specific period of time.

Effect of polymerization time and temperature: In the same work by Hyon et al. (Hyon et al., 1997), effect of polymerization time and temperature on conversion and molecular weight was investigated. As it is illustrated in Figure 2.6, the monomer conversion and M_v increased almost linearly with polymerization time up to a monomer conversion of 80%, and then decreased after passing a maximum when the reaction was allowed to proceed.

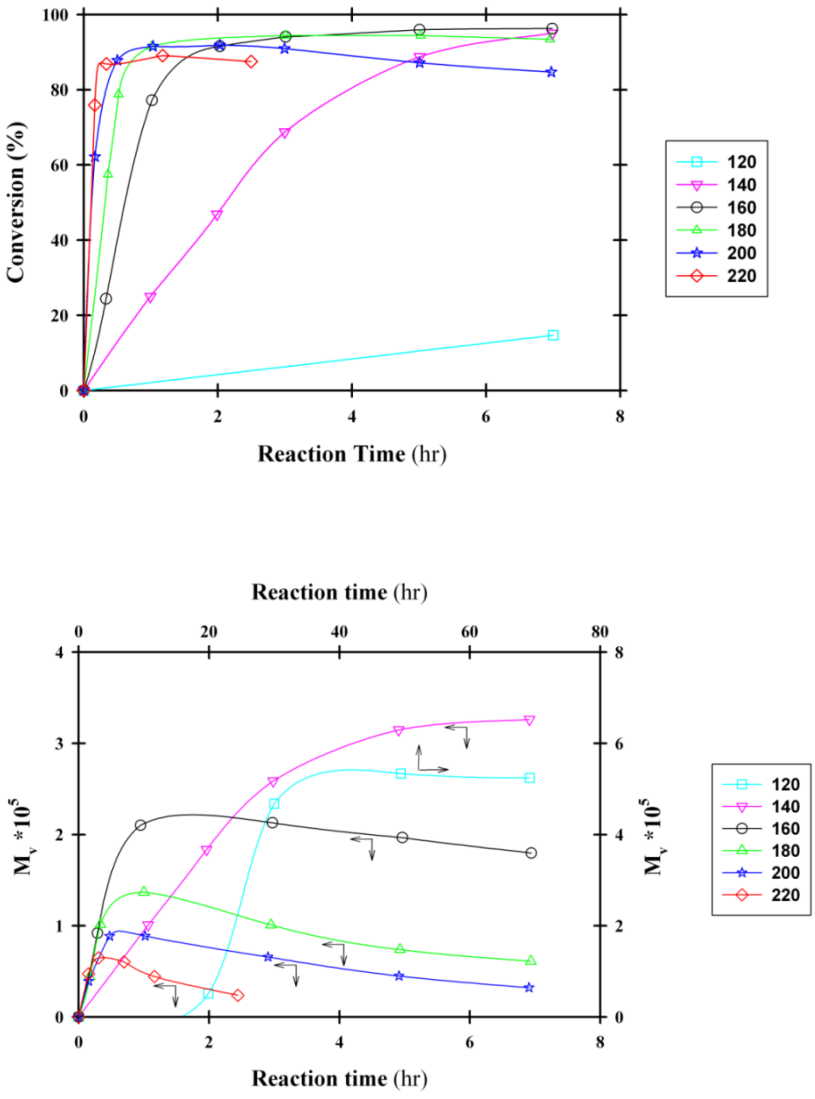

Figure 2.6. Effect of the reaction time and temperature on the conversion (top) and molecular weight (bottom) adapted from (Hyon et al., 1997)

This time dependence was pronounced at higher polymerization temperatures. These decreases at prolonged polymerization and higher temperatures were attributed to thermal depolymerization of resultant PLA.

Yu et al. also showed that polydispersity index, shown in Figure 2.7 as M_w/M_n, was increased as conversion approached 100% by prolonged reaction time because of the transesterification and chain scission reactions at high polymerization temperatures (Yu et al., 2011). It is noteworthy that molecular weight distribution broadening was significant above 80% monomer conversion, in agreement with results presented in Figure 2.6.

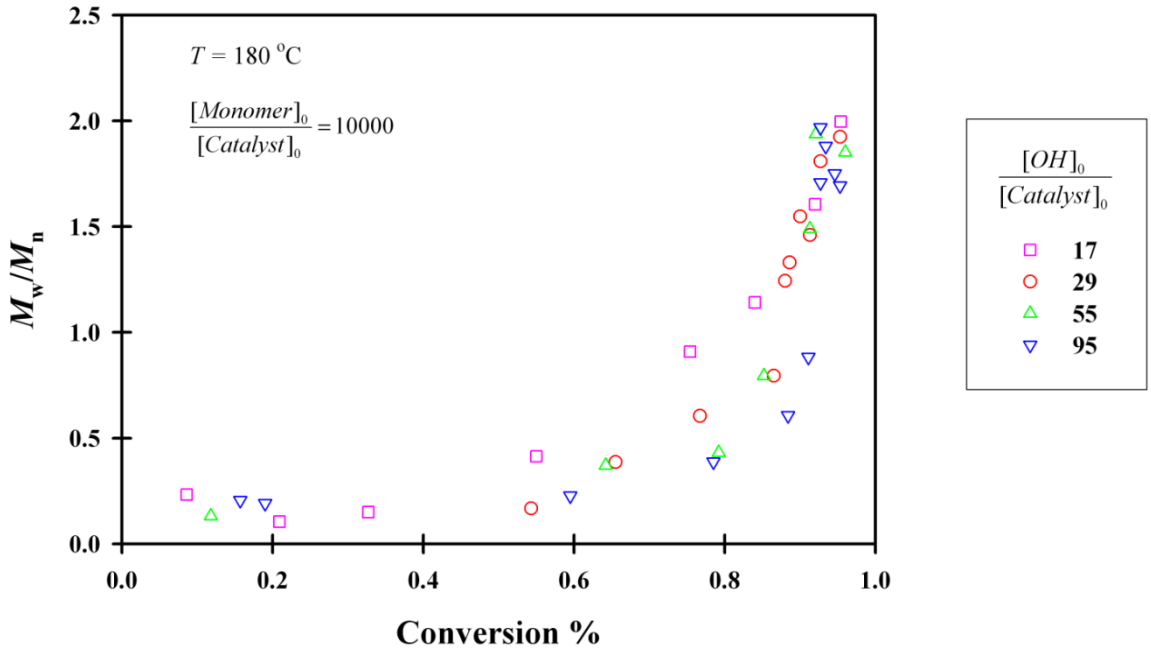

Figure 2.7. Variation of polydispersity index with conversion adapted from (Yu et al., 2011)

2.2 PLA properties

It is essential to understand PLA thermophysical and rheological properties in order to optimize its processing conditions and product quality. These properties which are particularly important for film blowing process, the intended application for this study, are introduced in this section. As it was mentioned in section 2.1.1 stereochemistry is a determining factor in PLA properties. Therefore, the role of chain composition (L and D monomers) on PLA properties is explained where applicable.

2.2.1 Thermophysical properties

Glass transition temperature (T_g) is an important property that determines heat deflection temperature (HDT) and service temperature, above which polymer becomes soft and loses strength to bear load. T_g of polymers is a function of molecular weight and can be predicted by the Flory-Fox equation:

$$T_g = T_g^{\infty} - \frac{K}{M_n} \qquad \textbf{(2.1)}$$

where M_n is the number average molecular weight, T_g^{∞} is the glass transition temperature at infinite molecular weight and K is a constant. For PLA, T_g is also a function of optical purity or the concentration of L and D repeating units in a chain (Jamshidi et al., 1988; Witzke, 1997; Dorgan et al., 2005-a). Flory-Fox equation constants are given for poly(L-lactide) (PLLA) according to Equations (2.2) and (2.3) as functions of X_D, the molar fraction of D units, (Saeidlou et al., 2012):

$$T_g^{\infty} = \frac{13.36 + 1371.68X_D}{0.22 + 24.3X_D + 0.42X_D^2} \qquad \textbf{(2.2)}$$

$$K = 52.23 + 791X_D \qquad \textbf{(2.3)}$$

By increasing the concentration of D units in PLLA, a decrease in T_g is observed. Maximum T_g for optically pure PLLA is about 60 ^{o}C which is lower in comparison with polystyrene (~ 95 ^{o}C) or polyethylene terephthalate (~ 80 ^{o}C). This is one of main drawbacks of PLA that limits it applications.

Besides the amorphous phase, PLA chain optical purity directly affects the crystalline phase. In fact, PLA can be semi-crystalline or completely amorphous. Different crystal types have been identified for PLA, the most frequently occurring is α type crystal with a pseudo-orthorombic cell structure with cell dimensions of a = 1.07 nm, b = 0.595 nm, and c = 2.78 nm, containing two 10_3 helices (Okihara et al., 1991). The extent of crystallinity and melting temperature (T_m) depend on the concentration of L and D repeating units in PLA chains (Bigg, 1996; Kolstad, 1996; Witzke, 1997; Hartmann, 1998; Bigg, 2005). Maximum crystallinity and melting temperature for α type crystal are about 40% and 180 ^{o}C, respectively, for pure PLAs made from L-lactide or D-lactide (known as PLLA and PDLA). As illustrated in Figure 2.8 and

Figure 2.9, by increasing the content of the opposite repeating unit in PLLA chains, melting point is decreased. Increase of D units higher than 10%, results in a completely amorphous PLA.

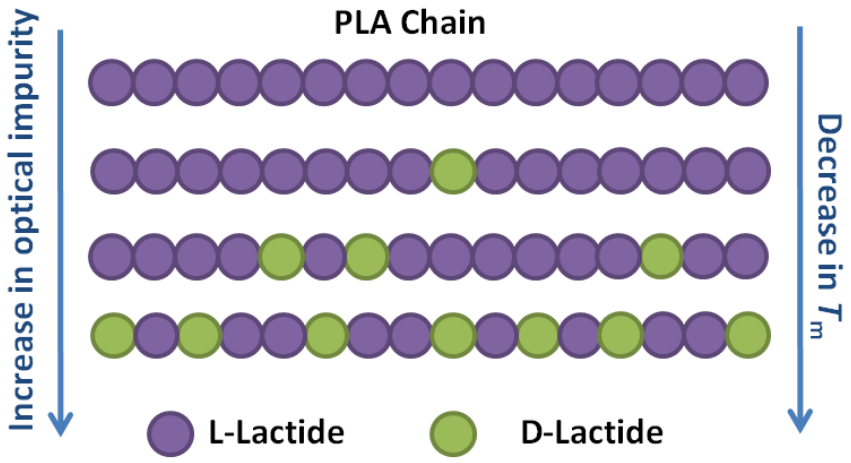

Figure 2.8. Schematic of PLA chains with different levels of optical purity and melting point

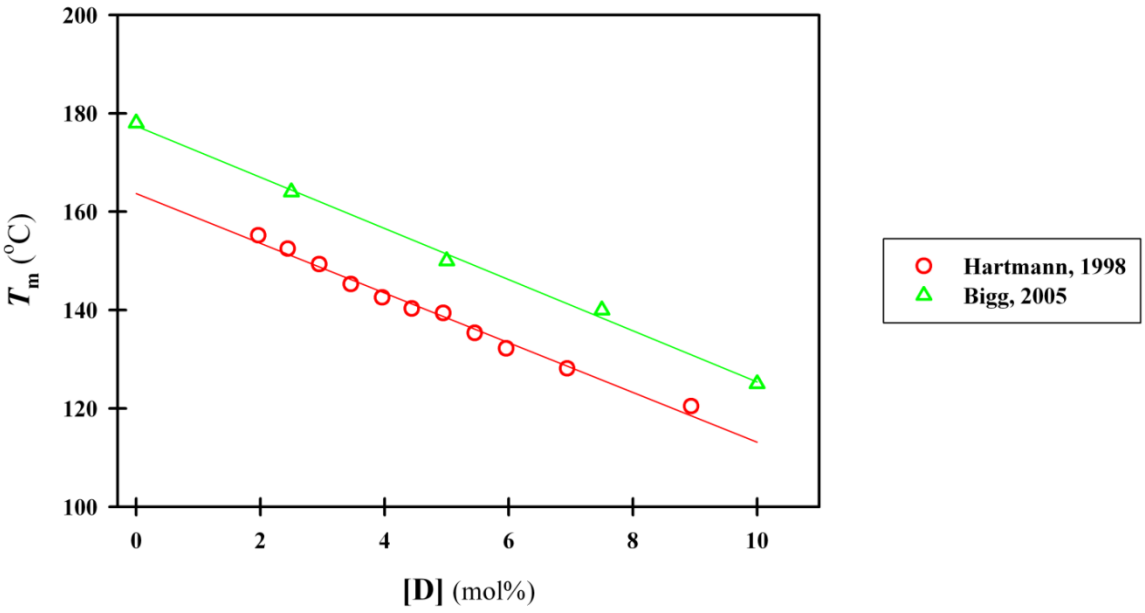

Figure 2.9. Variation of melting temperature of PLLA with D unit concentration, adapted from (Hartmann, 1998; Bigg, 2005)

One particularity about PLA crystallization behavior is that although opposite repeating units in PLA chain can hinder its crystallization, when PLLA and PDLA chains are mixed, they can co-crystallize and form a crystal type called stereocomplex. Ikada et al. for the first time reported the stereocomplex formation between two enantiomeric forms of PLA (Ikada et al.,

1987). They mixed PLLA and PDLA in solution state and precipitated the solution to obtain stereocomplex. They reported that the optimum blending ratio for stereocomplex formation is 1:1. Cell structure for stereocomplex is triclinic with dimensions of a = 0.916 nm, b = 0.916 nm and c = 0.870 nm, in each cell one PLLA and one PDLA chain segment are located assuming a 3_1 helical conformation (Okihara et al., 1991). Researchers have also produced stereoblock PLA chains to readily produce stereocomplex crystal by improving the mixing of L and D segments at molecular level (Kakuta et al., 2009; Tsuji et al., 2010; Rahaman and Tsuji, 2013). However, restrictions in chain mobility caused by the connection of opposite segments led to less stereocomplex formation in comparison with PLLA/PDLA blends. These two methods for stereocomplex formation are schematically illustrated in Figure 2.10.

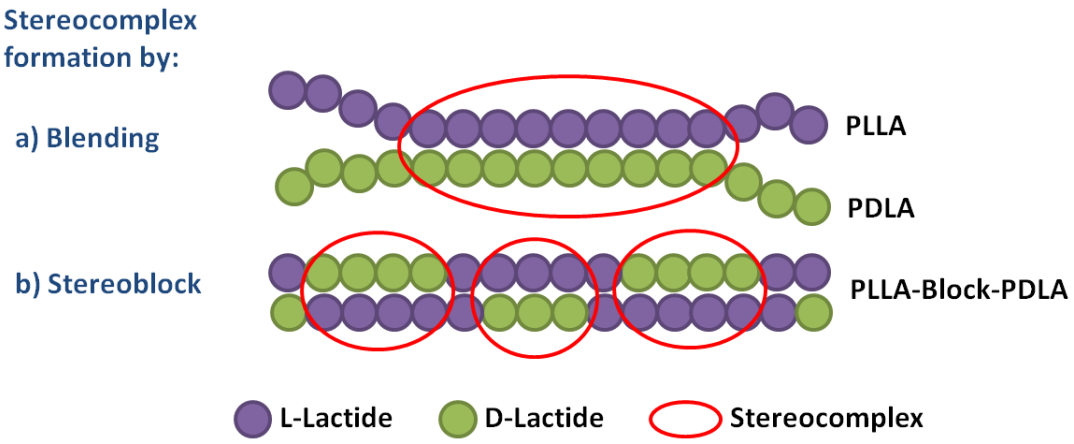

Figure 2.10. Schematic of stereocomplex formation methods

The crystal formed from the co-crystallization of PLLA and PDLA melts at about 50 ^{o}C higher than homopolymer crystals. Moreover in X-ray diffraction (XRD) analysis (Figure 2.11), stereocomplex crystals can be distinguished from homo-crystals as the peaks associated to PLA stereocomplex appear at 2θ equal to 12^{o}, 21^{o} and 24^{o} while homo-crystal peaks appear at 15 ^{o}, 16^{o}, 18.5^{o} and 22.5^{o} (Ikada et al., 1987). Peaks are presented in Figure 2.11.

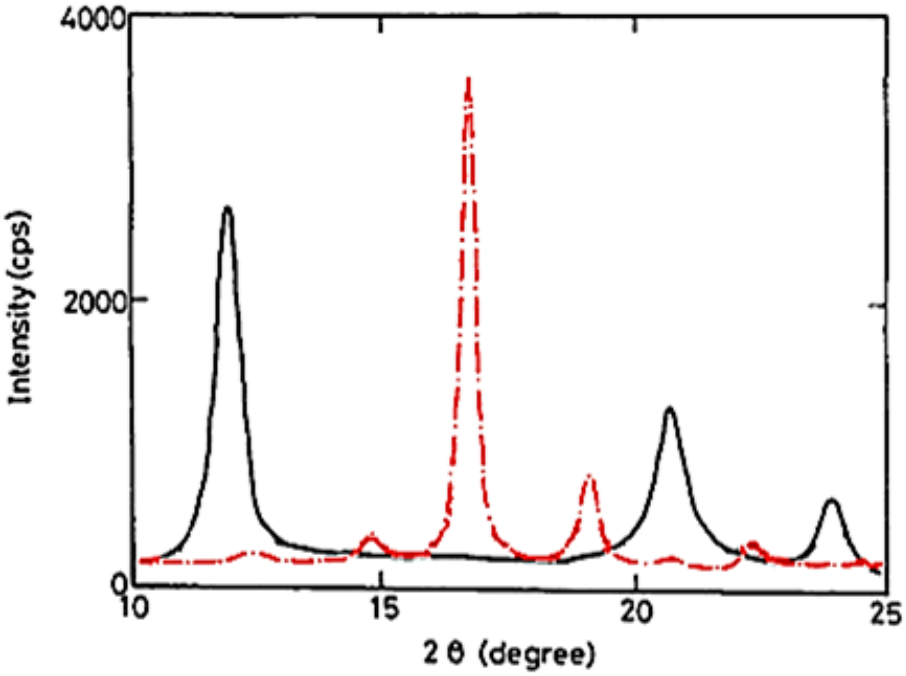

Figure 2.11. XRD patterns for PLA stereocomplex (solid line) and homocrystal (dash dot line) adapted from (Ikada et al., 1987)

Another determining aspect for crystallinity is thermal history. PLA is known as a polymer with very slow crystallization kinetics. Thus, even if high purity PLA is subjected to fast cooling rates from the melt, final product will have a low crystalline content. Usually PLA is not crystallized completely from the melt and shows cold crystallization behavior upon subsequent heating (Androsch and Di Lorenzo, 2013; Ravari et al., 2013). This can be used to increase the crystallinity of final product. Other methods such as adding nucleating agents (Kolstad, 1996; Nam et al., 2006; Tsuji et al., 2006; Kawamoto et al., 2007; Wen and Xin, 2010), plasticizers (Kulinski and Piorkowska, 2005; Xiao et al., 2009; Sungsanit et al., 2012) or their combination (Li and Huneault, 2007; Xiao et al., 2010) may also be used for increasing the number of crystallization sites and chain mobility; therefore, enhancing the overall crystallization kinetics of PLA.

High crystallinity may be favorable or not, depending on the end-use application. For instance, it is not suitable for injection molded parisons used in blow molding process, but desirable for injection molded articles where high thermal stability is needed. Moreover, the crystalline morphology and spherulite size are critical parameters. Especially, for transparent

packaging applications, spherulite size should be under the wavelength of visible light to have a clear product.

The most common method to measure the crystallinity of polymers is using the differential scanning calorimetry (DSC) technique. By heating a sample with a specific thermal history above its melting point and measuring the heat of fusion (ΔH_m) and heat of cold crystallization (ΔH_{cc}), its crystallinity can be determined based on the following equation:

$$Crystallinity\ (\%) = \frac{\Delta H_m - \Delta H_{cc}}{\Delta H_{m,100\%}} \times 100 \qquad \textbf{(2.4)}$$

Different values have been reported for ΔH_m of 100% crystalline PLLA or PDLA homopolymers which are presented in Table 2.1. Most commonly, 93 J/g is used in the literature as the reference value.

Table 2.1. Enthalpy of fusion for 100% crystalline PLA

Author, Year	$\Delta H_{m,100\%}$ (J/g)
(Fischer et al., 1973)	93
(Loomis et al., 1990)	140
(Tsuji and Ikada, 1996)	82
(Miyata and Masuko, 1998)	135
(Huang et al., 1998)	100

PLA density at room temperature is approximately 1.25 g/cm^3 and may vary slightly by crystallinity. Also its melt density can be approximated using Equation (2.5) by Witzke (Witzke, 1997):

$$\rho(g/cm^3) = \frac{\rho_{150℃}}{1 + \alpha_1(T(℃) - 150)} \qquad \textbf{(2.5)}$$

where $\rho_{150} = 1.1452$ and α_1 is the thermal expansion coefficient equal to 7.4×10^{-4} °C^{-1} for PLA.

2.2.2 Rheological properties

Melt processing is the main method to give shape to PLA; therefore, it is important to know its melt rheological behavior in different flow fields to determine the processing conditions. One of the most important characteristics of polymer melts is zero-shear viscosity (η_0). Commonly, η_0 is proportional to $M_w^{3.4}$ above the critical entanglement molecular weight (M_c) for linear polymers. Witzke (Witzke, 1997) introduced a model by using Williams-Landel-Ferry (WLF) equation in which he correlated the zero-shear viscosity of PLA to its M_w, temperature and chain composition (amount of meso-lactide and L-lactide):

$$\eta_0 = (a_1 + a_2 W_{meso} + a_3 W_{L-mer}) \left(\frac{M_w}{100{,}000}\right)^{3.38} \times exp\left(\frac{-C_1(T(°C) - 100)}{C_2 + (T(°C) - 100)}\right) \quad (2.6)$$

where W_{meso} and $W_{L\text{-}mer}$ are the initial weight fractions for meso-lactide and L-lactide, respectively, a_1 = -13,000, a_2 = -142,000, a_3 = 112,000, C_1=156±1.6, and C_2 = 110±11 ^oC. This equation is useful for L-lactide content of more than 50% and temperatures between T_g and T_g+100 ^oC. According to this relation, at a certain molecular weight and temperature, by increasing the D unit concentration in PLLA chain its zero-shear viscosity is reduced. Besides the power values of 3.38 proposed for PLA by Witzke, Palade et al. (Palade et al., 2001), Cooper-White and Mackay (Cooper-White and Mackay, 1999), and Dorgan et al. (Dorgan et al., 1999), reported 3.6, 4 and 4.6, respectively. Later, Dorgan et al. found that zero-shear viscosity of PLA is scaled with $M_w^{3.4}$ and the higher values reported previously were resulted from small data sets (Dorgan et al., 2005-a). The relationship between η_0 and M_w is also reported for star PLAs having different number of arms and summarized in Table 2.2.

Table 2.2: zero-shear viscosity and molecular weight relation for PLAs

Polymer type	T (°C)	Equation	Ref.
Linear PLA	180	$\log(\eta_o^*) = 3.4\log(M_w) - 14.26$	(Dorgan et al., 2005-a)
Linear PLA	150	$\log(\eta_o^*) = 3.4\log(M_w) - 13.2$	(Othman et al., 2011)
4-arm stars	180	$\log(\eta_o^*) = 9.8\log(M_w) - 46.3$	(Dorgan et al., 1999)
6-arms stars	180	$\log(\eta_o^*) = 9.9\log(M_w) - 47.4$	(Dorgan et al., 1999)

Zero-shear viscosity becomes more sensitive to molecular weight variations when chain structure is star shaped instead of linear. Therefore, at a similar molecular weight, η_0 of a star polymer may be higher or lower than linear one as demonstrated in Figure 2.12. In this figure η_0-M_w data for linear and star PLAs are presented for comparison. Positive or negative deviation from the linear polymer benchmark is associated to the possibility of branch entanglement as a consequence of number of arms and total molecular weight.

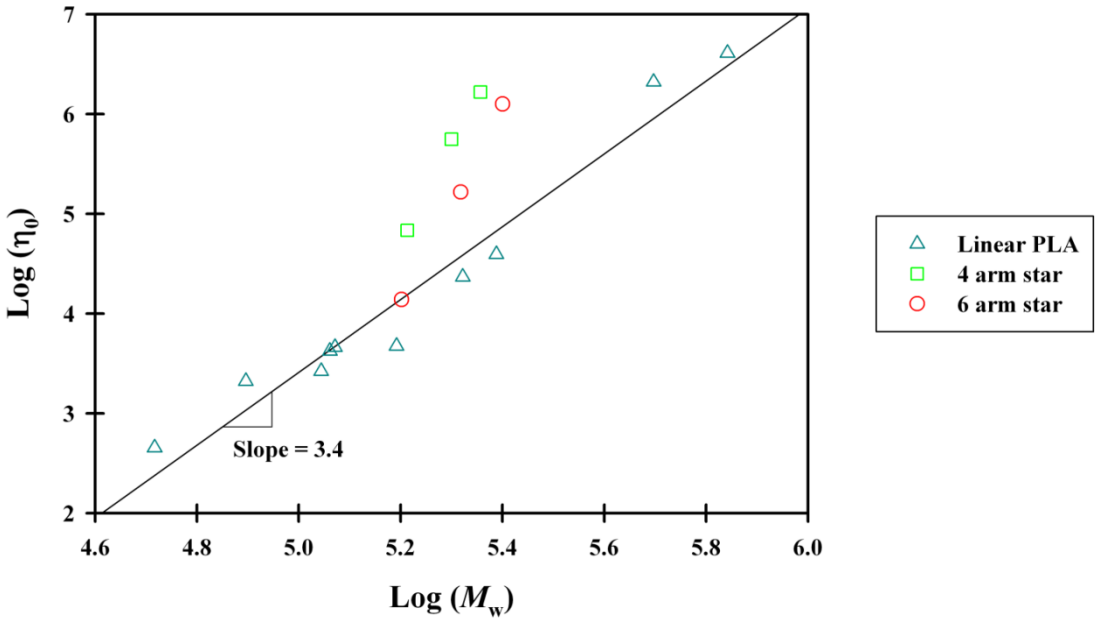

Figure 2.12. Deviation of star PLAs from linear PLA behavior in logaritmic plot of η_0-M_w at 180 °C, adapted from (Dorgan et al., 1999; Palade et al., 2001)

Rheological characterizations are also used to calculate some fundamental chain parameters. Critical molecular weight for entanglement (M_c) is calculated from the logarithmic scale η_0-M_w plot and is the molecular weight at which the slope of the line changes from 1 to 3.4. Entanglement molecular weight (M_e) is calculated according to Equation ((2.7) (Ferry, 1961):

$$M_e = \frac{\rho RT}{G_N^0} \qquad \textbf{(2.7)}$$

where ρ is the melt density, R is the universal gas constant, T is the temperature and G_N^0 is the plateau modulus. Different values of M_c (9000-16000 g/mol) and M_e (4000-10500 g/mol) have been reported in the literature for PLA (Grijpma et al., 1994; Cooper-White and Mackay, 1999; Dorgan et al., 2005-a; Othman et al., 2011). This inconsistency is because of different stereochemistry, temperature and polydispersity of tested PLAs.

Characteristic ratio (C_∞) is a measure of chain flexibility that can be estimated from melt rheological properties according to the following equation (Fetters et al., 1999):

$$C_\infty = 10 m_b \rho^{-\frac{2}{3}} (M_e)^{-1/3} / l_0^2 \qquad \textbf{(2.8)}$$

where m_b is the relative molecular mass per backbone bond and l_0^2 is the mean square bond length. Different values of C_∞ have been reported in the literature for PLA (Grijpma et al., 1994; Joziasse et al., 1996; Cooper-White and Mackay, 1999; Blomqvist, 2001; Dorgan et al., 2005-a; Dorgan et al., 2005-b). Recently it was showed that a value of 6.5 ± 0.9 is reliable, implying that PLA is a flexible polymer (Dorgan et al., 2005-a; Dorgan et al., 2005-b).

Besides shear flow, elongational flow is a major part of complex flow fields existing in polymer melt processing techniques. Especially in processes such as film blowing, thermoforming and foaming, understanding the polymer behavior in elongational flow is essential. Extensional rheometry is a powerful technique that can provide valuable information about the rheological behavior of polymers. One of the convenient methods for extensional rheometry is using Sentmanat Extensional Rheometer (SER) universal testing platform, shown schematically in Figure 2.13.

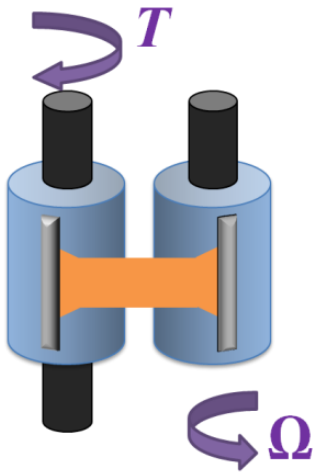

Figure 2.13. Schematic of Sentmanat Extensional Rheometer (SER) universal testing platform

This geometry consists of two drums with a radius *R* that rotate at an angular speed Ω in opposite directions. Rectangular sample is fixed on the drums by two clamps and is extended from both sides so that the stretch zone length (*L*) is constant and midpoint is stationary during the test. Hencky strain rate and time dependent extensional viscosity or tensile-stress growth coefficient (η_E^+) are calculated according to Equations ((2.9) and ((2.10), respectively:

$$\dot{\varepsilon}_H = \frac{2\Omega R}{L} \qquad \textbf{(2.9)}$$

$$\eta_E^+ = \frac{\mathrm{T}(t)}{2R\dot{\varepsilon}_H A_0 (\frac{\rho_S}{\rho_M})^{2/3}} \exp(\dot{\varepsilon}_H t) \qquad \textbf{(2.10)}$$

where T is the measured torque signal, A_0 is the cross-sectional area of the specimen in the solid state, ρ_S is the solid state density, and ρ_M is the melt density of the polymer. Two types of behavior are observed when η_E^+ is plotted as a function of time. When polymer chains are relaxed faster than the characteristic time of the test ($\frac{1}{\dot{\varepsilon}_H}$), η_E^+ increases up to a steady state plateau value as shown by number 1 in the diagram of Figure 2.14. However, if the relaxation time of polymer is longer than characteristic time (Kasehagen and Macosko, 1998) or if strain induced crystallization happens (Hadinata et al., 2007; Sentmanat et al., 2010; Chellamuthu et al., 2011), extensional viscosity deviates from a plateau behavior and continuously increases until the failure of the sample, a behavior known as strain hardening (number 2 in the diagram of Figure 2.14).

Strain hardening is an important phenomenon which is referred to as a self-healing mechanism since a more uniform deformation happens by transfer of stress to less extended and weaker locations, while in the absence of such mechanism, deformed specimen would fail at the continuously thinning locations.

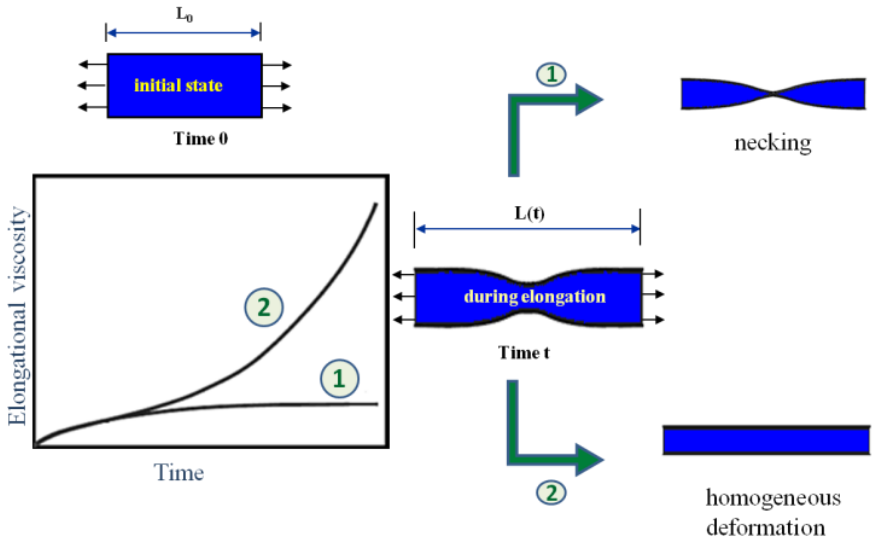

Figure 2.14. Typical response of specimen under extensional flow and its relation to elongational viscosity behavior

There is not an extensive amount of literature on extensional flow characterization of neat PLA and available data is not consistent; both behaviors have been reported (Palade et al., 2001; Sinha Ray and Okamoto, 2003; Yamane et al., 2004; Othman et al., 2011). This inconsistency may be the result of different characterization modes (squeezing vs. extensional flow), temperatures, molecular weights and molecular weight distributions. Palade et al. (Palade et al., 2001) investigated the melt rheology of PLA with L content between 96 to 100%. They used tris(nonylphenyl) phosphite (TNPP) to stabilize PLA during the tests and presented the extensional data for PLA for the first time, showing that it revealed strain-hardening behavior at 180 ^{o}C. Othman et al. (Othman et al., 2011) as well characterized a PLA thermally stabilized with TNPP in extensional mode in the temperature range of 90 to 130 ^{o}C. PLA exhibited strain hardening at 90 ^{o}C which was diminished by increasing temperature, contradicting the findings of Palade et al. In another work, Yamane et al. (Yamane et al., 2004) observed strain hardening in biaxial extensional flow for a high molecular weight PLA with broad distribution (M_w = 230 kg/mol, PDI = 2.3) at 190 ^{o}C, whereas no strain hardening was reported by Sinha Ray and

Okamoto (Sinha Ray and Okamoto, 2003) at 170 ^{o}C for a PLA with M_w = 180 kg/mol and PDI = 1.6.

2.3 PLA applications and processing

Considering that PLA has enantiomeric monomers which result in amorphous and semi-crystalline grades, it can be manufactured with a wide range of properties. It can be converted into different products such as film, sheet and fiber. on existing processing equipments (Lim et al., 2008). PLA is used mainly for packaging, medical and fiber applications (Gupta et al., 2007; Ahmed and Varshney, 2011; Ulery et al., 2011). PLA resins can be designed specifically for various forming processes such as injection molding, extrusion, blow molding, thermoforming, film forming, or fiber spinning (Henton et al., 2005; Lim et al., 2008). The key parameters that should be controlled are D-isomer content, molecular architecture and molecular weight. In all melt processing techniques, PLA should be dried first; otherwise, significant molecular weight reduction will happen as a result of hydrolytic degradation.

Among the variety of available processes, film blowing will be explained, as it is our concern to improve PLA processability for this forming technique.

2.3.1 Film blowing

Description of the process: Film blowing is the most common way of producing plastic films. Figure 2.15 is a schematic of film blowing process. In this process, pellets are molten by a single screw extruder and polymer is pushed through an annular die to form a tube. Air is blown from the die center to inflate the tube into a thin bubble. It is also drawn to orient the chains for better mechanical properties. The bubble is cooled down by exposure to ambient air and the cooling air blown around it by an air ring; reaching a height called freeze or frost line where it solidifies. At the top of machine, it is collapsed in nip rolls and taken up by the winder.

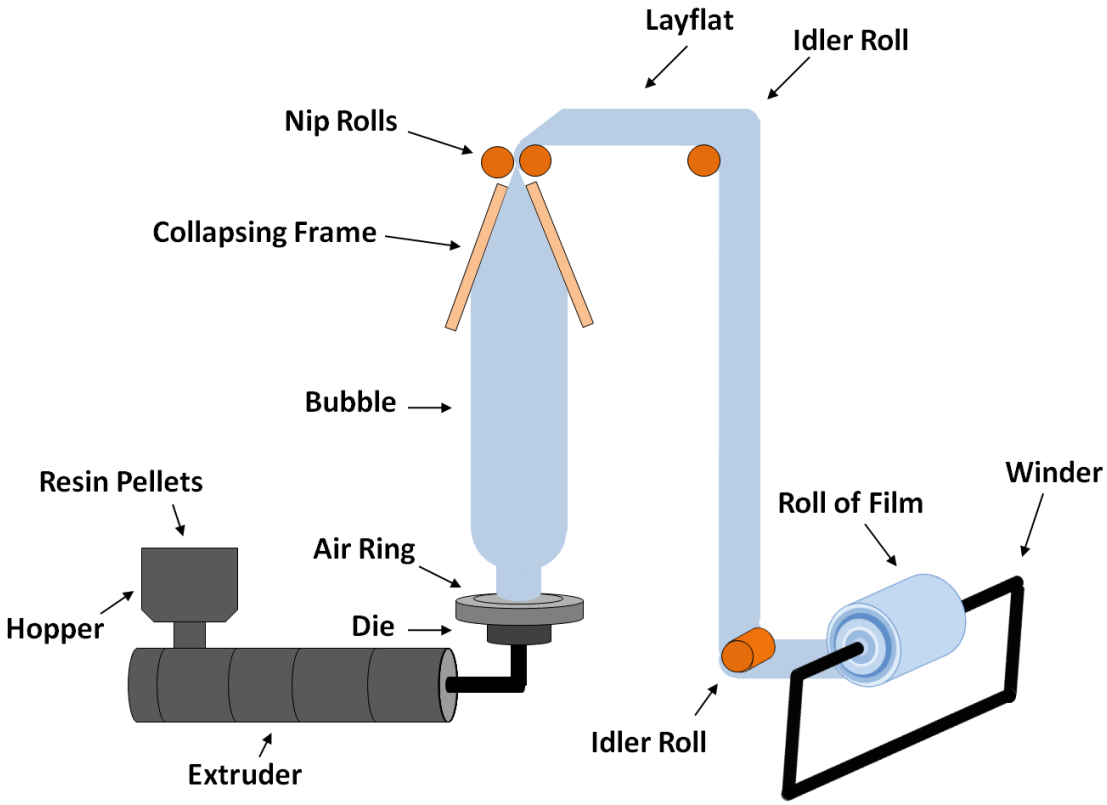

Figure 2.15. Film blowing line

Two important parameters in this process are blow up ratio (BUR) and draw down ratio (DDR). BUR is defined as the ratio of bubble diameter to the die diameter and is a measure of elongation of film in the transverse direction (TD) of the machine.

$$BUR = \frac{bubble\ diameter}{die\ diameter} = \frac{0.637 \times layflat\ width}{die\ diameter} \quad \textbf{(2.11)}$$

DDR is the ratio between the film winding speed and the average speed at die exit and is a measure of elongation in the machine direction (MD). Equation (2.12) gives the relation between DDR and BUR:

$$DDR = \frac{die\ gap}{film\ thickness \times BUR} \qquad \textbf{(2.12)}$$

By varying BUR and DDR, films with different thicknesses and orientations can be produced. Due to biaxial orientation in film blowing compared to uniaxial orientation in extrusion film casting process, final product has better mechanical properties. Additionally, in film blowing process, different film widths and sizes can be produced with a single die without trimming; therefore, the amount of waste material is less compared to casting process. Another advantage of this process is that making bags for packaging applications is done easily due to annular shape of the product. On the other hand, cooling is more efficient in cast film compared to blown film because it is done by chill roles or water. Moreover, controlling film thickness is more difficult in film blowing. Another disadvantage of film blowing process is that polymer usually has a lower melt flow index (MFI) compared to those used in extrusion film casting to ensure the bubble stability. Therefore, production rate of film blowing process is less than extrusion film casting. The main challenge in film blowing process is bubble stability which is the key to a continuous production and homogenous film properties. Different kinds of instability have been identified as shown in Figure 2.16, including bubble sagging, breathing, dancing and resonance. Low density polyethylene (LDPE) is known as the most stable polymer for this process because of its long-chain branched structure.

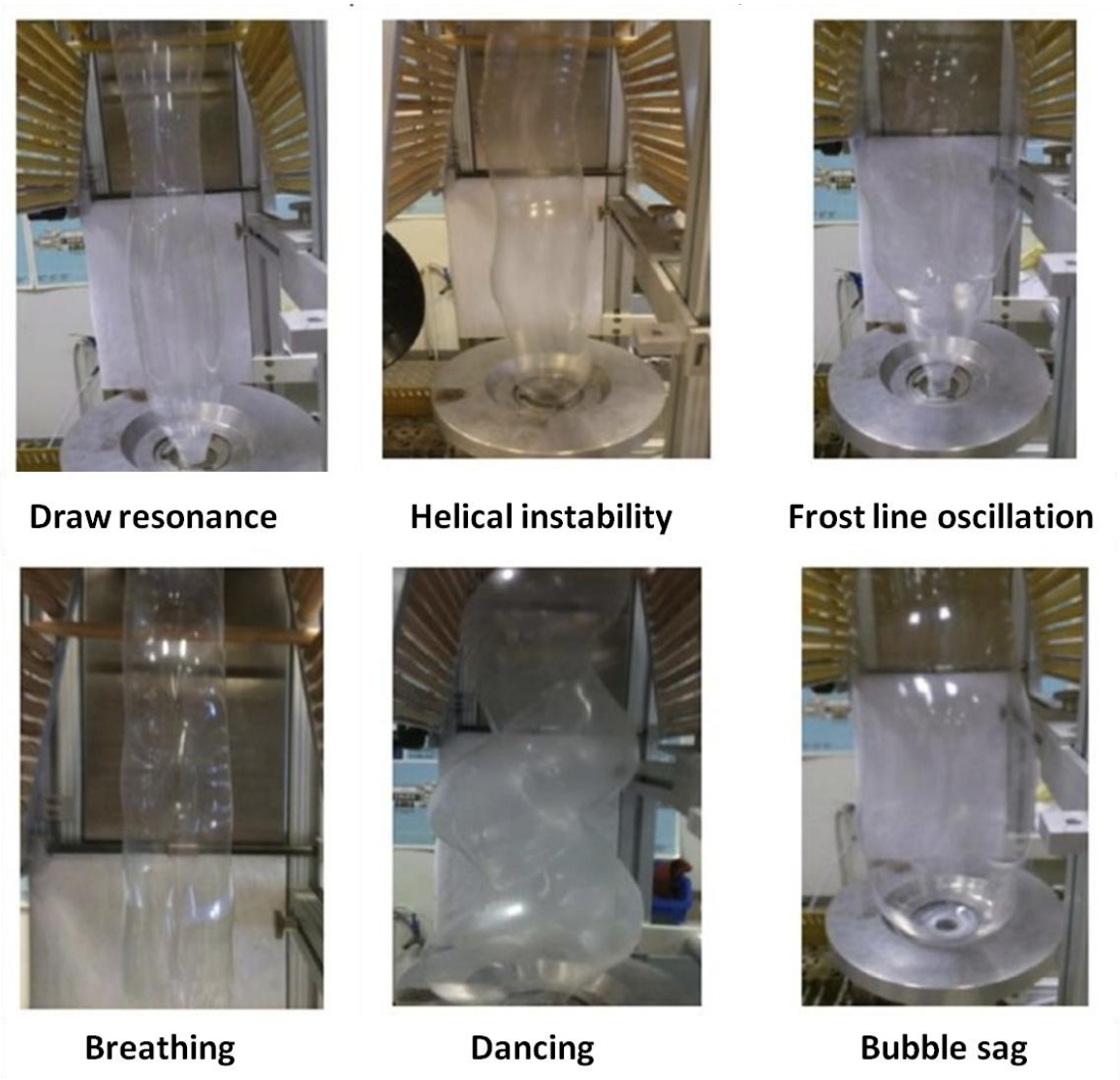

Figure 2.16. Various bubble instabilities in film blowing process (Mallet et al., 2014)

In the case of PLA, there is a shortage of scientific literature on the stability and operating window improvement for its film blowing process. While PLA is a low melt strength polymer which makes its processing very difficult, only few studies have dealt with improving PLA film blowing process. Plastics Suppliers Inc. patented a PLA film blowing process in which they claim to produce PLA blown film without any need for additives (Tweed, 2006). The key point was to increase melt viscosity four to eight times via internal cooling the die mandrel by air or liquid. However, this technique results in a decreased polymer flow through the die and hence a reduced production rate and higher costs. Mallet et al. (Mallet et al., 2014) studied a number of commercial resins and showed that the processing window is very narrow; especially when die temperature was set at 180 ^{o}C. To overcome this problem, they reduced die temperature to 150

^{o}C. Lower molecular weight resins were unstable at most tried conditions whereas higher molecular weight grades were stable at low DDR and became unstable by increasing this parameter.

Research on PLA film blowing is mainly focused on the enhancement of film properties such as tensile, impact resistance, tear resistance, permeability and degradability by blending with other polymers, plasticizers and nanoparticles. Enhanced orientation in film blowing process was employed to increase barrier properties of PLA/layered silicate nanocomposite films. Orientated clay platelets in PLA films were shown to decrease oxygen and water vapor permeability up to 50% and CO_2 permeability up to 80% (Thellen et al., 2005; Zenkiewicz et al., 2010). Blending PLA with other polymers has been used to improve the processability and final film properties simultaneously. These polymers are preferably bio-based and/or biodegradable to have a completely degradable or bio-based film. Plasticizers such as adipate and citrate esters where used to prepare PLA/thermoplastic starch (TPS) biodegradable blown films (Shirai et al., 2013). Biodegradable agricultural mulch films have also been introduced recently based on the film blowing of PLA/poly(hydroxibutyrate) (PHB) blends compatibilized by maleic anhydride (MA). Biodegradation rate was increased by 45% compared to virgin PLA films (Jandas et al., 2013). Combination of polydiethylene glycol adipate as plasticizer and acrylic impact modifier was shown to effectively increase the elongation at break as well as the tear strength of PLA blown films (Zhang et al., 2014).

2.4 Modifications to improve PLA melt strength

PLA has a low melt strength which is problematic in processes such as blow molding, film blowing, low density foaming and thermoforming where high melt strength is required. The following part is dedicated to the key studies that involve improvements in this aspect.

2.4.1 Structure modification

Different parameters affect the rheological properties of polymeric materials. For each polymer, its molecular weight, molecular weight distribution and chain structure have direct effects on rheological properties. Especially in terms of chain structure, usually molecules with long-chain branching have higher melt strength and elasticity depending on the number of

branches, their length and chain architecture, i.e. comb-like, multi-arm star, H-shaped or more complex architectures.

Melt strength improvement by structure modification for polyolefins is the subject of many scientific studies. La Mantia and Acierno (La Mantia and Acierno, 1985) showed that adding 50% low-density polyethylene (LDPE) with long-chain branching structure to high-density polyethylene (HDPE) increased its melt strength 1.5 to 2 folds. Another study verified that 10-20% LDPE can be added to linear low density polyethylene (LLDPE) to improve its strain hardening without significantly altering its crystallization behavior (Ajji et al., 2003). Similar results on the addition of long chain branched polypropylene (PP) to linear PP is reported as well (Tabatabaei et al., 2009). By comparing polyethylenes of almost similar molecular weights, but different levels of long chain branching, Wood-Adams observed that first normal stress coefficient increased by increasing the degree of long chain branching and was much more sensitive to long chain branching than viscosity (Wood-Adams, 2001). Molecular dynamics simulations has also confirmed that by increasing shear rate, the first normal stress difference (N1) becomes higher for branched polymers compare to linear one (Jabbarzadeh et al., 2003).

Similar to the presented works that give evidence about the enhancement of melt strength and rheological behavior of polyolefins by incorporation of branched polymer to the system, structure modification is adapted for PLA to improve its melt rheological properties. However, mainly shear flow rather than elongational is studied in these works. Regarding the importance of branched structure for enhancing rheological properties, different methods has been used to obtain a branched PLA; i.e. free radical branching, chain extension and direct branched PLA synthesis are explained hereafter.

2.4.1.1 Free radical branching

One strategy to generate branched PLA and improve the processability of PLA is to add a proxide during melt processing. Proxide decomposes at the process temperature and produces free radicals that attack polymer chains and produce other free radicals on them. This process continues and results in the branching and molecular weight distribution increase and possibly cross-linking depending on peroxide concentration. Lauroyl proxide was used up to 1% in a reactive extrusion process to modify PLA melt rheology. Complex viscosity and elastic modulus were increased up to 50% (Dean et al., 2012). Dicumyl peroxide at 0.3% concentration was

reported to increase complex viscosity of PLA by four times (You et al., 2013). Dorgan et al. characterized melt rheology of a peroxide initiated branched PLA and its blends with linear PLA (Dorgan et al., 2000; Lehermeier and Dorgan, 2001). Based on their results, zero-shear viscosity and elasticity increased with increasing the branched PLA content. Also tensile properties of the blends did not vary too much with each other, suggesting the possibility of adjusting rheological characteristics to desired values by blending, without compensation of mechanical properties. Peroxide initiated branched PLA is also used for melt spinning application (Cicero et al., 2002), showing strain hardening behavior and a higher initial elongational viscosity compared to linear structure.

Other studies exist on the use of peroxides to increase PLA molecular weight, while their rheological significance is not discussed (Sodergard and Nasman, 1994; Sodergard et al., 1995; Carlson et al., 1998). In a report by Sodergard et al. (Sodergard et al., 1995), M_n and M_w were almost doubled with 0.1% tert-butyl peroxybenzoate. Further increase in M_w more than 3 times was observed by 3% peroxide; however, M_n did not change significantly, showing that side chains and cross-links were increasing. Branched PLA through reactive extrusion by 2,5-dimethyl-2,5-di-(ti-butylperoxide) was produced by Carlson et al. They determined the optimum temperature and peroxide concentration to be 170-180 ^oC and 0.1-0.25%, respectively (Carlson et al., 1998).

2.4.1.2 Chain extension

Another way to impart branching, improve PLA melt viscosity and reduce degradation and chain scission is employing chain extenders. Chain extender is a multifunctional additive which links the end groups of polymer chains to each other. Two frequently used materials for PLA chain extension are tris(nonylphenyl) phosphite (TNPP) (Lehermeier and Dorgan, 2001; Palade et al., 2001; Cicero et al., 2002; Dorgan et al., 2005-a; Othman et al., 2011) and an epoxy functional styrene-acrylic oligomer (Al-Itry et al., 2012; Meng et al., 2012). Functional groups in these chain extenders react with PLA chain ends and give rise to a branched structure with a higher molecular weight than unmodified PLA.

To improve PLA foaming behavior, Mihai et al. used 1.5-2% chain extender and obtained low density foams as a result of enhanced melt rheology (Mihai et al., 2010). The tan (δ) (ratio of loss to storage modulus, G''/G') decreased with increasing chain extender content, meaning that

elasticity of the melt was increased. Specimens without chain extender did not show strain-hardening behavior and were broken before the maximum extension; On the other hand, samples with chain extender were elongated to the maximum strain and showed strain-hardening behavior.

Using the same chain extender was reported by Plastemart for blown film PLA (Plastemart, 2010). 2% addition of a 30% active masterbatch to PLA 4042D from NatureWorks resulted in increase of molecular weight from 124,000 to 185,000 g/mol, and 50% increase in elongation. They claimed better bubble stability and increased bubble size; however, films were hazy when chain extender was used.

2.4.1.3 Direct branched PLA synthesis

As mentioned in section 2.1.2.2, an advantage of ROP is the flexibility to design and fabricate polymers with desired structures to manipulate their final properties. Although producing non-linear polymers is possible in polycondensation method through copolymerization with multifunctional monomers, ROP is more practical and reliable since there is no concern about the crosslinking of final product and there is more control on the chain structure.

Structure of PLA depends on the alcohols used as initiators (Korhonen et al., 2001). Mono- and bifunctional alcohols yield linear polymers, while alcohols with hydroxyl functionality higher than two result in branched polymers. Some examples of the possible polymer structures are illustrated in Figure 2.17.

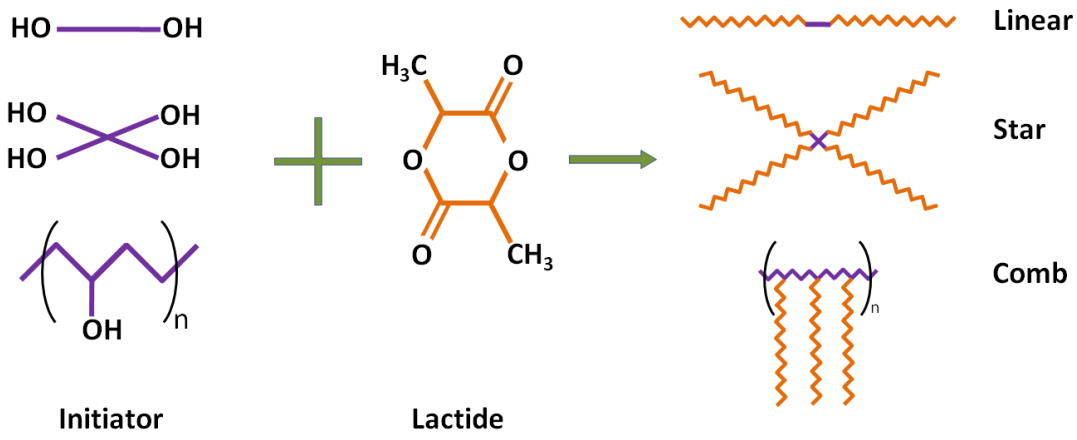

Figure 2.17. Reaction scheme of the PLA polymerization with different initiators

Dorgan and Williams compared star-shaped PLAs of 4 and 6 arms produced by ROP with linear PLA in shear mode and showed that zero-shear viscosity and shear thinning increased with branching (Dorgan et al., 1999).

In above examples, the only junction for branches is the initiator. In order to produce a long chain hyper-branched polymer in which the branching points are distributed along the polymer chain, an alteration in the polymerization is required. For this purpose, initiation sites which are hydroxyl groups should be distributed along the chain and to do so, it is possible to add a small quantity of a cyclic co-monomer with OH group on its ring that can copolymerize with the lactide monomer in the ring opening polymerization. As a result, in the course of polymerization, initiation sites are located in the growing chains that can start new branches in a tree shaped manner. Consequently, compared to other branched structures in which the branch number was controlled by the initiator type, in this case branch number is controlled by the monomer feed composition.

Pitet et al. used glycidol to produce PLA with such a branched structure (Pitet et al., 2007). They showed low temperature (80 ^{o}C) solution polymerization of lactide initiated by glycidol resulted in linear chains having the epoxide group at one end, while bulk polymerization at high temperature (130 ^{o}C) produced hyper-branched polymer in which glycidol ring opening made branching points. Wolf and Frey produced branched and hyper-branched PLA using 5-hydroxymethyl-1,4-dioxane- 2-one (5HDON) as the co-monomer in the range of 1-20 mol% of the feed (Wolf and Frey, 2009). Using $Sn(Oct)_2$ as the catalyst resulted in approximately 50% of 5HDON conversion into branching points and the rest was mainly chain initiator and a small portion was consumed in linear segments. Structures of glycidol, 5HDON and schematic of hyper-branched structure are presented in Figure 2.18.

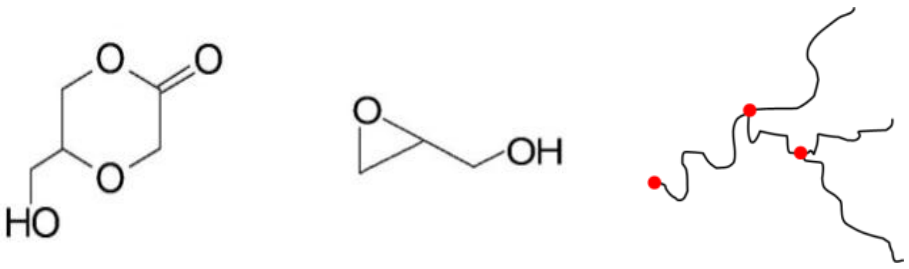

Figure 2.18. Chemical structure of 5HDON (left), glycidol (center) and schematic of hyper-branched structure with dots representing the comonomer

2.4.2 Blending

Another melt strength modification strategy for PLA, other than modifying chain structure, is blending with other polymers. In the following section, this approach is explained.

PLLA/PDLA stereocomplex: One way of increasing melt viscosity and elasticity of PLA is stereocomplex formation by blending the two stereochemically different PLAs, PLLA and PDLA. This mechanism is illustrated in Figure 2.19. Stereocomplex melting point is higher than PLA processing temperature; therefore, crystallites are remained in the melt. Consequently, chains are connected through this junctions and turn into a higher molecular weight branched structure. If a chain connects two or more of its counterpart chains it also acts as a physical cross-link (Tsuji and Ikada, 1999; Yamane et al., 2004).

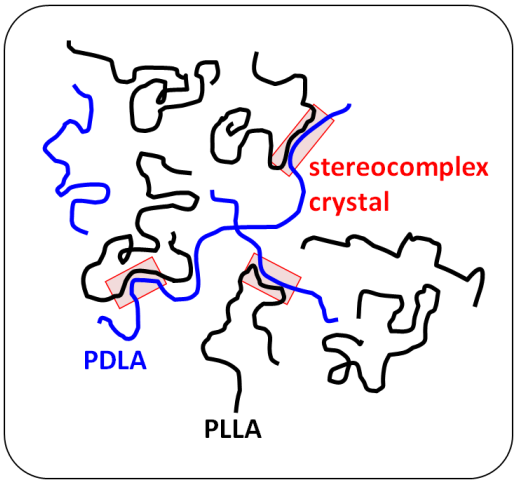

Figure 2.19. Branching and physical cross-linking by stereocomplex formation between stereochemically different PLA chains

Formation of a three dimensional network through stereocomplex formation was first indicated by Tsuji et al. (Tsuji et al., 1991). They found out that an irreversible gel was formed in concentrated PLLA/PDLA solutions. Dried gel showed only a single endothermic peak at 216 ^{o}C in DSC experiment, implying the existence of stereocomplex crystals. Later they investigated the mechanical properties of solution blended PLLA/PDLA cast films and showed that compared to non-blended films, films containing stereocomplex had better mechanical properties and their elastic modulus did not drop significantly by increasing temperature until above the stereocomplex melting point (Tsuji and Ikada, 1999). Yamane et al. studied the effect of PDLA addition to PLLA on its shear and biaxial extensional flow behavior. Steady shear measurements at 190 ^{o}C showed increase in viscosity for PLLA when blended with small amount of PDLA at

low shear rate region. Similar results were obtained in dynamic measurements at 190 ^{o}C. Complex viscosity (η^*), storage and loss moduli (G' and G'') increased by increasing PDLA content. It was shown that below the melting point of stereocomplex crystals, η^* at frequency of 0.1 s^{-1} for samples containing 5% PDLA was about four times of neat PLLA and the difference between viscosities becomes small at the melting point of stereocomplex, confirming that origin of the difference in viscosity between PLLA and blended sample was the formation of stereocomplex. In addition, in biaxial extensional measurements in squeezing mode, PLLA showed a slight strain hardening effect which is intensified with addition of a small amount of PDLA. Positive effect of PLA stereocomplex on low frequency viscosity increase was also demonstrated by Rahman et al. (Rahman et al., 2009).

PLA Blends with other polymers: Blends of PLA with other polymers are now more conventional, especially those in which both components are biodegradable. The most important ones are mainly blends of PLA with thermoplastic starch (TPS) (Huneault and Li, 2007; Mihai et al., 2007; Li and Huneault, 2011) and copolyesters such as poly(butyleneadipate-co-butyleneterephthalate) (PBAT) (Li et al., 2011; Sirisinha and Somboon, 2012; Wang et al., 2013), Poly(butylene succinate-co-adipate) (PBSA) (Ojijo et al., 2012; Eslami and Kamal, 2013) and Poly(3-hydroxybutyrate-co-3-hydroxyvalerate) (PHBV) (Boufarguine et al., 2013; Ma et al., 2013). The main reasons for fabrication of PLA blends with other polymers are reducing production costs, achieving better processability and improving PLA properties such as toughness, barrier properties and HDT. Since the subject of this research is the improvement of PLA processability in film blowing, some commercial PLA blends for this application are presented.

FKuR Kunststoff GmbH has developed different film blowing grades using PLA, a biodegradable copolyester and specialized compatibilizers: Bio-Flex F1130 consists about 10% PLA. This blend has similar processability and properties with LDPE and is not a transparent film. Bio-Flex F2110 is more similar in properties and feels to HDPE with about 30% PLA content and has applications like deep freeze packaging and waste bag. Also, Bio-Flex A4100 CL is a clear biodegradable film with similar feel to PP which consists about 75% PLA.

BASF has also introduced a completely biodegradable plastic called Ecovio, which is based on PLA and PBAT. Ecovio contains about 45% PLA and can be used for film blowing

applications. However, it has a high water vapor transmission rate. Due to high toughness of PBAT, its blending with PLA results in reduced tensile strength and modulus; however, elongation and toughness are increased.

2.5 Challenges and objectives

Based on the literature review, one may conclude that the main concern regarding PLA processing is its low melt strength and elasticity which is not studied comprehensively in literature. Additives such as chain extenders or peroxides were mainly added to PLA during its processing to prevent the molecular weight and viscosity reduction rather than improving the melt strength. In addition, no study has been reported on a real control of the final polymer structure and properties in those reactive processes. Moreover, melt processing of PLA containing stereocomplex crystal has not been studied intensively. Therefore, the main objective of this work is to improve PLA processability by enhancing its melt strength, intended for film blowing application. The following specific goals are identified to achieve the main objective of this project:

1. Synthesize and characterize PLA with different branched architectures to evaluate the correlation between their structure and properties
2. Study the effectiveness of chemical and physical branching strategies (blending branched PLLA or PDLA with linear PLA, respectively) on melt rheology enhancement
3. Study the homocrystallization and stereocomplex formation behavior of PLA with different branched structures
4. Employ the modified PLA blends in film blowing process and evaluate the processing window expansion and final film properties

2.6 Original contributions

This work has put forward a number of original contributions regarding the crystallization and rheological behavior of PLA in relation to its molecular chain architecture. In the first step of the project where structure-properties relationships were studied, the relation between chain branching and spherulite nucleation at elevated crystallization temperatures was clearly demonstrated. In addition, the strain hardening behavior in uniaxial extensional rheometry was revealed for synthesized branched architecture PLAs. In the second part where the effect of

chemical and physical branching on PLA rheological properties was studied, the extensional rheology of branched PLA containing stereocomplex crystals was an original aspect. PDLAs with star shaped, comb like and hyper branched chains were used for the first time for PLLA rheological property modification. In the third phase, pure effect of branched architecture on PLA homocrystallization and stereocomplex formation was studied, demonstrating enhanced homocrystallization kinetics with up to 14 fold decrease in crystallization half-time, increased stereocomplex formation by branching at very high crystallization temperatures and different internal morphology of stereocomplex and homocrystal spherulites. Finally, the last phase of the project was a study of the role of physical and chemical branching on PLA processability in film blowing and final film properties. Film blowing of PLA containing synthesized branched architectures as well as stereocomplex crystals was performed for the first time, identifying a wider operating window than has previously been reported.

CHAPTER 3. METHODOLOGY

In this section, our methodology to achieve each specific objective concerning the materials and equipments, experiments and characterization tests are presented.

The first step in this project was to synthesize branched polymers with desired architecture and molecular weight. Based on the advantages of ring opening polymerization to polycondensation, which was discussed in details previously, ROP was chosen as the synthesis route. It helps to achieve a high molecular weight PLA in a short reaction time and desired chain architecture is obtained based on the structure of the initiating molecule. Star shaped, comb like and hyper branched PLAs were synthesized and preliminary rheological and thermal characterizations were performed to evaluate their potential to be used as modifiers in next steps. In the second phase, detailed rheological study was conducted on branched PLAs, their blends with linear PLA as well as blends of stereochemically different chains to evaluate the role of chemical branching and physical branching (i.e. by stereocomplex formation between PLLA and PDLA chains) on different rheological characteristics such as zero-shear viscosity, shear thinning, extensional viscosity, etc. A comprehensive study on the crystallization of branched PLAs was conducted in the third step. Isothermal and non-isothermal crystallization were studied to examine the role of chain architecture on crystallinity, kinetics and crystalline morphology. Finally, in the last part of the project, chosen blends were processed in a film blowing line with BUR and TUR as variables to determine the operating conditions at which process was stable. In addition, different film properties were measured and compared with those obtained for a commercial resin as a reference.

3.1 Materials

Materials used in this work are summarized in Table 3.1. Initiators are chosen based on the desired chain architecture. All the materials were used as received without further treatment.

Table 3.1: List of materials used in this project

Function	Name	Chemical formula	M_w (g/mol)	T_m (°C)	Supplier
monomer	L-lactide D-lactid	$C_6H_8O_4$	144	95	Purac
catalyst	stannous octoate	$C_{16}H_{30}O_4Sn$	405	-20	Aldrich
initiator	1,3-butanediol	$C_4H_{10}O_2$	90	-50	Sigma
initiator	pentaerythritol	$C_5H_{12}O_4$	136	260	Sigma-Aldrich
initiator	triglycerol	$C_9H_{20}O_7$	240	30	Sigma-Aldrich
initiator & co-monomer	glycidol	$C_6H_6O_2$	74	-54	Sigma-Aldrich
solvent	chloroform	$CHCl_3$	119	T_b = 61	Aldrich
solvent	Methanol	CH_4O	32	T_b = 65	LaboratoireMat
linear PLA	4032D	$(C_3H_4O_2)_n$	101,000	170	NatureWorks

3.2 Polymer synthesis

Measured quantities of monomer, initiator and catalyst were added to a reaction vessel under inert atmosphere in a glove box where it was sealed. Ring-opening bulk polymerization reactions were conducted under inert atmosphere at 180 ^{o}C for one hour to reach a chemical conversion of more than 90% according to the literature. Finally, the reactor was cooled to room temperature to stop the reaction. Resulting polymer was dissolved in chloroform and precipitated in excess of methanol. Precipitated material was filtered, washed with methanol and dried under reduced pressure. Pentaerythritol, triglycerol and glycidol were employed as initiators to produce four-arm star, comb like and hyper branched PLA, respectively. Schematic of the reaction setup is illustrated in Figure 3.1.

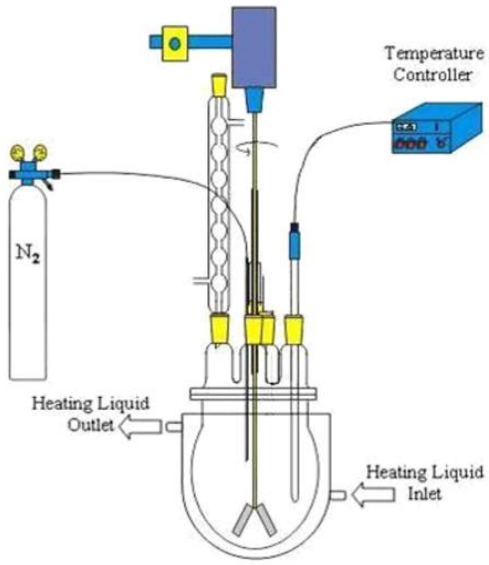

Figure 3.1. Schematic of polymerization setup

3.3 Blending process

After the preparation of adequate amount of each polymer, melt blending of branched PLLAs and PDLAs with commercial PLA at specific blending ratios was performed with a twin-screw extruder. Leistritz ZSE 18mm co-rotating twin-screw extruder was used for this purpose, operating at 190 ^{o}C and a rotation speed of 100 rpm. In the case of linear/branched PLLA blends, branched PLLA concentration was set at 10, 20 and 30%. For linear PLLA/branched PDLA, blends were prepared with 5, 7 and 10% of branched PDLA.

3.4 Film blowing process

The films were prepared using a Labtech Engineering Extrusion Line having a single-screw extruder with 20 mm screw diameter and length/diameter ratio of 30. An annular die with a diameter of 50 mm and 1.5 mm die gap was connected to the extruder to form the tube. The die temperature was set at 190 ^{o}C for PLLA and 200 ^{o}C for PLLA/PDLA blends. Different TUR and BUR were obtained by adjusting the winding speed and amount of air in the bubble, respectively.

3.5 Characterizations

3.5.1 Fourier Transform Infrared Spectroscopy

This technique was used as a proof for the nature of the synthesized polymer. By comparing the main absorption peaks related to each chemical bond with databases, it is possible to identify the synthesized polymer as well as possible residual impurities. Fourier transform infrared spectroscopy (FTIR) analysis was done with a Perkin Elmer Spotlight 200 (Waltham, MA) apparatus equipped with a Germanium ATR crystal. Measurements were performed with a resolution of 4 cm^{-1} and accumulation of 32 scans at wavelength range of 650-4000 cm^{-1} and room temperature.

3.5.2 Nuclear magnetic resonance (NMR)

^{1}H-NMR analysis was performed by a Bruker AV500 spectrometer operating at 700 MHz. A 30 degree pulse, an acquisition time of 2.6 second and a recycling delay of 2 second were used for all experiments. All spectra were collected at 25 ^{o}C.

3.5.3 Size Exclusion Chromatography

Weight average molecular weight (M_w) and polydispersity index (PDI = M_w/M_n) can be obtained using size exclusion chromatography (SEC). In the case of linear polymers, refractive index detector can be employed to obtain the molecular weight relative to the polystyrene standards. However, to obtain the molecular weight for branched polymers, an instrument with light scattering detector should be used. In this case, the absolute value for molecular weight can be measured. Molecular weight and molecular weight distribution of samples were obtained by performing SEC using a Viscotek GPCmax equipped with Wyatt DAWN light scattering system operating at 25 ^{o}C and flow rate of 1 $mL.min^{-1}$. The eluant was THF stabilized by 250 ppm BHT and 0.049 mLg^{-1} was chosen as the value of refractive index increment (dn/dc).

3.5.4 Polarimetry

The specific optical rotation [α] of PLLAs was measured in chloroform at a concentration of 1g/dL at 21.4 ^{o}C using a Jasco P-1020 Polarimeter.

3.5.5 Differential Scanning Calorimetry

Differential scanning calorimetry (DSC) can be used to measure glass transition temperature (T_g), melting point (T_m), crystallization temperature (T_c) as well as enthalpies of fusion (ΔH_m) and crystallization (ΔH_c). Also, this technique can be applied to study the crystallization kinetics and measure the crystallinity (X_c) of polymers. To evaluate the crystallinity of samples, one needs to know the enthalpy of fusion for the 100% crystalline polymer. DSC analysis was conducted using a TA instrument DSC Q 1000.

3.5.6 Rheological analysis

Shear flow: Disk shaped (25 mm diameter, 1 mm thickness) specimens for shear mode rheometry were prepared by compression molding, using a hydraulic press, at 190 ^oC. In case of PLLA/PDLA blends, enough time was given in the mold to produce the stereocomplex structure. Using dynamic shear flow measurement, various material functions and thermal stability of the samples can be determined. Frequency sweep tests were performed using an MCR 301 rheometer (Anton Paar) at 190 ^oC in a wide frequency range of 0.1 to 100 rad/s. Samples preparation and rheological characterizations were done under nitrogen atmosphere to minimize degradation.

Elongational flow: Rectangular (20×13×0.7 mm) specimens for extensional rheometry were prepared by compression molding, using a hydraulic press, at 190 ^oC. Materials were dried overnight in a vacuum oven at 80 ^oC prior to molding. In case of PLLA/PDLA blends, enough time was given in the mold to produce the stereocomplex structure. Uniaxial extensional viscosity measurements were performed by an ARES rheometer (TA Instruments) equipped with a Sentmanat Extension Rheometer (SER) universal testing platform from Xpansion Instruments. Elongational tests were performed at 180 ^oC. Sample preparation and extensional characterization were done under nitrogen atmosphere to minimize degradation.

3.5.7 Optical microscopy

The crystalline morphology of the specimens such as size and density of spherulites can be observed using optical microscopy. OPTIPHOT-2 optical microscope equipped with a programmable hot stage (Mettler FP82HT) was employed to observe the crystallization behavior of samples. Thermal procedure was decided based on the crystallization mode (isothermal and dynamic) and crystal type (stereocomplex and homocrystal).

3.5.8 X-ray diffraction

X-ray diffraction (XRD) measurements were performed using Bruker D8 Discover apparatus. The generator was set up at 40 kV and 40 mA and a copper CuKα radiation (λ=1.54056 A°) was selected. The samples were scanned in the 2θ range of 10 to 30 degree under scanning rate of 0.05 °/s to identify PLA crystalline structure. Afterward, at 2θ corresponding to observed peaks, φ scan at the rate of 1^{o}/s was performed to estimate crystal orientation.

2D-WAXD measurements were performed out using a Bruker Venture diffractometer equipped with a Photon 100 CMOS Detector, a Helios MX optics and a Kappa goniometer. The film - detector distance was 70 mm, and the data collection was carried out in 1024 x 1024 pixel mode with exposition of 300s.

3.5.9 Haze

To compare optical properties of the produced films, haze measurement was performed by Perkin-Elmer Lambda 1050 High Performance Spectrometer in the wavelength range of 300 to 800 nm. This spectrometer has a 150 mm integrating sphere with a small port fraction (less than 5%). Light trap module was used to eliminate specular reflection and measure the transmitted light scattered more than 2.5° from the axis of the incident light.

3.5.10 Tensile

The tensile testing of films was carried out using INSTRON-3365 (USA). Young modulus, tensile strength and elongation at break were measured by extending rectangular specimens of 25 mm wide and 75 mm long at a speed of 5 mm/min.

According to the presented methodology, different steps of this project are illustrated in Figure 3.2.

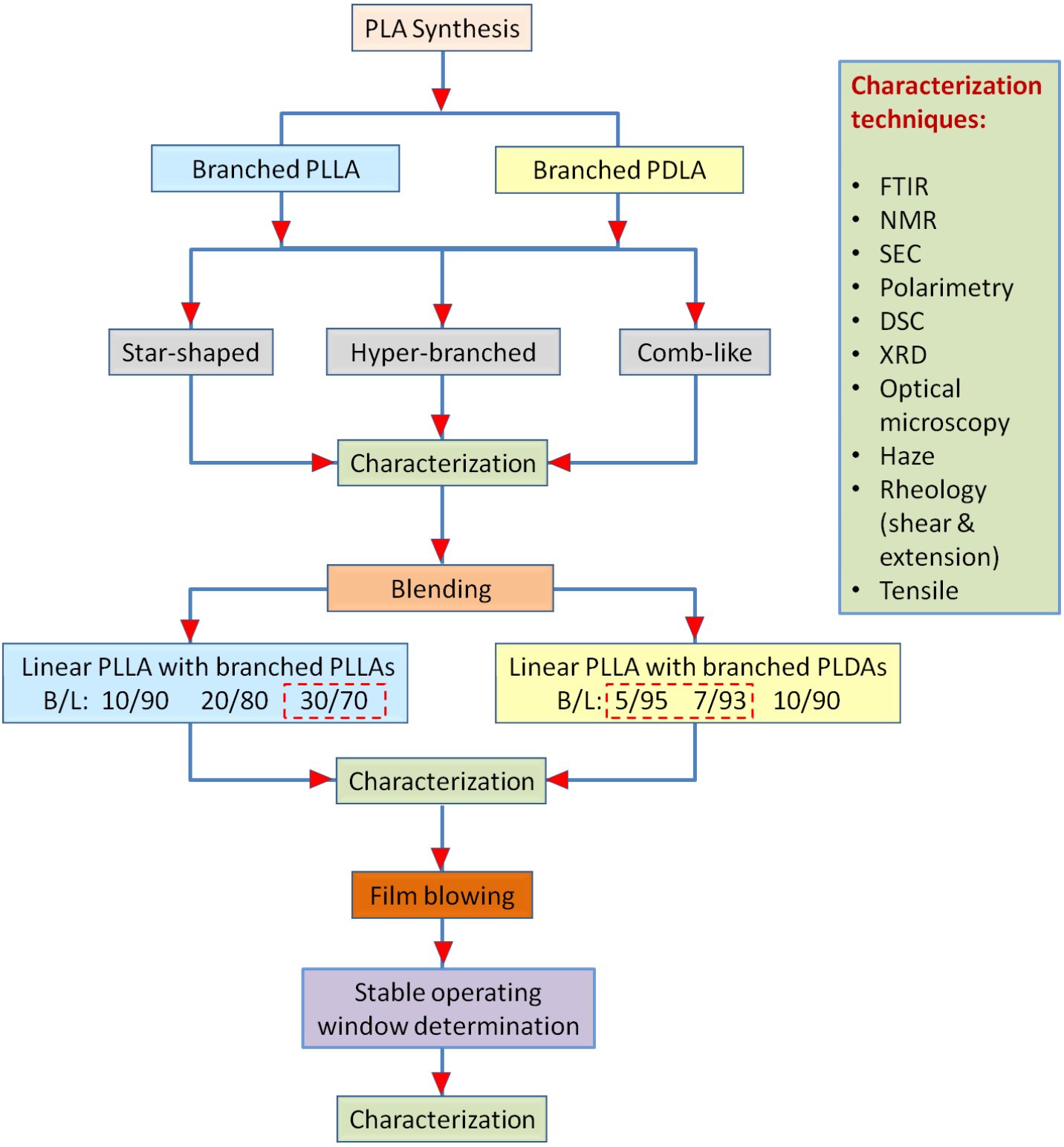

Figure 3.2. Flowchart of project steps

CHAPTER 4. ORGANIZATION OF ARTICLES

The main findings of this work are presented as four original scientific articles in the following sections, each corresponding to a specific objective stated earlier. The first paper accepted in Journal of Polymer Science Part B: Polymer Physics is presented in Chapter 5. In this chapter the experimental results of the first step of the project are presented which includes the synthesis and characterization of polylactides with different branched architectures. Star shaped, comb like and hyper branched PLAs were synthesized using ring opening polymerization and characterized by SEC, FTIR, DSC, optical microscopy and extensional rheometry techniques. Also a commercial resin with linear chain architecture was used as a reference. In Chapter 6, which is the second paper submitted to Journal of Rheology, the focus is on the detailed rheological characterization of branched PLAs and their blends with linear one. It explains the influence of two branching strategies, i.e. chemical and physical on rheological properties of such systems. Chemical branching is the direct synthesis of desired architectures and blending them with linear PLA, while physical branching is accomplished by the formation of stereocomplex crystals between PLLA and PDLA chains. Both shear and extensional rheology was employed to assess the suitability of these modification strategies on PLA melt rheology. Also DSC technique was used to confirm the formation of stereocomplex crystals. In Chapter 7, the third paper, submitted to Polymer, is presented which is a comprehensive study dedicated to crystallization of branched PLAs since in addition to melt rheology, crystallization is influenced by chain architecture. DSC and hot-stage optical microscopy were used in isothermal and non-isothermal modes to investigate the kinetics, crystallinity and morphology of branched PLAs crystallized in the form of homocrystal and stereocomplex. In addition, crystallization of linear PLA was studied and compared to branched PLAs. Another aspect of this section was the enhancement of linear PLA crystallization by blending with branched PLAs and using stereocomplex crystals as nucleating agent. Finally, in the last phase of the project which is presented in Chapter 8 and submitted as the fourth paper to International Polymer Processing, processability of the prepared blends as well as the commercial resin is explored in a film blowing process. Different operating conditions are examined to determine the regions of process stability. In addition, crystallization, optical and mechanical properties of prepared films are determined to understand the role of modification strategies and processing conditions on final film properties.

CHAPTER 5. ARTICLE 1: SYNTHESIS AND CHARACTERIZATION OF POLYLACTIDES WITH DIFFERENT BRANCHED ARCHITECTURES

Sahar Nouri, Charles Dubois, Pierre G. Lafleur

CREPEC, Chemical Engineering Department, Ecole Polytechnique, C.P. 6079, Succ. Centre ville, Montreal, QC, H3C 3A7 Canada

Correspondence to: Charles Dubois (E-mail: *Charles.dubois@polymtl.ca*)

ABSTRACT Star-shaped and comb-like poly(L-Lactide)s (PLA) are produced by employing multifunctional initiators and hyper branched structure is prepared using a cyclic co-monomer with hydroxyl group. FTIR, Size Exclusion Chromatography (SEC) and H-NMR techniques are employed to characterize the synthesized polymers, validating the formation of desired structures with chain lengths above the critical length for entanglement. After characterization of synthesized polymers, the effect of branching on PLA properties is investigated by comparing the crystallization and rheological behavior of branched PLAs to those of a linear commercial grade. Differential scanning calorimetry and optical microscopy observations reveal a remarkable improvement in PLA crystallization due to the nucleation role of branching points. Moreover, synthesized polylactides exhibit strain hardening behavior during elongational viscosity measurements by an SER platform. Significant improvements in crystallization and elongational rheology behavior of the synthesized polymers support the achievement of branched polymer structures.

KEYWORDS: nonlinear polymers; ring-opening polymerization; structure-property relations; polylactide; crystallization; extensional viscosity

5.1 Introduction

In recent years, polylactide (PLA) has been the focus of many researches due to its good mechanical and optical properties, its compostability under industrial conditions, as well as the possibility to produce this polymer from annually renewable resources. PLA is a polyester that

can be synthesized via two different polymerization reactions. The monomer, lactic acid possesses both hydroxyl and carboxylic acid groups. Consequently, it can be polymerized through a polycondensation reaction (Moon et al., 2000; Marques et al., 2010). Considering that this is an equilibrium reaction, removing traces of water at the late stages of the reaction becomes very difficult which prevents achieving a high molecular weight polymer. In the second polymerization route, lactide which is the cyclic dimmer of lactic acid is transformed to PLA through a ring-opening polymerization (ROP) reaction (Korhonen et al., 2001; Pitet et al., 2007; Kim et al., 2009). The main advantages of ROP are obtainable high molecular weights and shorter reaction time compared to polycondensation. Tin 2-ethylhexanoate or stannous octoate ($Sn(Oct)_2$) is the most common catalyst used for PLA synthesis (Pitet et al., 2007). In addition, presence of a molecule bearing hydroxyl group acting as a nucleophile is necessary to initiate ROP.

One interesting aspect of lactide ring-opening reaction is the flexibility in designing different molecular architectures by employing multifunctional initiators. Different branched structures such as star-shaped with arm numbers from 3 to 6,(Dechy-Cabaret et al., 2004; Biela et al., 2005; Mehta et al., 2005; George et al., 2009; Moravek et al., 2009; Darensbourg and Karroonnirun, 2010; Malberg et al., 2010; Ren et al., 2010; Zhao et al., 2010; Perry and Shaver, 2011) dendrimers,(Zhao et al., 2002; Adeli and Haag, 2006; Ouchi et al., 2006; Gottschalk et al., 2007; Atkinson and Vyazovkin, 2012; Zhang et al., 2012) comb-like (Wang and Wang, 2011; Yuan et al., 2012) and barbell-like molecules (Lu et al., 2012; Zhao et al., 2012) are synthesized by applying this strategy. An alternative procedure for the in-situ synthesis of branched PLA is to use comonomers bearing initiation groups such as 2,2-bis (hydroxymethyl) butyric acid in the presence of a tertiary amine, glycidol and 5-hydroxymethyl-1,4-dioxane-2-one (Gottschalk and Frey, 2006; Pitet et al., 2007; Wolf and Frey, 2009; Zhao et al., 2012). These molecules are inserted into the growing chains and become new branching points. Therefore, branches are distributed along the polymer chain and their content is determined based on the molar ratio of comonomer to lactide.

Chemically homologous chains with linear and branched structures may reveal different properties. For PLA, branching is reported to influence rheological properties such as complex viscosity and elastic modulus(Dorgan et al., 2000; Lehermeier and Dorgan, 2001; Dean et al., 2012; Wang et al., 2012; You et al., 2013) and consequently its melt processing(Mihai et al.,

2010; Ren et al., 2013). Also different reports exist regarding the effect of branching on PLA chain dynamics or segmental mobility(Sakamoto and Tsuji, 2013; Sakamoto and Tsuji, 2013), glass transition and nucleation(Wang et al., 2012; Fang et al., 2013; Phuphuak and Chirachanchai, 2013) which may accelerate or delay the crystallization process as well as melting behavior and crystallization mechanism. Most of the work in this area is based on PLA branching by reactive processes such as free radical branching or chain extension with undefined structures. Meanwhile there is a lack of fundamental studies on directly synthesized branched PLAs taking into account the pure effect of different chain architectures on final properties. Thus, the aim of this study was to investigate the relation between the chain structure and critical properties, particularly crystallization and extensional rheology of high molecular weight branched PLAs prepared by multifunctional initiators or initiator-comonomer molecules. More specifically, it was intended to improve the viscosity in extensional flow and crystallization behavior of PLA, which are critical aspects in terms of processability and final properties, through the modification of polymer chain structure and expand the opportunities for application of this environmentally friendly polymer. A comparison of the elongational rheology and crystallization behavior of branched PLAs with a commercial linear one, to elucidate the influence of branched architecture on PLA properties, supports the significant improvements in this regard.

5.2 EXPERIMENTAL

5.2.1 Materials

L-lactide (≥99.5%) was purchased from Purac biochem and used as the monomer in the ring-opening polymerization. Tin (II) 2-ethylhexanoate (~95%) from Aldrich was employed as polymerization catalyst whereas 1,3-butanediol, pentaerythritol, triglycerol and glycidol initiators were supplied from Sigma-Aldrich. Chloroform (99%, Aldrich) and methanol (99%, LaboratoireMat) were the solvents used for purification of final product. Commercial linear PLA was the semicrystalline grade 4032D from NatureWorks. All the materials were used as received without further treatment.

5.2.2 Polymer Synthesis

Mixture of monomer, catalyst and initiator was added to a reactor under inert atmosphere in a glove box, where it was sealed. Ring-opening bulk polymerization reactions were conducted under inert atmosphere at 180 ^{o}C for one hour to reach a chemical conversion of more than 90% according to the literature (Hyon et al., 1997). Tin (II) 2-ethylhexanoate, $Sn(Oct)_2$, was used as the catalyst at a concentration of 0.03 mol% in all cases. Pentaerythritol, triglycerol and glycidol were employed as initiators to produce four-arm star, comb like and hyper branched PLA, respectively. At the end of reaction, the reactor was cooled to room temperature. Resulting polymer was dissolved in chloroform and precipitated in excess of methanol while being agitated. Precipitated material was filtered, washed with methanol and dried under reduced pressure.

5.2.3 Characterizations

Fourier transform infrared spectroscopy (FTIR) analysis was done with a Perkin Elmer Spotlight 200 (Waltham, MA) apparatus equipped with a Germanium ATR crystal. Measurements were performed with a resolution of 4 cm^{-1} and accumulation of 32 scans at wavelength range of 650-4000 cm^{-1} and room temperature. The specific optical rotation [α] of PLLAs was measured in chloroform at a concentration of 1g/dL at 21.4 ^{o}C using a Jasco P-1020 Polarimeter. ^{1}H-NMR analysis was performed by a Bruker AV500 spectrometer operating at 700 MHz. A 30 degree pulse, an acquisition time of 2.6 second, a recycling delay of 2 second were used for all experiments. All spectra were collected at 25 ^{o}C. Molecular weight and molecular weight distribution of samples were obtained by performing size exclusion chromatography (SEC) using a Viscotek GPCmax equipped with Wyatt DAWN light scattering system operating at 25 ^{o}C and flow rate of 1 $mL.min^{-1}$. The eluant was THF stabilized by 250 ppm BHT and 0.049 mLg^{-1} was chosen as the value of refractive index increment ($\frac{dn}{dc}$) (Podzimek, 2011). Diffrential scaning calorimetry (DSC) was conducted using a TA instrument DSC Q 1000. For dynamic tests, thermal history was removed by keeping the samples at 200 ^{o}C for 3 min. Subsequently, specimens were cooled to 25 °C at a rate of 10 $°C.min^{-1}$ to observe their crystallization behavior and heated back to 200 ^{o}C to record their cold crystallization. For isothermal tests, after removing thermal history at 200 ^{o}C, samples were rapidly cooled to 120 ^{o}C and isothermally crystallized. OPTIPHOT-2 optical microscope equipped with a programmable hot stage (Mettler FP82HT) was employed to observe the crystallization behavior of synthesized polymers and compare it

with the behavior of a commercial grade PLA. Thin films, prepared by hot press, were first melted completely at 200 ^{o}C for 3 min to remove their thermal history. Afterwards, for non-isothermal observations, specimens were cooled at a rate of 10 ^{o}C.min^{-1} to room temperature while for isothermal characterization, they were kept at 140 ^{o}C for 10 min. Elongational viscosity measurements were performed by an ARES rheometer (TA Instruments) equipped with a Sentmanat Extension Rheometer (SER) universal testing platform from Xpansion Instruments. Materials were dried overnight in a vacuum oven at 80 ^{o}C prior to molding. Rectangular specimens (20×13×0.7 mm) were prepared by compression molding, using a hydraulic press, at 190 ^{o}C. Sample preparation and extensional characterization were done under nitrogen atmosphere to minimize degradation. Elongational tests were performed at 170 ^{o}C.

5.3 Results and discussion

5.3.1 Polymerization

Our goal was to compare the synthesized polymers with the commercial grade linear PLA at similar molecular weights and also to have a branch length well above the critical length for entanglement, which is suggested to be about 9000 g/mol by Dorgan et al. (Dorgan et al., 2005-a) Accordingly, for star and comb architecture initiators, there is a range of acceptable functionalities. Thus, four-arm star and five-arm comb like structures were selected. Figure 5.1 shows the chemical structure of monomer, linear PLA, initiator molecules and the schematic structure of PLA expected from each one. Pentaerythritol and triglycerol have multiple hydroxyl groups and therefore the growth of PLA branches from them results in star-shaped and comb-like molecules, respectively.

lactide hydroxylic initiator Polylactide

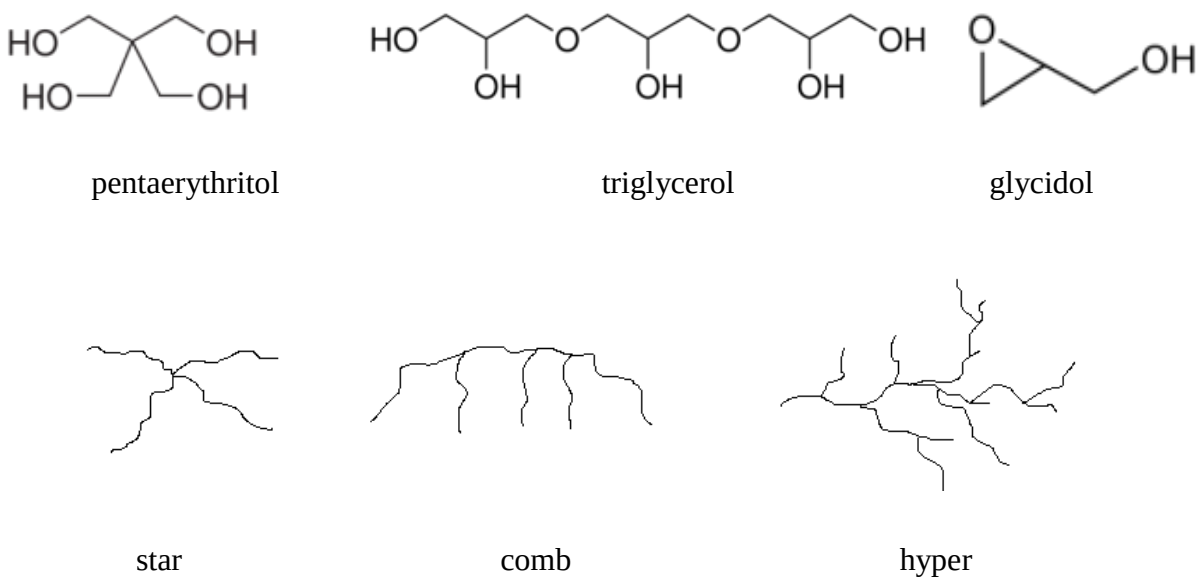

Figure 5.1. Chemical Structure of Polymerization Components and Schematic Structure of Final Polymers

On the other hand, glycidol is a cyclic molecule bearing a single hydroxyl group; therefore, simultaneous incorporation of glycidol in PLA chain by opening the ring and the growth of PLA from OH group results in a hyper-branched architecture.

Initiator concentration for star and comb like architecture was calculated according to Equation (5.1):

$$[I] = \frac{[lactide]_0}{M_{target}} \times M_{lactide} \times X_c \qquad \textbf{(5.1)}$$

where $[I]$ is the molar concentration of initiator, $[lactide]_0$ is the initial molar concentration of monomer, M_{target} is the desired molecular weight of product, $M_{lactide}$ is the molecular weight of lactide, and f_c is a correction factor equal to the degree of monomer conversion, $f_c = \frac{W_{PLA}}{W_{0,lactide}}$. $W_{0,lactide}$ is the initial weight of the monomer, and W_{PLA} is the weight of the final product.

According to a preliminary test, a conversion of 90% under the applied polymerization conditions was retained for the purposes of initiator concentration calculations (f_c = 0.9). In case of the hyper branched architecture, it was not possible to exactly determine the number of branches since the process is randomly governed. However, based on the results of Pitet et al.,(Pitet et al., 2007) a monomer to initiator ratio of 250 led to a M_n of 101,000 $gmol^{-1}$.

Therefore, this initiator concentration was selected to achieve the desired molecular weight. For all synthesis the catalyst concentration was fixed to 0.03 mol.%, which is in the range of optimum concentration to efficiently polymerize lactide and avoid acceleration of degradation in future processing steps due to presence of residual catalyst.(Hyon et al., 1997)

5.3.2 Polymer Characterization

All the synthesized polymers were characterized by FTIR technique and results were compared to the linear commercial PLA to assess the extent of the polymerization reaction. FTIR specta are illustrated in Figure 5.2, showing similar characteristic peaks.

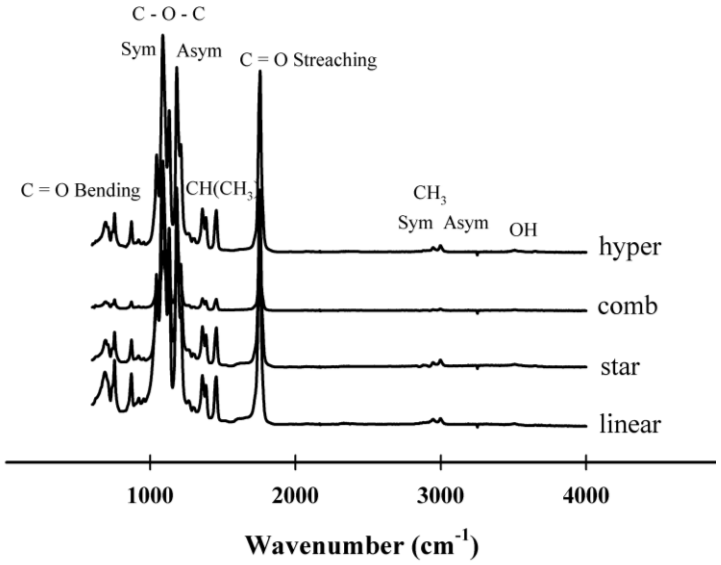

Figure 5.2. FTIR Spectra of Polylactides

The characteristic absorption band at 3520 cm^{-1} is due to the –OH stretching; (Idage et al., 2010) a very strong absorption peak at 1758~1763 cm^{-1} corresponds to the C=O stretching vibration and the absorption peak at 757cm^{-1} is associated with the –C=O bending vibration. The absorption peaks at 2996 and 2946 cm^{-1} are attributed to the asymmetric and symmetric $–CH_3$ vibration. The absorptions at 1452~1457 cm^{-1} and 1382~1389 cm^{-1} reveal the presence of $–CH(CH_3)$ (Fraschini et al., 2005; Ling et al., 2009), while the weak peak at 2879 cm^{-1} is associated with the –CH stretching vibration. The peaks at 1186~1245 cm^{-1} and 1095~1130 cm^{-1} are due to the asymmetric and symmetric –C–O–C– vibration, and all of those FTIR characteristic peaks confirm that the PLA was successfully produced. A very weak signal at

932~934 cm^{-1}, which is typical of –CH bond on the ring of lactide, is observed, indicating the presence of a small amount of residual monomer in the sample.

The specific optical rotation [α] was measured for all polymers. The value of [α] was equal to -154^{o} for synthesized PLLAs and -151^{o} for commercial PLLA.

Molecular weight and molecular weight distribution are known as the main characteristics of polymers, since they have significant effects on different properties. Size exclusion chromatography was employed to compare molecular weight characteristics of the synthesized polymers with commercial linear one. SEC signals are plotted versus the elution volume in Figure 5.3. It is clear that all the polymers are in the same range of molecular weight and possess similar distributions. Therefore, it is possible to compare the effect of chain structure on their properties.

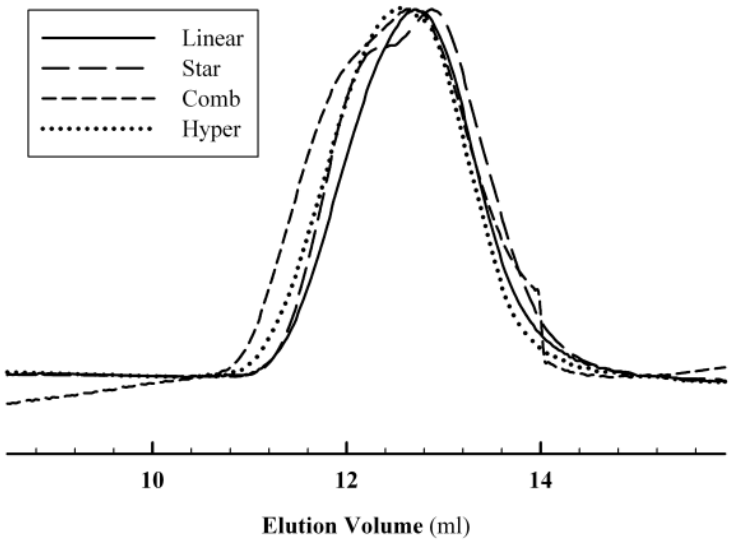

Figure 5.3. SEC Signal versus Elution Volume for PLAs

Table 5.1 reports the feed compositions for the synthesized polymers as well as the SEC data in more details. Synthesized polymers have a narrow molecular weight distribution, similar to the commercial linear grade which is due to the living nature of the ring opening polymerization of lactide. A little higher polydispersity index (PDI) for the comb-like structure might be the result of steric hindrance of close hydroxyl groups on each other. Moreover, the

average molecular weight of each arm in star and comb structure was obtained by dividing M_n to the functionality of their initiator. However, it is not possible to determine this parameter for hyper-branched PLA due to the dual role of glycidol in chain initiation and branching.

Table 5.1. Feed Compositions and Molecular Weight of Samples

Designation	Monomer	Initiator	$\frac{\text{Initiator}}{\text{Monomer}}$ [a]	Catalyst	$\frac{\text{Catayst}}{\text{Initiator}}$ [a]	M_n [b]	PDI	Average branch molecular weight [b]
Linear	–	–	–	–	–	75,000	1.35	–
Star	L-lactide	pentaerythritol	0.1	St $(Oct)_2$	0.03	89,000	1.38	22,250
Comb	L-lactide	triglycerol	0.1	St $(Oct)_2$	0.03	85,000	1.74	17,000
Hyper	L-lactide	glycidol	0.4	St $(Oct)_2$	0.03	89,000	1.39	–

[a] mol%. [b] $gmol^{-1}$

^{1}H-NMR was employed to explore chain structure of PLAs and determine the real branch number. NMR spectrum for linear PLA is shown in Figure 5.4. Two characteristic peaks for PLA chains are methine proton of the end group next to terminal hydroxyl group at 4.38 ppm (A) and the methine proton of the repeating unit at 5.18 ppm (B). In the case of branched PLAs, characteristic peaks of initiators can be used to determine the real number of functional groups participating in the ring opening polymerization reaction. The region of interest is identified with a dashed oval and magnified NMR spectra for synthesized branched PLAs in this region are shown in Figure 5.4 as well.

For star PLA synthesized with pentaerythritol, presence of initiator in the polymer structure and initiation of the reaction from hydroxyl groups was confirmed by observing the peaks at 4.1 and 4.2 ppm associated to methylene protons neighboring the reacted OH. Also absence of the peak at 3.5 ppm for the same group when it is connected to non-reacted OH group suggested that all OH groups participated in the ring opening reaction. Therefore, the 4-arm star shaped structure was successfully produced.

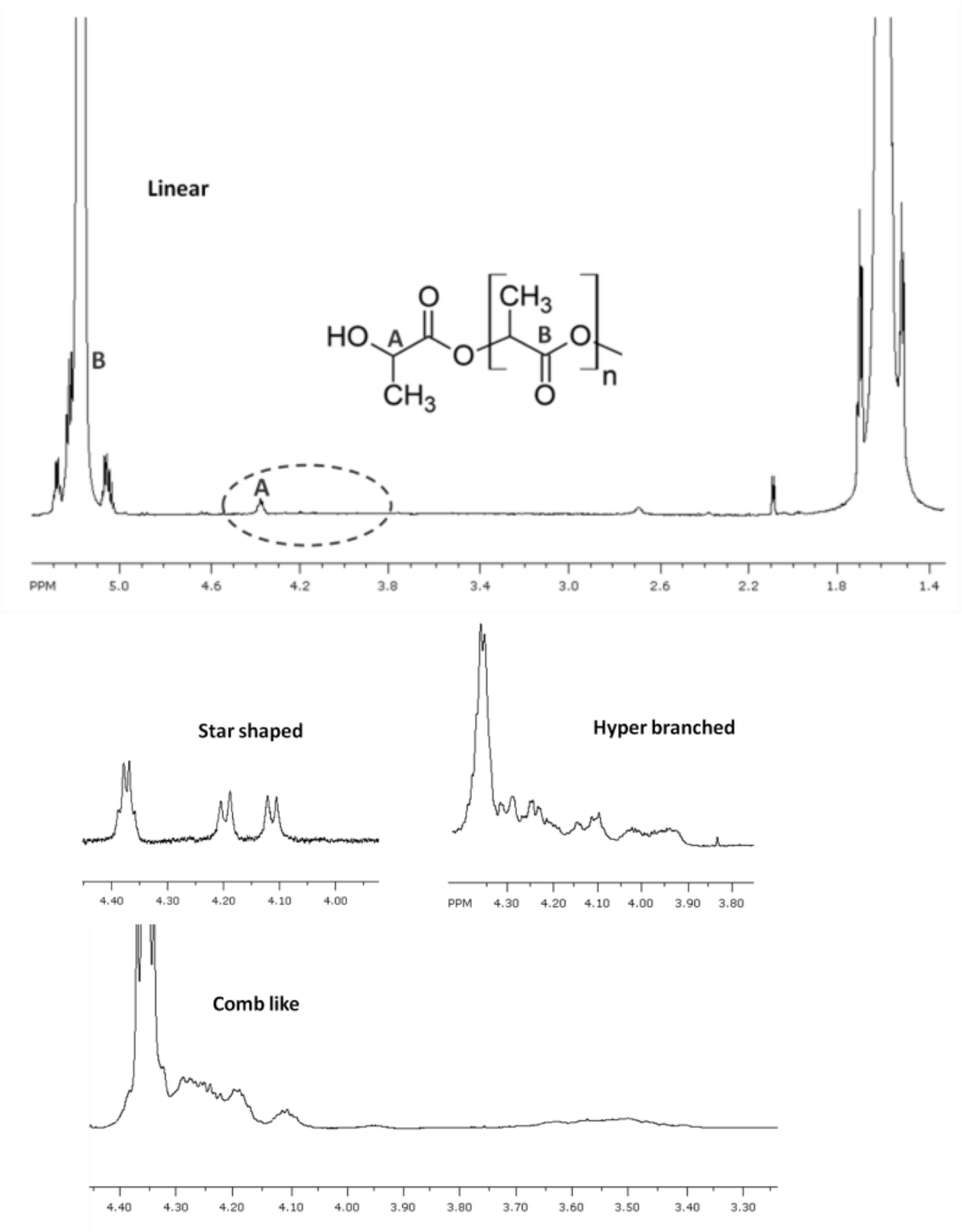

Figure 5.4. HNMR spectra of PLAs with different chain architectures

For comb like PLA, characteristic peaks for methylene and methine protons adjacent to non-reacted and reacted OH groups appear at 3.5 and 4.1-4.3 ppm, respectively. A very low intensity peak appeared at 3.5 ppm, showing that some hydroxyl groups remained unreacted in the system. Due to the overlap of the peaks for methine proton of the end group next to terminal OH with methylene and methine protons neighboring the reacted groups of the initiator at 4.3 ppm, it was not possible to calculate the exact number of arms. However, it was approximated by comparing peak integrals associated to non reacted and reacted groups. A 94.6% participation of OH groups in ring opening reaction was estimated which is equal to an average branch number of 4.73 for each molecule. The wider molecular weight distribution for comb PLA may also be caused by this unequal share of reacted groups between polymer molecules. Finally, for hyper branched PLA, as a result of the complex structure of the molecule it was not possible to determine the real branch number. Initiator also acted as a comonomer and was distributed in the chain, making junctions for new branches. In terms of the NMR spectrum shape, this was translated into a high number of broad overlapping peaks, indirectly proving the formation of hyper branched structure.

5.3.3 Properties of Branched PLAs

Variation in the chain architecture of polymers can lead to a remarkable change in their properties. (Ajji et al., 2003; Tabatabaei et al., 2009; Mihai et al., 2010) Comparing the properties of the synthesized PLAs with a linear grade is a good approach to prove their branched structure.

Since crystallization behavior and rheological properties in extensional mode are sensitive to chain structure variations, these aspects are chosen for further investigation. In addition, it is interesting to see if branched structure can improve these two challenging aspects of PLA.

5.3.3.1 Crystallization

Differential scanning calorimetry was employed to compare the crystallization behavior of PLA samples in a non-isothermal procedure. Figure 5.5 presents the DSC thermograms of commercial and synthesized PLAs at a cooling rate of 10 $^{o}C.min^{-1}$. Results have been shifted along the vertical axis for the sake of clarification. Commercial linear PLA represented by a solid

line curve did not reveal a crystallization peak, in agreement with its slow crystallization. However, synthesized polymers were crystallized with crystallization peak temperatures around 102 ^{o}C and crystallization enthalpy varying from 6.6 to 9.8 J/g, corresponding to 7-11% crystallinity based on 93 J/g melting enthalpy of 100% crystalline PLA.(Fischer et al., 1973) This clearly shows a remarkable difference and improvement in crystallization behavior of the synthesized PLAs as compared to commercial linear one.

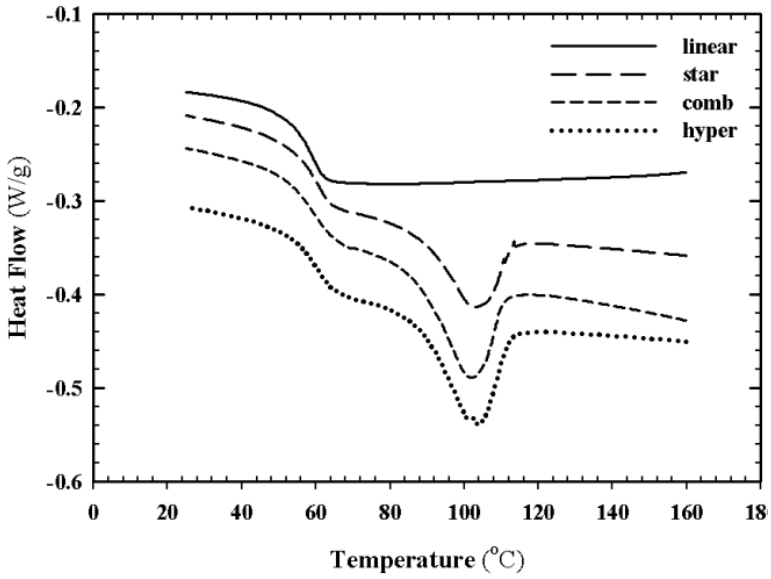

Figure 5.5. DSC Thermogram of PLA Samples at a Cooling Rate of 10 ^{o}C/min from the Melt

In addition, a subsequent heating cycle was conducted at the same rate to observe the cold crystallization of linear and branched PLAs. Data are summarized in Table 5.2. For linear PLLA a very small cold crystallization peak with an enthalpy of about 2 J.g^{-1} at peak temperature (T_{cc}) equal to 140 ^{o}C confirmed the slow crystallization. However, larger cold crystallization peaks with enthalpies of 10-13.5 J.g^{-1} were obtained at about 30 ^{o}C lower than T_{cc} of linear PLA. Thus, branched PLAs possessed better cold crystallization properties. Significant reduction in T_{cc} strongly suggests the nucleating effect caused by branching. T_g was about 58 ^{o}C for linear PLA and synthesized branched structures showed a slight increase in T_g up to 2 ^{o}C. Both decrease and increase in T_g between star shaped and linear PLA were reported by Sakamoto and Tsuji(Sakamoto and Tsuji, 2013). By changing chain structure from linear to branched, two parameters that influence glass transition temperature are altered. One is the segmental mobility

which decreases by branching since chains are more compact, restricted in motion and more entangled. The other is free volume which increases due to more flexible chain ends and this contributes to a decrease in T_g. Therefore, T_g may decrease or increase depending on which of the two counteracting parameters prevail. However, faster crystallization of synthesized branched structures relative to linear PLA implies that the slight increase in T_g was not detrimental for crystallization. Finally, total crystallinity obtained from the sum of crystallization upon cooling and heating was another proof of enhanced crystallization behavior by chain branching. For linear PLA a total crystallinity of 2.5% was obtained while branched PLAs crystallized about 10 times more.

Table 5.2. Thermal properties of PLA samples in dynamic mode at 10 ^{o}C.min^{-1}

Sample	**nonisothermal** (10 ^{o}C/min**)**					
	T_c (^{o}C)	ΔH_c (J/g)	T_g (^{o}C)	T_{cc} (^{o}C)	ΔH_{cc} (J/g)	X_c (%)
Linear	-	-	58.6	140.4	1.94	2.5
Star	102.5	6.6	60.4	112.7	13.5	24.1
Comb	101.5	8.9	59.1	111.7	10.1	22.2
Hyper	103.5	9.8	60.7	111.2	11.9	25.7

As mentioned earlier, branching had a positive effect on crystal nucleation. Also, the main difference between branched architectures was their branch content. Since nucleation is the controlling parameter at high temperatures, it was not possible to differentiate between branched structures in dynamic DSC at the applied conditions. Consequently, isothermal crystallization tests were conducted at 120 ^{o}C to better illustrate the difference between chain structures. Heat flow data versus time are plotted in Figure 5.6 to display the crystallization peaks obtained at 120 ^{o}C.

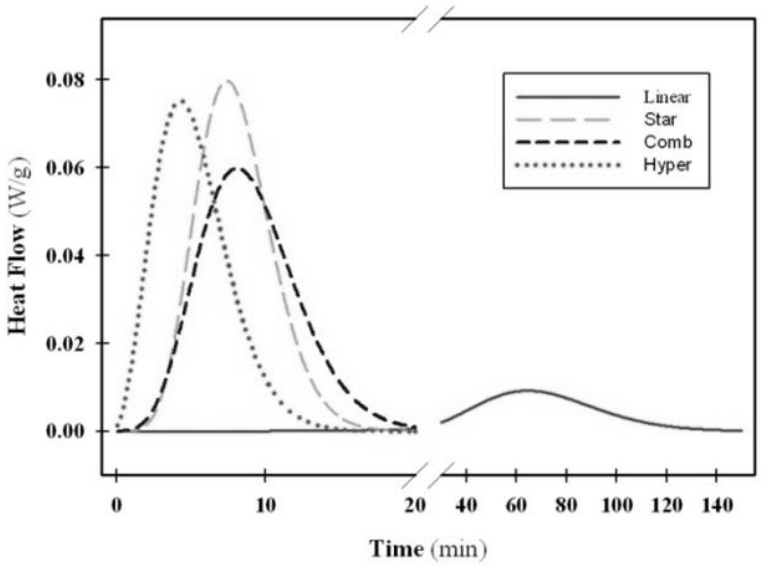

Figure 5.6. Crystallization peaks of PLAs at 120 °C

Linear PLA revealed a broad peak as expected from its slow crystallization at high temperatures. Branched PLAs on the other hand showed much narrower peaks. Among those, crystallization peak for hyper branched PLA started earlier which is a sign for better nucleation.

To investigate the effect of chain architecture on isothermal crystallization kinetics, crystallization fraction was calculated as a function of time, α(t), by integrating the peaks at time *t* divided by the total peak area. Kinetic curves attained are shown in Figure 5.7. Avrami model expressed with the following equation was used to fit the kinetic curves:

$$\alpha(t) = 1 - \exp\left[-(kt)^n\right] \qquad \textbf{(5.2)}$$

where *n* is the Avrami exponent and *k* is a rate constant.

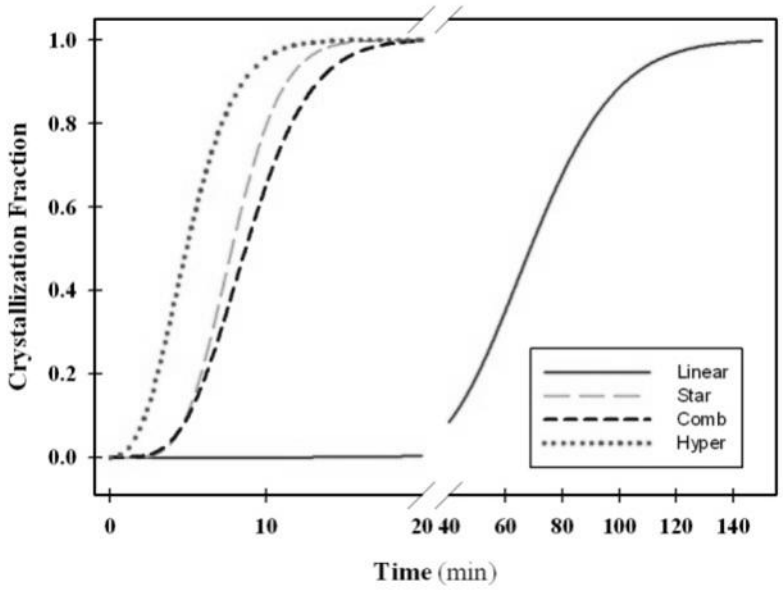

Figure 5.7. Crystallization fraction as a function of time at 120 °C

Avrami constants can be calculated by rearranging Equation (7.3) and plotting ln[-ln[1-$\alpha(t)$]] versus ln(t). n, ln(k) and regression coefficient (R^2) obtained from this procedure are summarized in Table 5.3.

From these data it is clear that rate constant is highest for hyper branched PLA followed by comb and star PLA. Additionally, Avrami exponent reduced from about 3 for linear PLA to 2.3 for hyper branched one indicating a change in nucleation mechanism.

Table 5.3. Avrami constants and crystallization half-times of samples

Sample	*isothermal at 120 °C*			
	n	**ln(*k*)**	**R^2**	**$t_{½}$ (min)**
Linear	2.99	-12.56	0.998	68.6
Star	3.6	-7.78	0.998	7.8
Comb	3.08	-7.06	0.998	8.7
Hyper	2.29	-4.02	0.999	4.9

Another important parameter is crystallization half time ($t_{1/2}$) or the time required to reach a crystallization degree of 50%. This parameter was calculated from Figure 5.7 and given in Table 5.3 for the four structures. Linear PLA had the longest $t_{1/2}$ about 69 min, while branched architectures resulted in one order of magnitude decrease in $t_{1/2}$. Hyper branched PLA had the

smallest half time equal to 5 min and for star and comb structures $t_{1/2}$ was longer by 3 to 4 min. These results clearly demonstrated the difference in crystallization behavior of various branched architectures.

Optical microscopy was utilized to explore the crystalline morphology of samples in a similar thermal history to further investigate the origin of the difference in crystallization behavior and have a better understanding of the effect of branched structure on this aspect. Images shown in Figure 5.8 were captured in a cooling procedure at a rate of 10 $^{o}C.min^{-1}$ from the melt. At 115 ^{o}C the first evidence of crystallization for the linear PLA was observed, which was not detectable in DSC experiments as a consequence of the lower sensitivity of the technique. Thus, for the synthesized polymers, this temperature was chosen for comparing the crystalline morphology. Star-shaped and comb-like polymers show higher spherulite density as compared to linear one. This effect is much more significant in case of hyper branched PLA where the image is covered completely with very small spherulites. A similar effect has been reported when a heterogeneous nucleating agent is added to PLA (Pan et al., 2009). To make sure that the observed difference between the commercial linear PLA and the synthesized ones does not originate from an impurity introduced into the system during polymerization and is only related to the chain architecture, a linear PLA was synthesized under the abovementioned polymerization conditions using 1,3-butanediol as initiator. Compared to the commercial PLA, the synthesized linear structure resulted in even lower spherulite density.

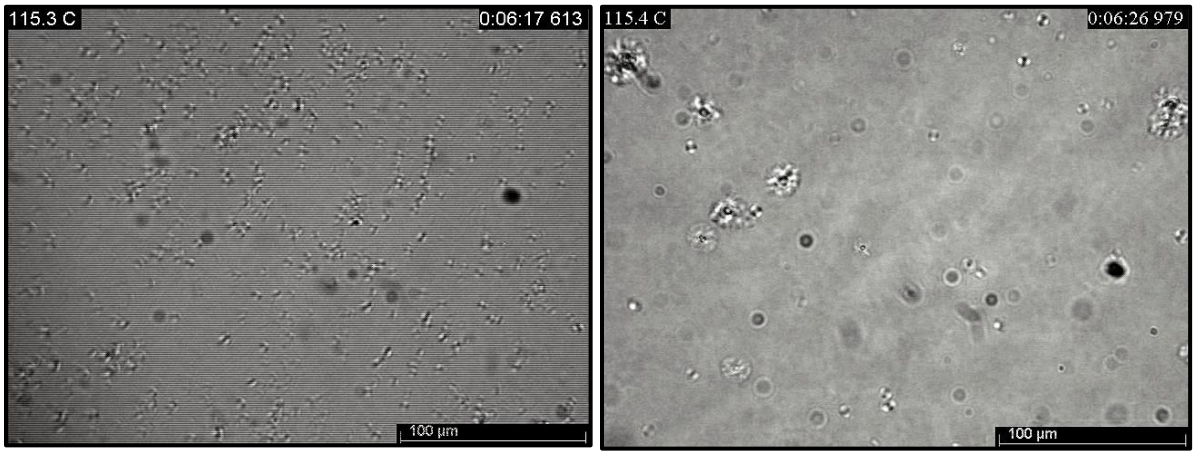

(a) **(b)**

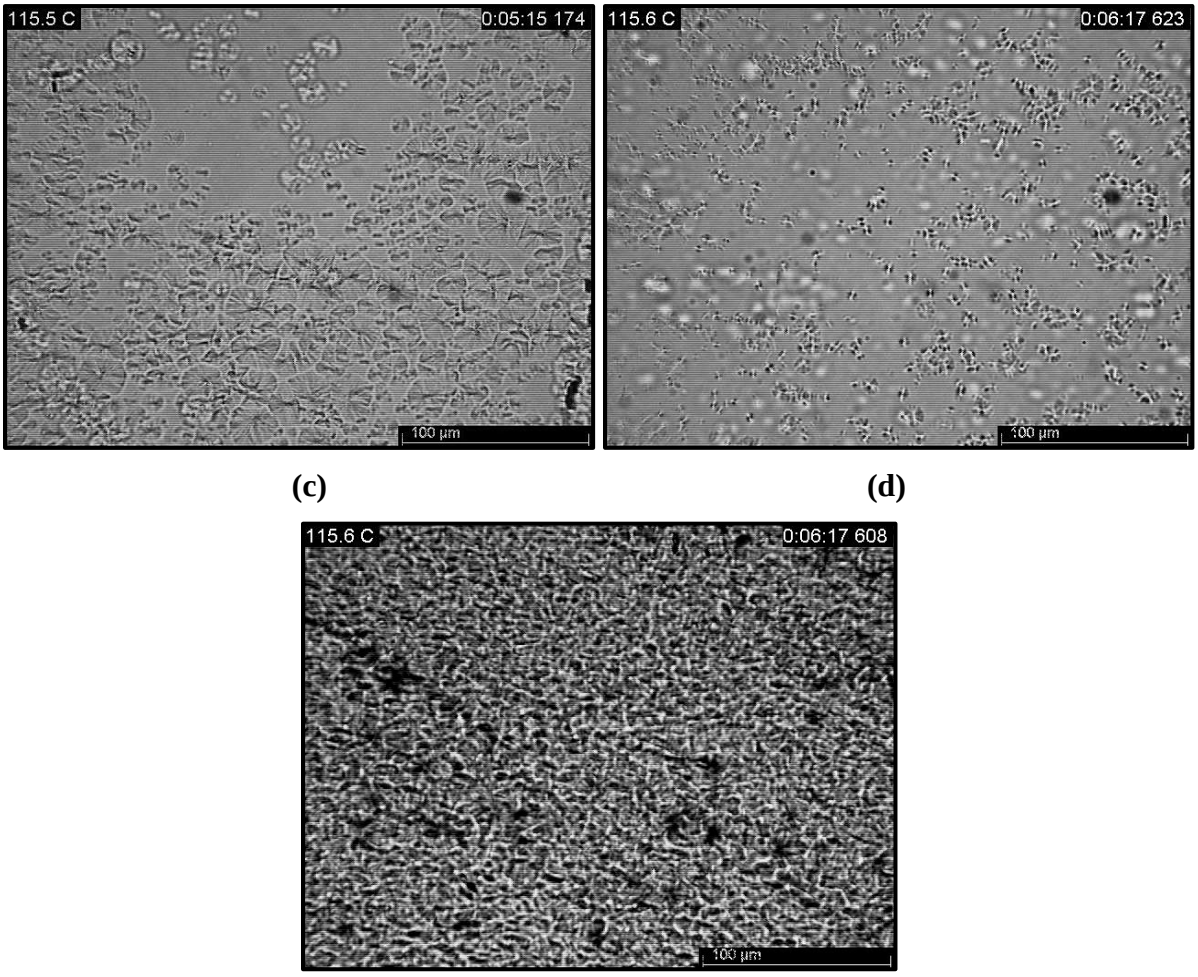

Figure 5.8. Optical microscopy micrographs in non-isothermal mode with cooling rate of 10 ^{o}C/min; a) commercial linear, b) synthesized linear, c) star, d) comb, and e) hyper; scale bar is equal to 100 µm

Effect of branching on PLA crystallization behavior was further investigated in isothermal mode and the results are presented in Figure 5.9. Since increasing crystallization temperature has a negative effect on crystal nucleation, to confirm the nucleation role of branched structures, a high temperature was selected at which neat linear PLA has a very low spherulite density (Tsuji et al., 2006; Yasuniwa et al., 2006). After 10 min isothermal crystallization at 140 ^{o}C, commercial linear PLA (Figure 5.9, a)) hardly shows any crystallization. Synthesized linear one also showed a similar spherulite density (Figure 5.9, b)). On the contrary, all the branched PLAs developed spherulites, the hyper branched PLA with the highest spherulite density as expected, followed by the comb-like and star architectures, in agreement with the amount of branching

points. Increased spherulite density by branching in optical microscopy images also confirms DSC results about the crystal nucleation effect of these structures. Two mechanisms may be proposed for this effect, increased number of polar terminal groups and their association or immobilization of chain segments by branching points. First mechanism is less probable since terminal groups have more mobility than chain segments closer to branching points and are usually considered as impurities that cannot participate in crystallization process. In addition, organic salts such as sodium stearate(Li and Huneault, 2007) and sodium benzoate(Penco et al., 2011) have been used for PLA to produce ionic end groups with stronger interactions to enhance nucleation; but no remarkable enhancement of crystallization was observed. Therefore, it is suggested that reduced segmental mobility caused by branching points is the main reason for increased crystal nucleation in branched structures.

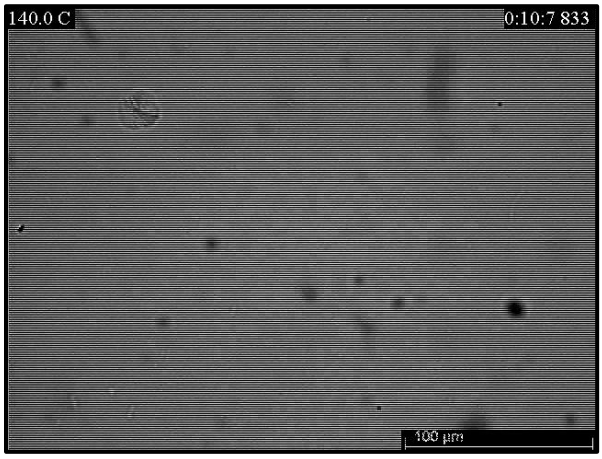

(a)

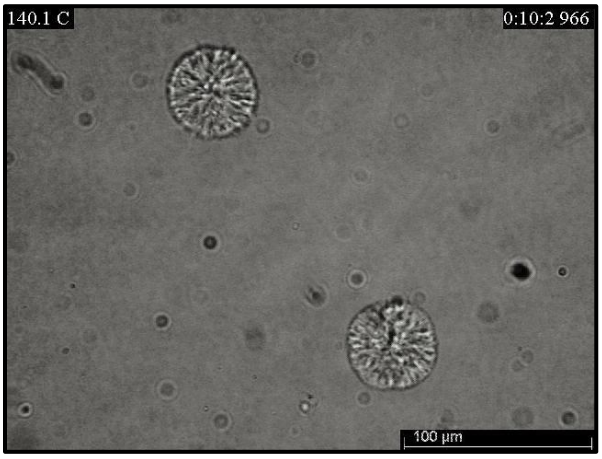

(b)

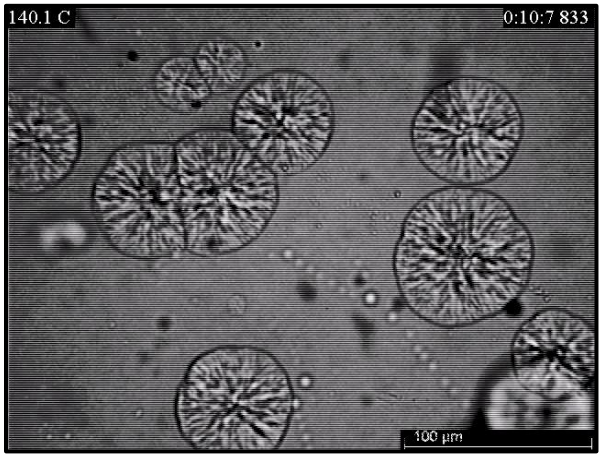

(c)

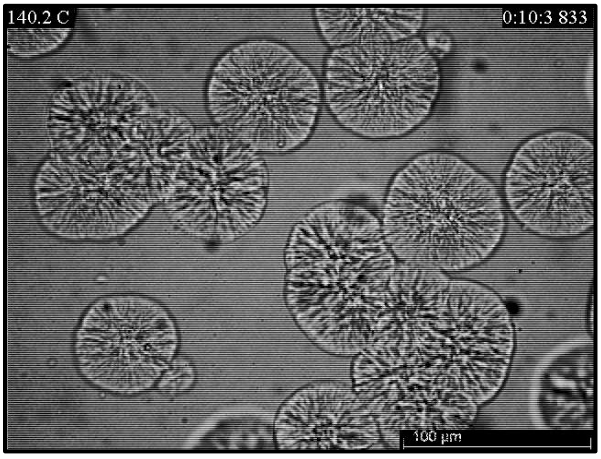

(d)

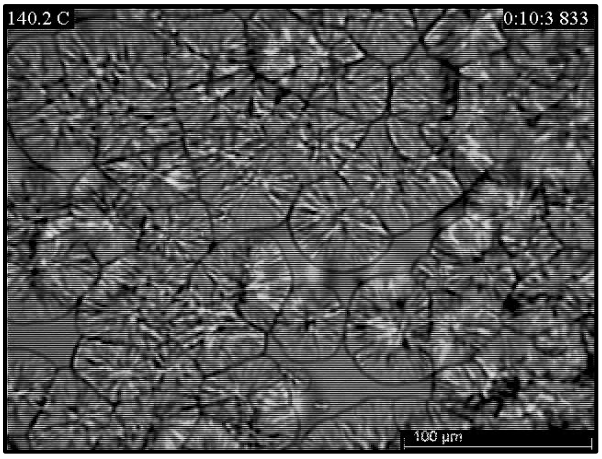

(e)

Figure 5.9. Optical microscopy micrographs in isothermal mode at 140 °C; a) commercial linear, b) synthesized linear, c) star, d) comb, and e) hyper; scale bar is equal to 100 µm

5.3.3.2 Extensional melt properties

Among the different rheological properties, the time dependent elongational viscosity, $\eta_E^+(t, \dot{\varepsilon}_0)$, is the most sensitive parameter to the chain architecture. In general, elongational viscosity initially increases with time until a plateau is reached. Then, depending on the polymer structure, further extension may lead to the failure of the sample or a sudden increase in viscosity, known as strain hardening behavior. The latter has been observed for some branched polymers, (Wagner et al., 2000; Tabatabaei et al., 2009; Mihai et al., 2010) and is a result of a lower disentanglement rate of their branched chains as compared to deformation rate. Therefore, elongational rheology is a powerful technique to show the presence of branched chains in a polymer structure. Elongational viscosities of the synthesized branched PLAs were compared with the linear one at a Hencky strain rate of 1 s^{-1}. For lower strain rates, data were noisy due to the transducer sensitivity limitation. Results are presented in Figure 5.10 and shifted for better visualization purpose. From this figure it is clear that there is a significant difference between linear and branched polymers. Commercial PLA, presented by circle in the graph, reached a viscosity plateau and failed just after a small increase at the end. This behavior is consistent with the linear chain architecture of PLA. However, synthesized branched PLAs revealed a pronounced strain hardening behavior after the plateau region which is an indication of long chain branching.

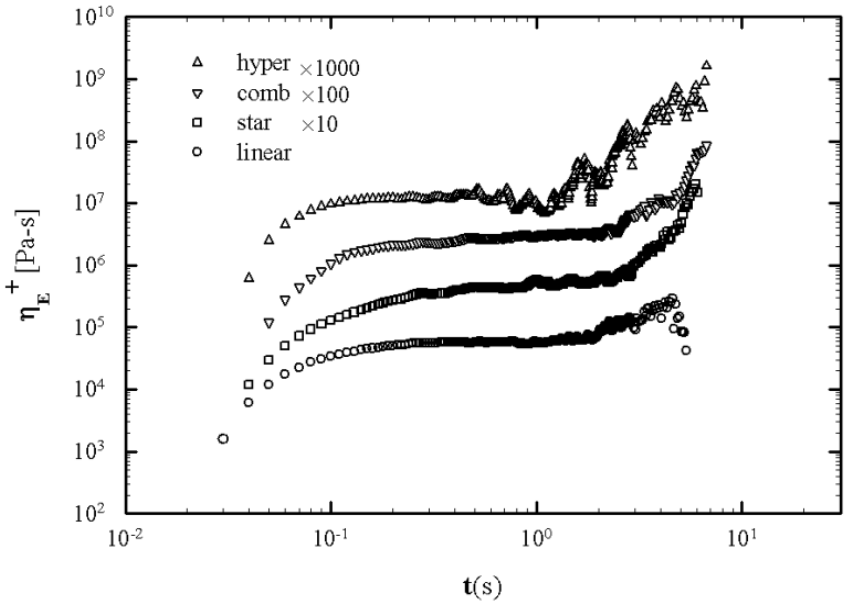

Figure 5.10. Elongational viscosity of PLA samples at 170 ^{o}C and Hencky starin rate of 1 s^{-1}

5.4 Conclusions

Branched PLAs were synthesized by different initiators through the ring opening polymerization of lactide. Based on the molecular structure of the initiators, resulting polymers were star-shaped, comb-like and hyper-branched architectures. Synthesized polymers were characterized using FTIR, GPC and NMR analyses. Accordingly, polylactides with narrow molecular weight distributions and different architectures were produced. Their molecular weights were in the range of a commercial linear grade which was used as a reference in this study. Crystallization and elongational rheology of the synthesized PLAs were compared to the commercial linear PLA. DSC thermograms obtained in dynamic mode revealed a noticeable difference in the crystallization from the melt and cold crystallization behavior of branched polylactides compared to linear one. In addition, isothermal crystallization at 120 ^{o}C revealed the difference between crystallization kinetics of synthesized branched architectures with fastest rate for hyper branched PLA. Further investigation on crystallization of the specimens by optical microscopy technique in isothermal and non-isothermal modes showed that the presence of branching points directly influenced the spherulite density by increasing the nucleation sites and improved significantly the crystallization behavior of PLA. However, linear PLAs (commercial and synthesized) did not show a considerable crystallization in similar conditions. Effect of branched structure was also obvious in elongational rheology. While linear PLA failed after a

viscosity plateau, branched polylactides exhibited a strain hardening behavior. Based on these results it can be concluded that branching is a practical approach to improve the crystallization and rheological properties of polylactide.

CHAPTER 6. ARTICLE 2: EFFECT OF CHEMICAL AND PHYSICAL BRANCHING ON RHEOLOGICAL BEHAVIOR OF POLYLACTIDE

Sahar Nouri, Charles Dubois, Pierre G. Lafleur

CREPEC, Chemical Engineering Department, Ecole Polytechnique, C.P. 6079, Succ. Centre ville, Montreal, QC, H3C 3A7 Canada

ABSTRACT This study was aimed at improving the process rheology of polylactide (PLA) melts by means of two strategies. In the first approach PLAs of different branched structures, i.e. star shaped, comb like and hyper branched were synthesized and blended with a linear grade analog. Shear and extensional flow rheometry tests were performed on pure materials and their blends to evaluate their rheological properties. It was shown that the presence of branched poly(L-lactide) (PLLA) increased the shear thinning, shear and extensional viscosity and elastic modulus of linear PLLA at the same time; the star shaped PLLA providing the most significant change. In the second strategy, poly(D-lactides) (PDLA) with similar molecular architectures were synthesized to have a double branching effect. In addition to the presence of branched architecture, physical cross-links due to the stereocomplex formation exist between PLLA and PDLA chains. Based on the rheological characterizations in shear and extensional mode, a greater improvement in PLA melt rheological properties was observed for blends containing stereocomplex structure as compared to linear/branched enantiopure blends.

6.1 Introduction

Using bio-based polymers for commodity applications has become a popular trend in recent years in search for more sustainable production, lesser environmental footprint and reduced dependency on fossil based polymers. Among those is poly(lactide) or PLA, a thermoplastic polyester with favorable mechanical, optical and barrier properties, which make it well-suited for packaging applications. Solution and melt rheological properties of commercial PLA with linear structure are studied in the literature to understand its fundamental chain properties and to determine processing conditions (Grijpma et al., 1994; Cooper-White and

Mackay, 1999; Dorgan et al., 1999; Palade et al., 2001; Dorgan et al., 2005-a; Dorgan et al., 2005-b; Othman et al., 2011). PLA zero-shear viscosity is reported to be proportional to $M_w^{3.4}$ above the critical molecular weight for entanglement (M_c); and M_c is estimated between 9000 to 16000 g/mol depending on stereochemistry, temperature and polydispersity. One major drawback of PLA is its low melt strength which is not sufficient for film blowing applications where melt elasticity is required to preserve dimensions and stability (Tweed, 2006; Mallet et al., 2014). There is limited literature on extensional flow characterization of PLA. Few studies have shown the lack of strain hardening behavior or very slight viscosity increase in extensional flow, confirming PLA's low melt strength (Palade et al., 2001; Sinha Ray and Okamoto, 2003; Yamane et al., 2004; Othman et al., 2011). Blending polymers is a common and straightforward means to achieve better properties although compatibility between the components is often an issue. In addition, in the case of PLA, the choice of modifying polymers is further narrowed if it is desired to keep the final product fully bio-based or degradable. The most important ones from a commercial point of view are thermoplastic starch (TPS), poly(butylenes adipate-co-terephthalate) (PBAT), poly(butylene succinate-co-adipate) (PBSA), poly(3-hydroxybutyrate-co-3-hydroxyvalerate) (PHBV) and poly(ε-caprolactone) (PCL) (Jiang et al., 2006; Sarazin et al., 2008; Gerard and Budtova, 2012; Gui et al., 2012). Another approach that has been put forward to improve PLA melt rheological properties is to alter its chain structure since the low melt strength is associated to the linear structure of PLA chains. One way of doing so is the reactive modification of linear PLA. Free radical branching in the presence of peroxides (Sodergard et al., 1995; Carlson et al., 1998; Takamura et al., 2008; Dean et al., 2012; Takamura et al., 2012) or by beam irradiation (Shin et al., 2010; Wang et al., 2011; Xu et al., 2014) have been employed to induce branching points and increase PLA molecular weight. In the same spirit, the addition of polyfunctional chain extenders to PLA can also lead to branching. Polyisocyanates were commonly used for PLA chain extension (Kylma et al., 2001; Tuominen et al., 2002; Di et al., 2005; Ren et al., 2006; Gu et al., 2008) owing to the presence of terminal hydroxyl groups on the polymer chains; however, due to their toxicity, the trend is shifting towards the use of other small molecules such as tris (nonylphenyl) phosphate (Lehermeier and Dorgan, 2001; Dorgan et al., 2005-a) and multifunctional epoxy-based chain extenders (Pilla et al., 2009; Mihai et al., 2010; Corre et al., 2011; Li and Huneault, 2011; Zhang et al., 2012; Cailloux et al., 2014). However,

these modifications are limited as cross-linking and gelation may occur if the process is not carefully controlled.

It is also possible to directly synthesize branched PLA with a variety of chain structures depending on the polymerization precursors. Initiating the ring-opening polymerization reaction of lactide with a multifunctional branched initiator leads to a PLA with structure similar to the initiator (Zhao et al., 2002; Hao et al., 2005; Adeli and Haag, 2006; Perry and Shaver, 2011; Zhang et al., 2012). Copolymerization of lactide with cyclic monomers having hydroxyl group on the cycle is another route to synthesize branched PLA (Pitet et al., 2007; Wolf and Frey, 2009). Although direct branched PLA synthesis, hereafter referred to as chemical branching, provides more control over the final chain structure as compared to reactive modification, there is not a considerable number of studies on the effect of defined branched structures on rheological properties of PLA, especially in extensional flow. Dorgan et al. studied the effect of chain structure on melt rheological properties of PLA for four and six arm stars in shear mode (Dorgan et al., 1999).

In addition to the previously indicated chemical modification routes, physical branching of PLA is possible through the co-crystallization of poly(L-lactic acid) or PLLA and poly(D-lactic acid) or PDLA. It is known that mixing of PLLA and PDLA chains generates a special crystalline phase called stereocomplex with a melting point about 50 ^{o}C higher than common PLA α crystal structure (Ikada et al., 1987). Due to the higher melting point of stereocomplex crystal compared to PLA α crystal, stereocomplex crystals remain in PLA melt and act as branching points and free chain segments act as branches on the opposite chains. This approach, hereafter referred to as physical branching, is schematically illustrated in Figure 6.1 in parallel with chemical branching.

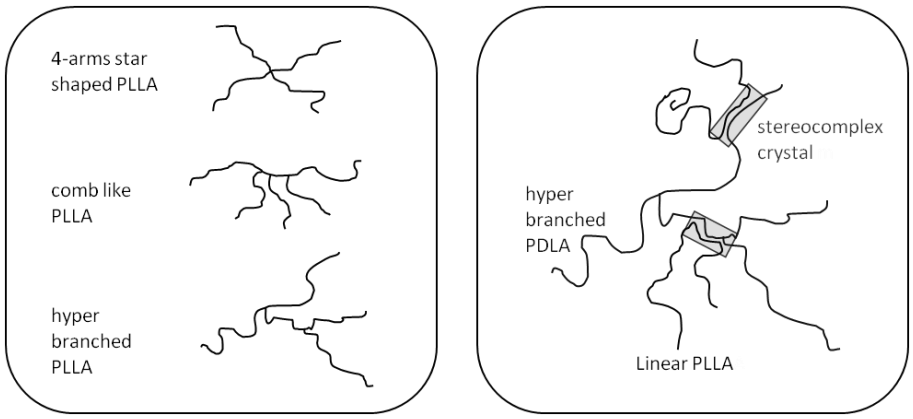

Figure 6.1. Schematic illustration of chemical (left) and physical (right) branching strategies

Due to its high melting point, PLA stereocomplex is widely investigated as a nucleating agent for PLA crystallization (Schmidt and Hillmyer, 2001; Tsuji et al., 2006; Rahman et al., 2009). However, the influence of this structure on PLA rheological properties has not been fully researched, especially in extensional flow rheometry. Few reports exist on the viscosity enhancement of PLLA with linear PDLA having low to intermediate molecular weights (Yamane et al., 2004; Rahman et al., 2009; Ahmed et al., 2014; Saeidlou et al., 2014). Among these studies, only Yamane et al. investigated the role of stereocomplex structure on elongational viscosity of PLA in a squeezing flow.

Accordingly, the aim of this work was to investigate in more details the chemical and physical branching strategies to establish a clear understanding of their effect on the rheological properties of PLA. Particularly, in chemical branching approach, three distinct branched structures were compared with linear PLA in shear and extensional flows. Also the physical branching route had two original aspects. Branched PDLA was used as a rheological modifier of linear PLLA for the first time. Therefore, a double branching strategy was employed. Uniaxial extensional rheometry of PLA stereocomplex system was another original aspect. Application of these strategies resulted in a remarkable increase in extensional viscosity and strain hardening behavior of PLA.

6.2 Experimental

6.2.1 Material

L-lactide and D-lactide were purchased from Purac biochem and used as monomers in the bulk ring-opening polymerization reaction to produce PLLA and PDLA respectively. Tin (II) 2-ethylhexanoate from Aldrich was employed as catalyst whereas pentaerythritol, triglycerol and glycidol initiators were procured from Sigma-Aldrich. Star shaped and comb like architectures were synthesized using pentaerythritol and triglycerol respectively as initiating molecules for the ring-opening polymerization of L-lactide. In addition, a hyper branched PLLA was synthesized through copolymerization of lactide with glycidol. The latter is a cyclic molecule that bears a reactive hydroxyl group. Thus, glycidol is introduced into PLA chain through the ring-opening reaction and can initiate a new branch by ring-opening of lactide via its hydroxyl group. ^{1}H-NMR analysis was done and confirmed the formation of branched structures as expected from the type of initiators and reaction condition. Details of this characterization are reported elsewhere (Nouri et al., 2015). Linear PLA was the semicrystalline grade 4032D from NatureWorks. Molecular weight of the commercial and synthesized PLAs was measured by size exclusion chromatography with a Viscotek GPCmax operating at 25 ^{o}C, using a THF stabilized by 250 ppm BHT as the eluant. Molecular weight data are summarized in Table 6.1

Table 6.1. Molecular Weight of Samples

Structure	**Initiator**	M_n (gmol^{-1})	M_w (gmol^{-1})	**PDI**
Linear	–	75,000	101,000	1.35
Star	pentaerythritol	89,000	123,000	1.38
Comb	triglycerol	85,000	148,000	1.74
Hyper	glycidol	89,000	124,000	1.39

6.2.2 Blend preparation

Synthesized and commercial PLAs were dried 12 hr at 80^{o}C before blending. Blends of linear and branched PLA were prepared using a Leistritz ZSE co-rotating twin-screw extruder with 18mm screw diameter and length/diameter of 40. The screw had three mixing zones with 30, 60 and 90^{o} elliptical elements in the first mixing zone, 30^{o} elliptical elements in the second mixing zone and 60^{o} elliptical elements in the third mixing zone. Blending was performed at 190

^{o}C and a rotation speed of 100 rpm. Residence time was approximately 3 min. In the case of linear/branched PLLA blends, branched PLLA concentration was successively set at 10, 20 and 30%. For linear PLLA/branched PDLA, blends were prepared with 5, 7 and 10% of branched PDLA.

6.2.3 Characterizations

Prepared blends were dried overnight in a vacuum oven at 80 ^{o}C prior to molding. Rectangular (20×13×0.7 mm) and disk shaped (25 mm diameter, 1 mm thickness) specimens for extensional and shear mode rheometry were prepared by compression molding, using a hydraulic press, at 190 ^{o}C. In case of PLLA/PDLA blends, enough time was given in the mold to produce the stereocomplex structure. Differential scanning calorimetry (DSC) was conducted using a TA instrument DSC Q1000 to confirm the formation of a stereocomplex in the samples. Time sweep tests were performed at the 190 ^{o}C and 1 Hz to evaluate thermal stability of the materials during blending and frequency sweep tests. G′ was stable for more than 20 min which is longer than the time required for blending and frequency sweep tests. This also confirms the adequacy of drying and absence of trasesterification which is considerable at temperatures above 200 ^{o}C (Jamshidi et al., 1988). Uniaxial elongational viscosity measurements were performed by an ARES rheometer (TA Instruments) equipped with a Sentmanat Extension Rheometer (SER) universal testing platform from Xpansion Instruments. Elongational tests were performed at 180 ^{o}C. To compensate the volumetric expansion upon melting in extensional tests, cross section area of the specimens was corrected with the factor $(\rho_s/\rho_m)^{2/3}$ where ρ_s and ρ_m are the solid and melt density, respectively. The following equation proposed by Witzke (Witzke, 1997) was used to estimate melt density at test temperature:

$$\rho\left(\frac{g}{cm^3}\right) = \frac{\rho_{150C}}{1 + \alpha_l(T(\,^{o}\mathrm{C}) - 150)} = \frac{1.1452}{1 + 0.00074(T(\,^{o}\mathrm{C}) - 150)} \qquad \textbf{(6.1)}$$

For samples containing stereocomplex crystals, stereocomplex crystal density was assumed equal to 1.274 g/cm^3 (Okihara et al., 1991) and melt density was corrected depending on the content of stereocomplex crystals. Also start-up tests were done at 180 ^{o}C and shear rate of 0.01 rad/s to determine the limit of linear response for extensional measurements. Frequency sweep tests were performed using an MCR 301 rheometer (Anton Paar) at 190 ^{o}C in a wide

frequency range of 0.1 to 100 rad/s. Initially, linear viscoelastic (LVE) region was determined from elastic modulus data obtained in strain sweep tests at 0.1, 1 and 10 Hz. At a strain of 5%, all materials were in the LVE region. Therefore, this strain amplitude was chosen for frequency sweep tests. Sample preparation and rheological characterization were done under nitrogen atmosphere to minimize degradation.

6.3 Results and discussion

6.3.1 Shear flow rheometry

6.3.1.1 Evaluation of chain architectures

Effect of chain structure on rheological properties of PLA was investigated by performing small amplitude oscillatory shear tests. Figure 6.2 shows the variation of complex viscosity as a function of frequency for PLLA with different chain architectures. Carreau-Yasuda model was fit to the experimental data to calculate zero-shear viscosity. Dashed lines in Figure 6.2 represent this model. It is clear that experimental data fit quite well in this model, except for comb structure which might be due to the shape of the curve at low frequencies. This imposes some uncertainty in the value of calculated zero-shear viscosity. However, it is clear that η_0 for comb structure is between the values calculated for hyper branched and star structures. Linear PLLA showed a zero-shear viscosity of 1960 Pa.s and a long Newtonian plateau typical of polymers having a linear chain structure. On the other hand, branched PLLAs revealed different behaviors. Generally, all branched PLLAs had higher zero-shear viscosities as compared to the linear one. η_0 was equal to 13400, 27300 and 34600 Pa.s for hyper-branched, comb-like and star shaped structures, respectively. Also they showed an intensified shear thinning response compared to the linear PLLA. Among the branched polymers, the shear thinning behavior of star shaped and comb liked PLLA was similar and much more significant than the hyper branched PLLA. Branch length was shorter for the latter, thus chain disentanglement became less significant in comparison to the longer and fewer branches in the case of star and comb like PLLA.

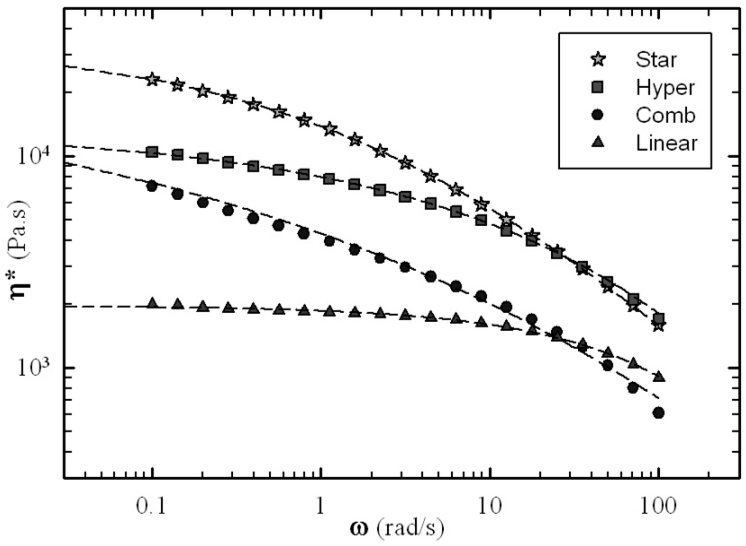

Figure 6.2. Complex viscosity as a function of oscillation frequency for linear and branched PLA with different branch structures

To better demonstrate the effect of structure on zero-shear viscosity and to account for the difference in M_w, η_0 values are compared in Figure 6.3 to predictions calculated relative to η_0 of linear PLA according to the following relationship (open symbols). Above the critical molecular weight for entanglement (M_c):

$$\frac{(\eta_0)_1}{(\eta_0)_2} = \left(\frac{M_{w,1}}{M_{w,2}}\right)^{3.4} \qquad \textbf{(6.2)}$$

which is also valid for PLA (Dorgan et al., 2005-a; Othman et al., 2011).

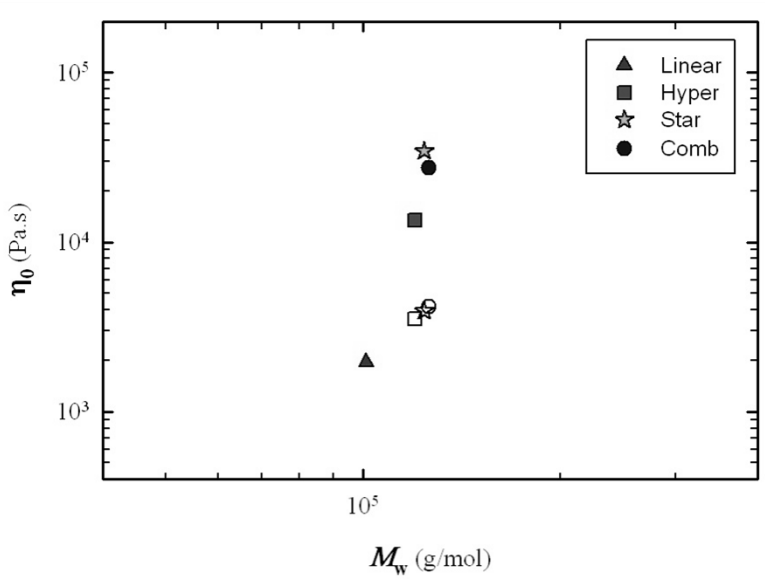

Figure 6.3. The zero shear viscosity as a function of molecular weight for linear and branched PLAs at 190 °C

In general, a deviation from the diagonal line is an indication of a branched structure and can be positive or negative, depending on different parameters such as number of branches, relative location of branches with respect to each other and branch molecular weight. A broader molecular weight distribution could be a possible reason for this deviation. However, since the validity of this relation is shown for linear PLA with PDI up to 2.3 (Palade et al., 2001; Dorgan et al., 2005-a) which is higher than the values reported in this work, the observed difference is more likely caused by the branched structure of synthesized PLAs. Dorgan showed that the positive deviation of η_0 of star PLA from linear chains happened when M_w was higher than a critical value for branch entanglement (M_b) (Dorgan et al., 1999). Also in a theoretical study, a model developed by Larson for predicting the linear viscoelastic properties of branched polymers suggested that at a constant molecular weight above M_c, η_0 increases to a maximum by increasing the branch content and then decreases sharply to below the η_0 of a linear structure (Larson, 2001). A similar trend was also demonstrated for randomly branched polyethylene based on the theory of Janzen and Colby (Janzen and Colby, 1999). The initial increase in η_0 at lower branch contents is due to the significant effect of branching points on chain relaxation while branches are entangled. However, after the maximum in η_0 is reached, higher branch content for a constant molecular weight is equal to shorter branches or backbone and compromise of branching effect by less entangled branches. When the branch content is so high that the branches are not entangled anymore, η_0 becomes lower than the linear structure. Therefore, the positive deviation

shown in Figure 6.3 confirms that for synthesized branched PLAs, the effect of introducing branching point on chain relaxation time and viscosity prevails on the negative effect of reduced molecular span and that branch lengths are well above the entanglement limit. The relative position of data points in Figure 6.3 for branched structures also confirms the importance of branch length decreasing in the following order: Star > Comb> Hyper.

In addition to complex viscosity, elastic modulus is another parameter that can provide an insight regarding the relation between polymer chain structure and its rheological response. Therefore, in Figure 6.4, *G*' is plotted as a function of oscillation frequency for the linear and three branched PLLAs. *G*' was proportional to ω^2 at low frequencies for linear PLLA as indicated with a slope of 2 in the log-log plot. This is known to be valid for polymers with a linear chain structure. On the other hand, star, comb and hyper branched samples revealed higher elastic modulus at low frequency region with a lower slope compared to linear PLLA between 1.03 to 1.39, which is in direct relation to their branched nature. In addition, *G*' for hyper branched PLLA was lower at low frequency region and the slope was higher than those of star shaped and comb like PLLA which substantiates the importance of branch length for higher inter-chain interactions and a more pronounced elastic behavior at lower frequencies.

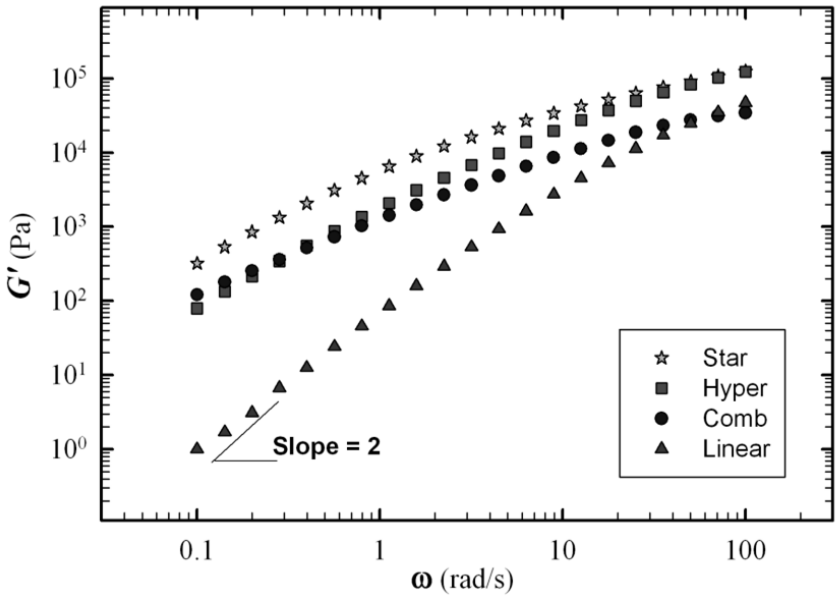

Figure 6.4. Elastic modulus as a function of oscillation frequency for linear and branched PLA with different branch structures

In addition to complex viscosity and elastic modulus, phase angle (δ) is another important parameter related to the chain microstructure and elasticity of the material. Figure 6.5 shows the variation of phase angle as a function of frequency for linear and branched PLAs. For linear PLLA and at low frequencies where the polymer behaves like a Newtonian fluid, δ was close to 90 degrees. By increasing the frequency beyond 1 rad/s, δ was reduced monotonically. This is known to be typical for polymers with a linear chain structure. On the other hand, branched PLAs exhibited a dissimilar trend. For all the branched PLAs, δ was located below the linear one and started to decrease initially as the frequency was increased. In addition, the star shaped and comb like PLA showed an inflection in the trend towards a plateau at higher frequencies that can be attributed to their longer branch length as compared to hyper branched PLA. Accordingly, Figure 6.5 is another indication of the difference in the chain architecture of branched PLAs and its role on their rheological response.

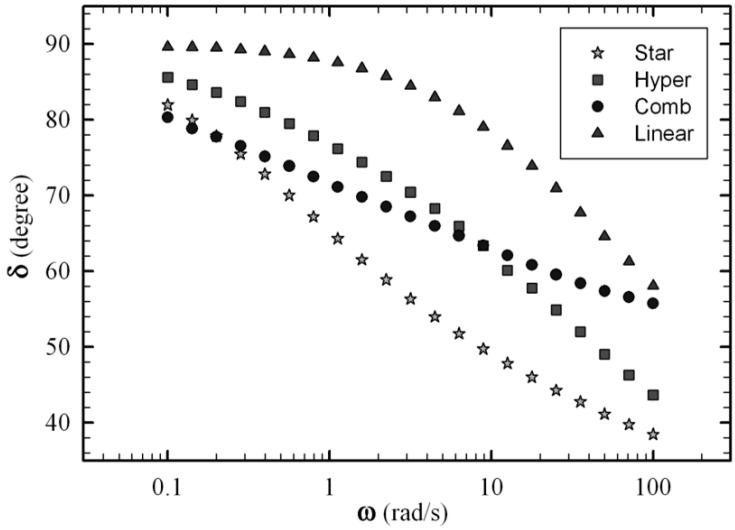

Figure 6.5. Phase angle as a function of oscillation frequency for linear and branched PLA with different branch structures

6.3.1.2 Linear / Branched PLLA blends

In the next step, after an evaluation of the relationship between chain architecture and melt rheological properties, star shaped, comb like and hyper branched PLLAs were blended at 10, 20 and 30% with linear PLLA to assess the modification role of a minor branched PLA fraction on the rheological properties of the blend. In Figure 6.6, complex viscosity is plotted versus oscillation frequency for blends based on star shaped PLLA as a representation of linear/branched PLLA systems. It is clear from this figure that the viscosities of the blends were

in-between those of the neat components and as the content of the branched PLLA increased, viscosities increased likewise and shear thinning behavior augmented.

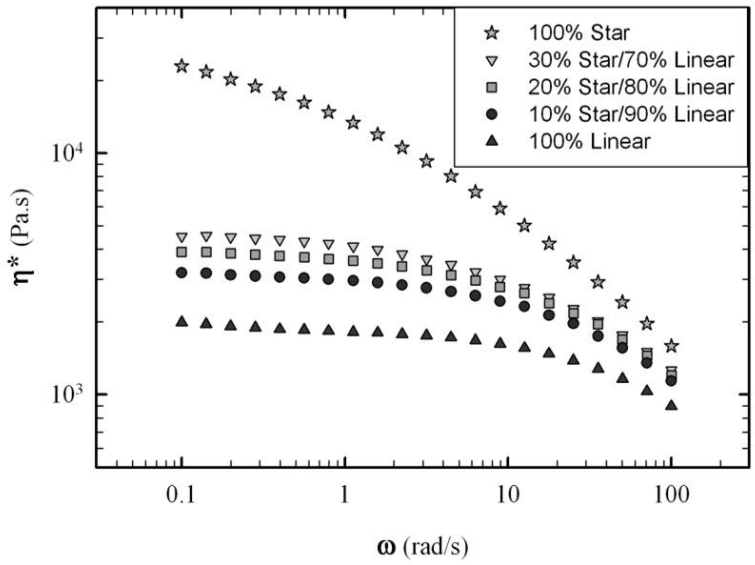

Figure 6.6. Complex viscosity as a function of oscillation frequency for linear and star shaped PLA and their blends

To better illustrate the effect of branch content on viscosity, η_0 obtained from the Carreau-Yasuda model was plotted as a function of branched PLLA content in Figure 6.7. In addition, a dashed line representing the logarithmic additivity rule was plotted to analyze general blend behavior. It is expressed with the following equation:

$$\log(\eta_0) = \sum \Phi_i \log(\eta_{0,i}) \qquad \textbf{(6.3)}$$

where Φ_i and $\eta_{0,i}$ are the volume fraction and zero-shear viscosity of component *i* respectively.

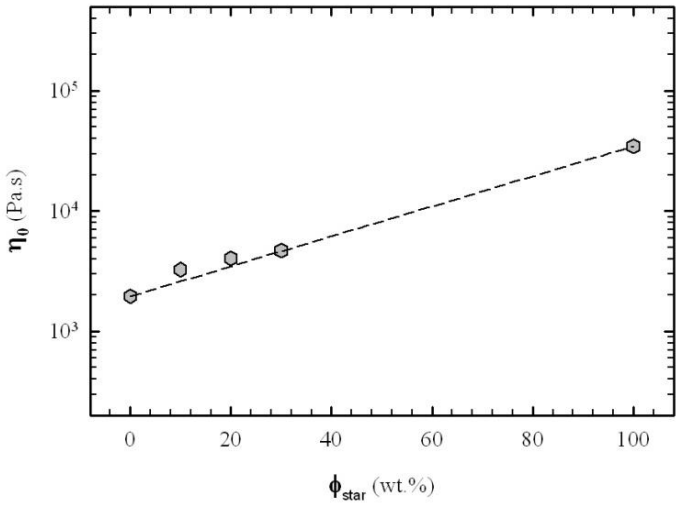

Figure 6.7. Zero-shear viscosity as a function of star shaped PLA content

According to Figure 6.7, the blends of linear and branched PLLA nearly followed the log-additivity rule with only a slight positive deviation. Following the log-additivity mixing rule or a positive deviation is often interpreted as miscibility of the components in the literature (Utracki, 2002). Also by taking into account the similarity in chemical nature and molecular weight of the components, these blends can be considered miscible.

6.3.1.3 Branching through stereocomplex formation

Stereocomplex crystals with a melting point higher than PLLA melt temperature remain in the system at the rheological characterization temperature and contribute to the increase of PLA melt viscosity. In this work for the first time the PDLAs chosen for PLA rheological property modification had branched architectures themselves. Accordingly, blends of linear PLLA with star shaped, comb like and hyper branched PDLAs (produced similarly to their PLLA counterparts) were prepared at branched PDLA contents of 5, 7 and 10%. Prepared samples for the rheological characterizations were first examined in DSC tests to verify the formation of stereocomplex structure and its quantity. Specimens were first kept at 190 ^{o}C for 3 min to simulate the preheating step in rheological tests, then heated at a rate of 10 ^{o}C/min to 240 ^{o}C. Figure 6.8 shows the DSC thermograms for blends of hyper branched PDLA and linear PLLA containing 5, 7 and 10% PDLA as a representative of linear PLLA/branched PDLA systems.

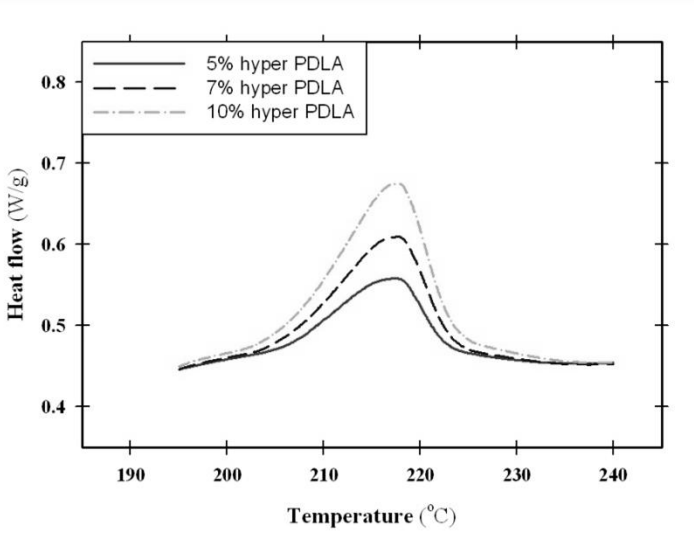

Figure 6.8. Stereocomplex melting peaks for blends of linear PLLA with hyper branched PDLA

Manifestation of endotherm peaks at 217 ^{o}C confirmed the presence of stereocomplex crystal structure which is associated to higher melting points than PLA homocrystals which melt at 170 ^{o}C. Stereocomplex crystallinities calculated based on the melting peak area are 5.9, 8.5 and 11.6% for 5, 7 and 10% PDLA respectively. Crystallinity calculation is based on melting enthalpy of 146 J/g for 100% crystalline PLA in the form of stereocomplex (Tsuji et al., 1992).

Figure 6.9 shows the complex viscosity as a function of frequency for hyper branched PDLA/ linear PLLA blends. Clearly, addition of branched PDLA to PLLA had a remarkable effect on complex viscosity. Viscosity and shear thinning behavior were both in direct relation with the concentration of branched PDLA. Complex viscosity at low frequencies showed a significant increase up to two orders of magnitude and no viscosity plateau was reached. This behavior is observed for systems with structure formation capability within the constituents, suggesting a high level of interaction and entanglement between chains as a result of stereocomplex formation and physical chain branching. Also, compared to linear PLLA/ branched PLLA blends, a higher degree of viscosity increase was achieved by a smaller amount of the modifying component in linear PLLA/ branched PDLA blends.

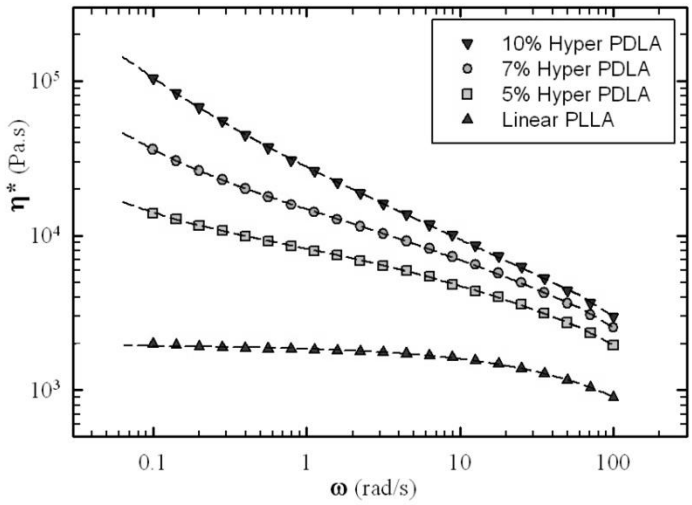

Figure 6.9. Complex viscosity as a function of oscillation frequency for linear PLLA and its blends with hyper branched PDLA

The increase in complex viscosity at low frequencies can be predicted with the Carreau-Yasuda model with an extra term standing for a yield stress:

$$\left|\eta^*(\omega)\right| = \frac{\sigma_y}{\omega} + \eta_0[1 + (\lambda\omega)^a]^{\frac{(n-1)}{a}} \qquad \textbf{(6.4)}$$

where σ_y is the yield stress. Model predictions were plotted as dashed lines in Figure 6.9, showing a good fit of the data to this model. Calculated yield stress was also plotted as a function of branched PDLA content in Figure 6.10 to determine the required PDLA for a rheological percolation. By interpolating the line passing from 5 and 7% PDLA data points to the zero yield stress, the calculated percolation threshold was equal to 4.4% PDLA.

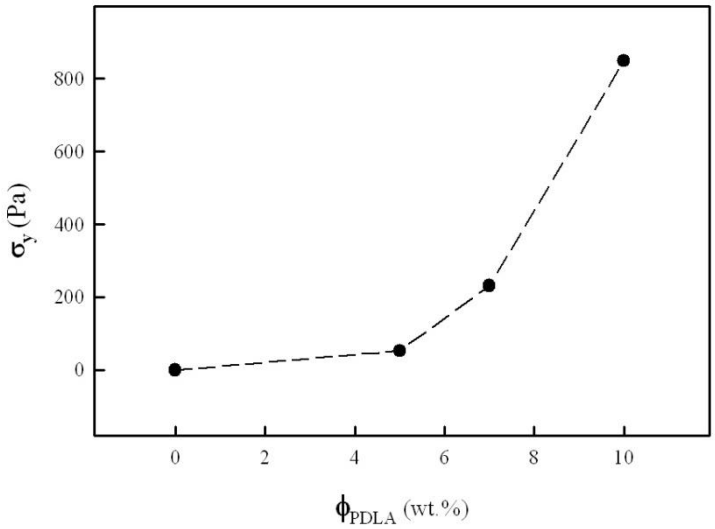

Figure 6.10. Yield stress as a function of hyper branched PDLA content

Phase angle as a function of frequency is plotted in Figure 6.11 for physically branched systems containing different concentrations of PDLA. In comparison to linear PLLA and linear/branched PLLA blends, a completely different behavior was observed. At low frequency end, δ was between 30^o to 70^o which is much lower compared to linear and chemically branched blends. This shows the more elastic nature of PLA in presence of stereocomplex crystals. Previously, it was observed that by increasing frequency, phase angle showed a decreasing trend. On the other hand, for stereocomplex systems, it first increased to a maximum and then decreased. This behavior shows that by increasing the frequency, the yield stress is overcame and as the frequency is further increased, material shows more elastic behavior. In addition this effect intensified as the content of PDLA was increased in the blends.

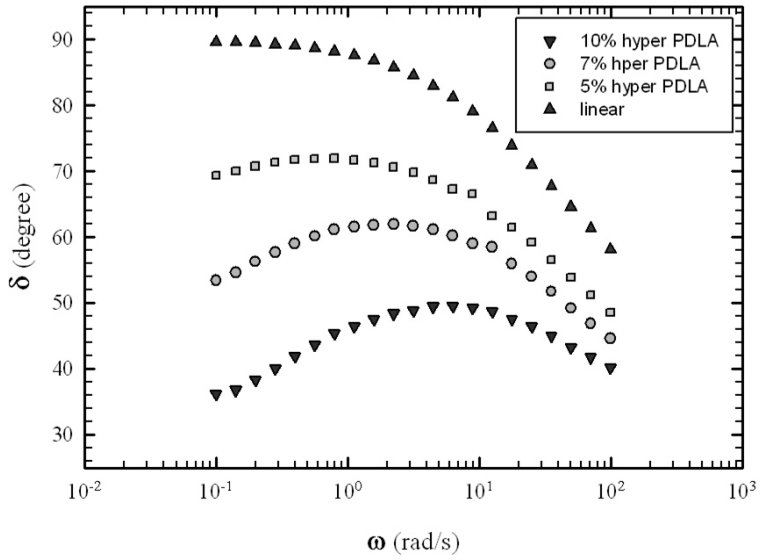

Figure 6.11. Phase angle as a function of oscillation frequency for linear PLA and its blends with hyper branched PDLA

Another method to investigate the effect of chain structure on melt properties is plotting the Cole-Cole diagram. In Figure 6.12 G′ vs. G″ is plotted for (a) linear and branched PLLAs and (b) linear PLLA / branched PDLA blends.

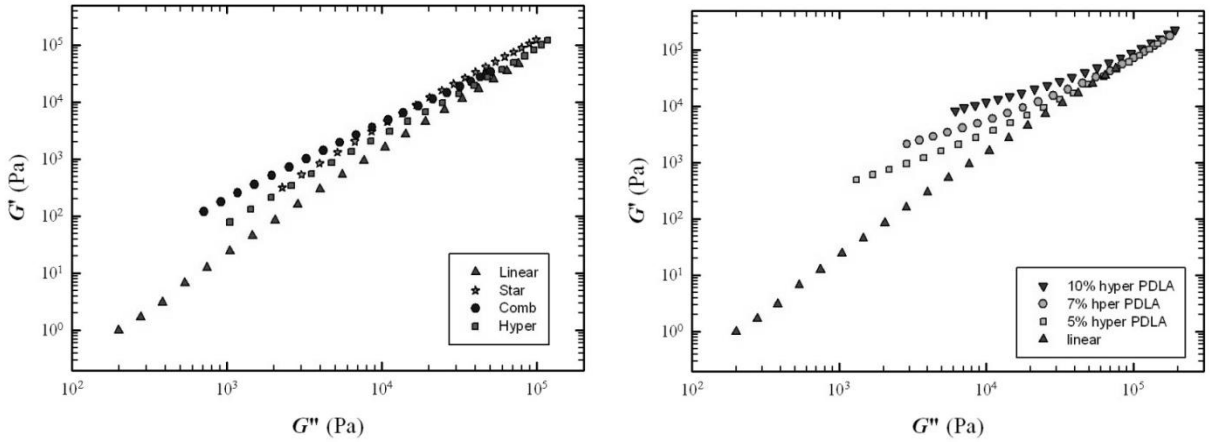

(a) (b)

Figure 6.12. Cole-Cole diagrams for (a) linear and branched PLLAs, (b) linear PLLA and its blends with hyper branched PDLA

In these types of plots, deviation from the behavior of linear molecules is an indication of changing the structure. Linear PLA showed a straight diagonal line which is typical for polymers

with a linear chain structure. On the other hand, branched PLLAs showed different levels of deviation from linear PLA, especially at lower G′ and G″ values. For stereocomplex systems, deviation from the linear structure was even further and G′ became less dependent to G″ in agreement with more elastic nature of these materials observed earlier. Therefore, physical branching revealed a stronger effect on chain structure evolution.

To explore the effect of branched PDLA architecture on viscosity increase, complex viscosity versus frequency data are presented in Figure 6.13 for blends having 5% of branched PDLA. Although branching caused by stereocomplex formation was showed to be more influential on viscosity than blending of chemically branched PLLAs with linear one, the type of PDLA chain revealed some effect on the total response obtained for simultaneous chemical and physical branching. Viscosity increase was highest for the blend having hyper branched PDLA followed by star shaped and comb like PDLA. Hence, having a shorter branch length is more favorable for stereocomplex formation between linear PLLA and branched PDLA.

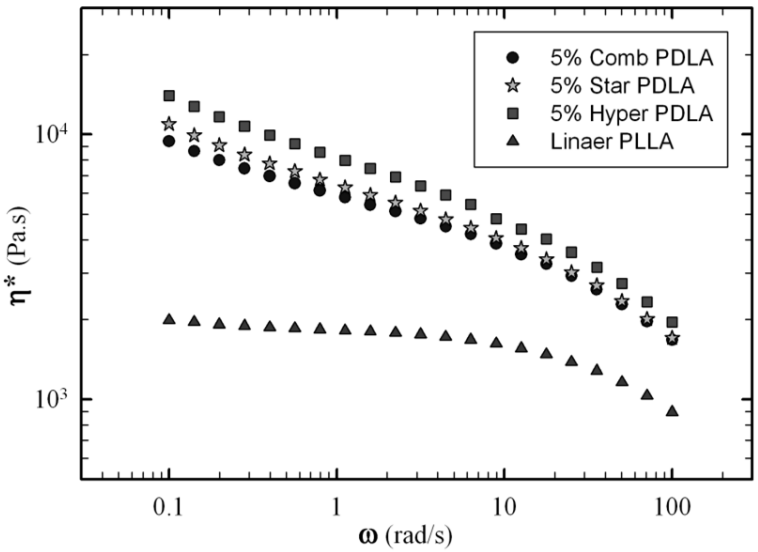

Figure 6.13. Complex viscosity as a function of oscillation frequency for linear PLLA and its blends with 5% branched PDLAs with different chain architectures

This is in agreement with DSC results where stereocomplex crystallinity calculated for 5% star and comb PDLA blends was lower than blends containing 5% hyper branched PDLA, i.e. X_c 4.7 and 4.5% compared to 5.9%. In fact in our previous work, the hyper branched structure was shown to be very efficient in PLLA homocrystallization due to a high nucleation density and

spherulite growth rate (Nouri et al., 2015). Therefore, it is believed that similar characteristics of hyper branched PLLA that promoted its homocrystallization would enhance the stereocomplex formation of hyper branched PDLA with PLLA. In addition, due to a higher number of branching points, stereocomplex formation with PLLA happened in more locations and resulted in a higher viscosity of the blend.

6.3.2 Uniaxial extensional rheometry

Extensional rheometry is another powerful technique that can provide valuable information about the rheological behavior of polymers in elongational flow fields which is important for many melt processing applications such as film blowing, blow molding, thermoforming, foaming etc. In our previous work, it was shown that unlike linear PLA, synthesized polylactides with different branched architectures revealed a strain hardening behavior in extensional rheometry tests (Nouri et al., 2015). Therefore time-dependent elongational viscosity, $\eta_E^+(t, \dot{\varepsilon}_H)$, as a sensitive parameter to the chain architecture was measured for branched PLAs as well as blends of linear/branched PLLA and linear PLLA/branched PDLA to investigate the effect of chemical and physical branching respectively on PLA extensional rheology. Tensile stress growth coefficient is defined as:

$$\eta_E^+ = \frac{\mathrm{T}(t)}{2R\dot{\varepsilon}_H A_0 (\frac{\rho_S}{\rho_M})^{2/3}} \exp(\dot{\varepsilon}_H t) \qquad \textbf{(6.5)}$$

where T is the measured torque signal, $\dot{\varepsilon}_H$ is applied Hencky strain rate, R is the radius of the windup drums, A_0 is the cross-sectional area of the specimen in the solid state, ρ_S is the solid state density, and ρ_M is the melt density of the polymer.

Effect of chemical branching: Figure 6.14 shows the elongational viscosity for linear and branched PLLAs obtained at a Hencky strain rate of 1 s^{-1}. In addition, open symbols represent three times the transient shear viscosity data, $3\eta^+(t)$, in the limit of low deformation for each structure.

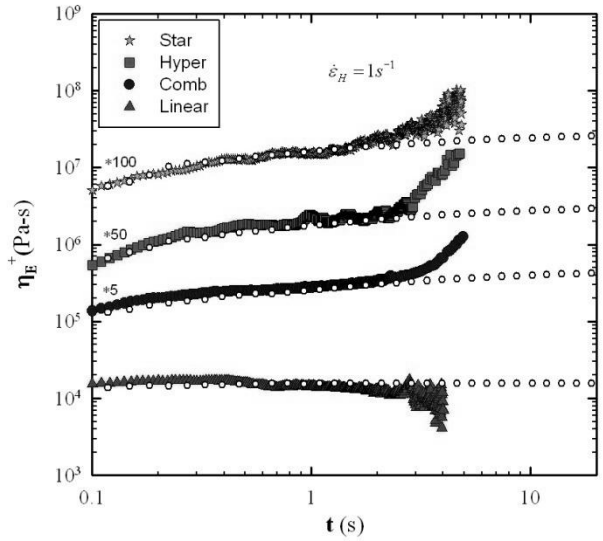

Figure 6.14. Elongational viscosity of linear and branched PLLA with different architectures at 180 °C

Linear PLLA reached a viscosity plateau and failed afterwards, as expected from its linear chain nature. On the other hand, branched PLLAs displayed an interesting and different response. Depending on the branch architecture, elongational viscosity started to increase after the plateau at strains of 1.5 to 2.5 and a strain hardening comportment was observed, indicating a considerable difference between the rheological response of the linear and branched PLAs. Since there was no evidence of stress induced crystallization for the branched PLAs, the strain hardening was attributed to the molecular structure and the reduced rate of chain disentanglement due to the presence of branches on polymer molecules.

Since an improvement in extensional viscosity was observed for branched PLLAs as compared to the linear one, it was desired to see if the addition of the branched molecules to the linear polymer had any influence on the rheological response of the linear PLA in elongational flow. In Figure 6.15, elongational viscosities of linear and star shaped PLLA and their blends containing 10, 20 and 30% of the star structure are compared at Hencky strain rates of 0.1, 1 and 5 s^{-1}. Data are shifted vertically for a better visualization. Also $3\eta^+(t)$ data for these materials are plotted (open symbols) to show the deviation from linear behavior by strain hardening. For all examined Hencky strain rates, linear PLLA failed after reaching a viscosity plateau. This happened due to the linear chain architecture and absence of any viscosity increase mechanism.

On the other hand, branched samples demonstrated a completely different response. At Hencky strain rates of 0.1 and 1 s^{-1}, star shaped PLLA and its blends revealed a significant strain hardening, which was more intense at lower Hencky strain rates. This clearly proved a promising contribution in reducing chain disentanglement rate and improving the rheological response of PLA in extensional mode. However, at a Hencky strain rate of 5 s^{-1}, star shaped PLLA and its blends with linear PLLA failed to show the strain hardening response due to a fast elongation rate and rupture of the specimens.

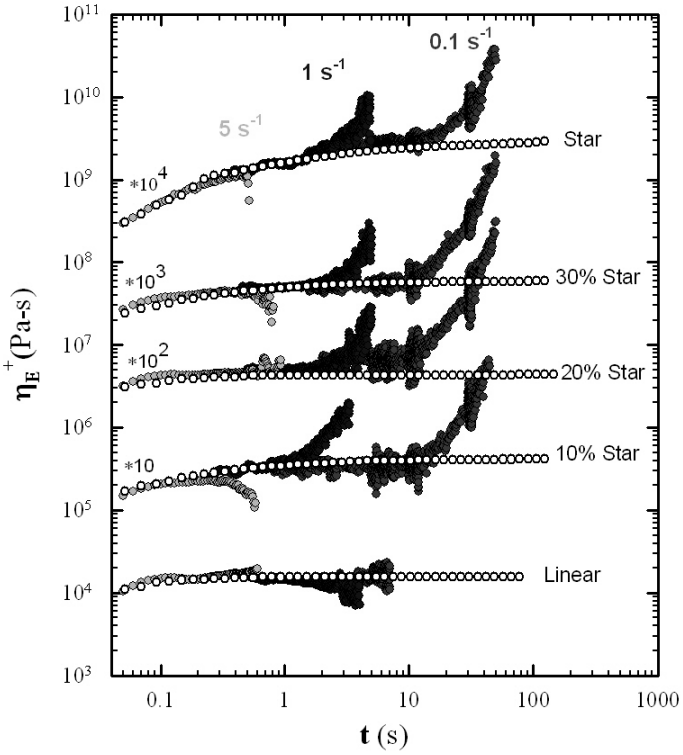

Figure 6.15. Effect of the addition of a branched PLLA to linear PLLA on elongational viscosity at 180 ^{o}C

Effect of physical branching: The role of physical branching through stereocomplex formation on PLA elongational viscosity was investigated for the blends of linear PLLA and branched PDLA. In Figure 6.16, elongational viscosity of linear PLLA and its blends containing 5% of the star shaped, comb like and hyper branched PDLA are compared at Hencky strain rates of 0.1 to 5 s^{-1}. Again, data are shifted vertically for a better visualization and open symbols represent the linear behavior calculated from start-up tests. It should be noted that for blends

containing 7 and 10% PDLA, viscosity was so high that samples were not extensible at test conditions and it was not possible to perform extensional rheometry characterization on them. From this figure, it is evident that the presence of PDLA in all three architectures had significant effect on PLLA extensional rheology. At Hencky strain rates lower than 5 s^{-1}, all samples revealed strain hardening behavior which was more pronounced at lower rates. In addition, contrary to the blends of linear and branched PLLA, in blends of linear PLLA with branched PDLA, the elongational viscosity was increasing progressively and did not reach a viscosity plateau. Strain hardening was also reported for blends of linear PLLA and PDLA by Yamane et al.; however, tests were performed in a biaxial squeezing flow at very low strain rates (0.01 - 0.05 s^{-1}) and extensional viscosity reached a plateau before strain hardening (Yamane et al., 2004). Finally, it should be noted that the remarkable change in elongational viscosity was achieved with only 5% of the branched PDLA, showing the effectiveness of this approach and in agreement with the results of shear flow rheometry. It is noteworthy that strain hardening effect was not essentially different between systems with different branched PDLA architectures. Thus, it is reasonable to say that the physical branching due to stereocomplex formation was the prevailing mechanism for observing the strain hardening behavior.

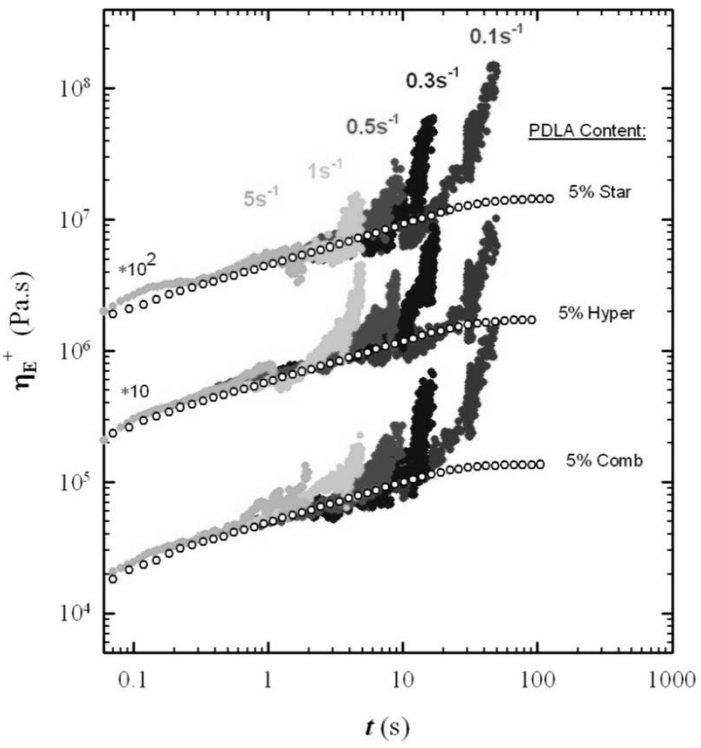

Figure 6.16. Effect of stereocomplex formation between branched PDLA and linear PLLA on elongational viscosity at 5% PDLA content at 180 ^{o}C

The observed strain hardening in branched systems can be explained by different mechanism. In principal, the relaxation mechanism is different between linear and branched structures. Linear chains use the reptation mechanism which is greatly suppressed in branched chains and relaxation is mainly through arm retraction. Therefore, disentanglement rate of branched molecules is decreased. Another reason is a change in entanglement density by branching. Depending on the number of branches and molecular weight, entanglement density may be increased or decreased by branching. In this study, based on the data presented in Figure 6.3 and the observed positive deviation, entanglement density was increased. Finally, in blends containing stereocomplex structure, two additional mechanisms contribute to strain hardening. One is the apparent broadening of molecular weight by physical connection of a portion of PLLA to PDLA chains by stereocomplex crystals, and the other reason is the gripping forces caused by the interaction of polymer chains with solid stereocomplex crystals.

6.4 Conclusion

The objective of this work was to investigate two potential strategies to improve the shear and extensional rheological properties of PLA. In the first approach, branched PLLAs with different chain architectures were synthesized and blended with linear PLLA. It was observed from shear flow rheometry of branched PLLAs that all of them had higher viscosity and elastic modulus at low frequencies compared to linear PLLA as well as an increased shear thinning behavior. Among the branched PLLAs, star shaped PLLA had the highest viscosity and elastic modulus which was associated to longer branches. Blends of the latter with linear PLLA containing 10, 20 and 30% branched structure revealed an increase in viscosity. A viscosity increase was evident even at 10% branch content and the phenomenon becomes more intense by adding more branched PLLA to the blend. In addition, elongational viscosity measurement of the branched PLLAs and their blends with linear PLLA showed a strain hardening behavior due to the presence of branched chains. The strain hardening was dependent on Hencky strain rate and

as the strain rate was increased to 5 s^{-1} samples were ruptured before demonstrating a viscosity increase.

In the second strategy, branched PDLAs were synthesized similar to their PLLA counterparts to benefit from a double branching approach, i.e. branched architecture and stereocomplex formation between PLLA and PDLA chains. Stereocomplex crystals are more stable than homocrystals because of specific molecular packing and PLLA/PDLA interchain interactions, thus remain in PLA melt. Shear flow rheometry of blends containing up to 10% branched PDLA showed a significant increase in viscosity and shear thinning and absence of a viscosity plateau. Comparison of the shear viscosity for blends containing 5% of different branched architectures suggested that hyper-branched PDLA had some advantage compared to star shaped and comb like PDLA that can be originated from an easier stereocomplex formation due to shorter branch length and nucleation effect of branching points. In extensional rheology experiments on the same blends, it was observed that elongational viscosity was progressively increased without reaching a plateau followed by a significant strain hardening. Meanwhile, by comparing the results from the rheological characterization of linear/branched PLLA blends with those from linear PLLA/branched PDLA blends it is concluded that the physical branching due to stereocomplex formation, which simultaneously increases branch content and apparent molecular weight, is a more effective mechanism to improve PLA rheological properties such as shear thinning, melt elasticity and strain hardening.

CHAPTER 7. ARTICLE 3: HOMOCRYSTAL AND STEREOCOMPLEX FORMATION BEHAVIOR OF POLYLACTIDES WITH DIFFERENT BRANCHED STRUCTURES

Sahar Nouri, Charles Dubois and Pierre G. Lafleur

CREPEC, Chemical Engineering Department, Ecole Polytechnique, C.P. 6079, Succ. Centre ville, Montreal, QC, H3C 3A7 Canada

ABSTRACT Effect of chain architecture on homocrystallization and stereocomplex formation behaviour of polylactide (PLA) in quiescent conditions was investigated by means of differential scanning calorimetry (DSC) and optical microscopy. Non-isothermal and isothermal crystallization of star shaped, comb like and hyper branched poly(L-lactides) (PLLAs) with similar molecular weights were studied and compared to a linear one. In dynamic mode, branched PLAs reached higher crystallinity and revealed much higher spherulite density as compared to linear PLA. Also blends of linear and branched PLA with different blending ratios revealed faster crystallization than neat linear PLA. Based on kinetic data obtained in isothermal crystallization experiments, much faster crystallization was achieved with a 4 to 14 fold decrease in crystallization half-time as a consequence of non-linear chain architecture. Crystallization upon cooling, reduced cold crystallization temperature, increased spherulite density and lower Avrami exponent values for branched PLAs in comparison to linear one suggest enhanced nucleation process as a result of a branched chain architecture. On the other hand, total crystallinity and growth rate were decreased by branching. Stereocomplex formation between linear PLLA and branched poly(D-lactides) (PDLAs) showed dependency of stereocomplex formation to branched architecture. Also, stereocomplex crystals nucleated PLA homocrystallization process while different internal morphology between stereocomplex and homocrystal spherulites was observed. These results confirm that chain architecture has a profound effect on the crystallization behavior of PLA.

KEYWORDS Polylactide, branched structure, crystallization, stereocomplex

7.1 Introduction

Application of bio-based polymers has surged throughout the past decade due to their reduced environmental impact as compared to traditional polymers. Polylactide (PLA) is a leading member of this family of polymers which has been in the spotlight; having the edge over competitive bioplastics because of its degradability and acceptable mechanical, optical and barrier properties. Existence of lactic acid in two stereo-isomer forms known as L and D results in a wide variety of PLA grades from the crystallization point of view. PLA can be completely amorphous or semi-crystalline with different melting temperatures and crystallinity depending on the amount and placement of L and D units in polymer chain (Bigg, 1996; Kolstad, 1996; Witzke, 1997; Hartmann, 1998; Bigg, 2005). Also, different crystal types have been identified for PLA, the most frequently occurring is α type crystal with a pseudo-orthorombic cell structure with cell dimensions of a = 1.07 nm, b = 0.595 nm, and c = 2.78 nm, containing two 10_3 helices (Okihara et al., 1991). For stereochemically pure PLAs with high enough molecular weights, melting temperature could be as high as 180 ^{o}C (Witzke, 1997; Bigg, 2005). Another PLA crystal type is known as stereocomplex crystal and was first reported by Ikada et al. (Ikada et al., 1987). Although opposite repeating units in PLA chain can hinder its crystallization, when PLLA and PDLA chains are mixed, they can co-crystallize and form stereocomplex. Stereocomplex cell structure is triclinic with dimensions of a = 0.916 nm, b = 0.916 nm and c = 0.870 nm, in each cell one PLLA and one PDLA chain segment are located assuming a 3_1 helical conformation (Okihara et al., 1991). The crystal formed from the co-crystallization of PLLA and PDLA melts at about 50 ^{o}C higher than homopolymer crystals.

It is well established that crystallinity is a major parameter in determining several polymer properties. In the case of PLA, slow crystallization and low crystallinity are among its main weaknesses (Saeidlou et al., 2012). Usually PLA does not crystallize completely from the melt and shows cold crystallization behavior upon subsequent heating (Androsch and Di Lorenzo, 2013; Ravari et al., 2013). This can be used to increase the crystallinity of final product. Other methods such as adding nucleating agents (Kolstad, 1996; Nam et al., 2006; Tsuji et al., 2006; Kawamoto et al., 2007; Wen and Xin, 2010), plasticizers (Kulinski and Piorkowska, 2005; Xiao et al., 2009; Sungsanit et al., 2012) or their combination (Li and Huneault, 2007; Xiao et al., 2010) may also be used for increasing the number of crystallization sites and chain mobility; therefore, enhancing the overall crystallization kinetics of PLA.

Another type of modification is changing chain architecture from linear to a branched one. Different methods have been used to produce branched PLA such as free radical branching (Dorgan et al., 2000; Dean et al., 2012; You et al., 2013), using chain extenders (Lehermeier and Dorgan, 2001; Cicero et al., 2002; Dorgan et al., 2005-a; Mihai et al., 2010; Othman et al., 2011), multifunctional initiators (Dorgan et al., 1999; Sakamoto and Tsuji, 2013; Sakamoto and Tsuji, 2013) or the combination of synthesis and chain extension methods (Wang et al., 2012), as well as copolymerization with other monomers (Wolf and Frey, 2009; Phuphuak and Chirachanchai, 2013). Although these studies revealed the effect of branching on changing PLA properties, their focus was mainly on melt rheology. Crystallization of branched PLA is explored to a smaller extent in comparison to linear PLA; especially for stereocomplex crystal. In addition, results are inconsistent from different aspects. There are some reports that branching increased the crystallization rate (Mihai et al., 2009; Mihai et al., 2010; Nofar et al., 2011) while other reports exist on slower crystallization by increased number of branches (Hao et al., 2005; Sakamoto and Tsuji, 2013). In addition, while some researchers presented a reduction in melting temperature by less perfect crystals (Wang and Dong, 2006; Wang et al., 2012), others showed that T_m was not affected by chain branching (Wang et al., 2012; Sakamoto and Tsuji, 2013). Also by increasing branch content, crystallinity (X_c) is reported to decrease or remain unaffected (Tsuji et al., 2005; Ouchi et al., 2006; Wang et al., 2012). Furthermore, most of the published data are on PLAs randomly branched through reactive processes that can influence their molecular weight. Therefore, the pure effect of chain architecture in well defined structures is less examined. In this work, we focused on this aspect by a comprehensive study of branched PLA crystallization kinetics and morphology. Homocrystallization of three branched chain architectures, i.e. star shaped, comb like and hyper branched PLA was compared with linear PLA as well as stereocomplex formation between linear PLLA and branched PDLAs. Interesting results were obtained on crystalline morphology and improvement of crystallization behavior for both crystal types.

7.2 Experimental

7.2.1 Materials

PLLA and PDLA with different branched architectures were synthesized by ring-opening polymerization of L-lactide and D-lactide (Purac Biochem, The Netherlands), respectively.

Reaction was conducted at 180 ^{o}C for one hour under the nitrogen atmosphere. Tin(II) 2-ethylhexanoate (Aldrich) was used as the catalyst at a concentration of 0.03 mol%. Pentaerythritol and Triglycerol (Sigma-Aldrich) were used as initiator to prepare star shaped and comb like polymers, while Glycidol (Sigma-Aldrich) was used as initiator-comonomer to produce hyper branched structure. Molecular weight and its distribution was obtained using a Viscotek GPCmax equipped with light scattering detector. To confirm the structure of synthesized materials, ^{1}H-NMR characterization was performed by a Bruker AV500 spectrometer. M_n and PDI of star shaped PLA were equal to 89 kg/mol and 1.38, respectively. Base on the NMR data, absence of non-reacted hydroxyl groups of the initiator indicated that four-arm star structure was successfully synthesized. Therefore, the average arm molecular weight was 22.25 kg/mol. M_n and PDI of comb like PLA were equal to 85 kg/mol and 1.74, respectively. According to NMR analysis, 94.6% of hydroxyl groups were reacted. Thus, average backbone and arm molecular weights were 36.2 and 17.9 kg/mol. For hyper branched structure, M_n of 89 kg/mol and PDI of 1.39 were obtained. Although it was not possible to quantify the branch density because of the complex structure of this polymer, formation of randomly branched structure was verified from NMR characterization. More details regarding the synthesis and structure characterization including NMR spectra can be found in a previous paper by this group (Nouri et al., 2015). In addition, a commercial linear PLLA (4032D from NatureWorks) with a molecular weight of 101 kg/mol was used in this study as a reference and for blending purpose. Polymers are identified with two letters; X-Y. The first letter (X) indicates the stereochemistry of PLA, L for PLLA and D for PDLA. The second letter (Y) represents the chain structure, L for linear, S for star shaped, C for comb like and H for hyper branched PLA. For example, D-H means PDLA with hyper branched structure.

7.2.2 Blending

To study the effect of synthesized polymers on the crystallization behavior of commercial PLA, different blends were prepared by melt blending. Prior to the process, polymers were dried at 80 ^{o}C for 12 hours. A Leistritz ZSE 18mm co-rotating twin-screw extruder operating at 190 ^{o}C and a rotation speed of 100 rpm was used to prepare the blends.

7.2.3 Characterizations

Differential scanning calorimetry by TA instrument DSC Q1000 was performed to study the isothermal and non-isothermal crystallization behavior as well as melting of the specimens. In dynamic mode, after removing thermal history at 200 ^{o}C for homocrystal or 240 ^{o}C for stereocomplex, samples were cooled to 20 °C and then heated again at a rate of 10 °C/min. For isothermal mode, after removing thermal history, samples were rapidly cooled to crystallization temperature and enough time was given to complete the crystallization process. Hot-stage optical microscopy observations were conducted to evaluate crystalline morphology (spherulite size and density) and spherulite growth rate. OPTIPHOT-2 optical microscope equipped with a programmable hot stage (Mettler FP82HT) was employed using similar thermal procedures as in DSC tests. Samples were in the form of thin films, prepared by hot pressing technique.

7.3 Results and discussion

7.3.1 Homocrystallization

In the first step, PLLA homocrystallization (absence of PDLA chains) in non-isothermal and isothermal modes at quiescent conditions was studied from different aspects, including kinetics, crystallinity and morphology.

7.3.1.1 Non-isothermal crystallization

Crystallization of linear, star shaped, comb like and hyper branched PLLAs in non-isothermal conditions were compared through DSC characterizations. Thermal history of the specimens was removed by melting at 200 ^{o}C for 3 min. Temperature was then reduced to 20 ^{o}C at a rate of 10 ^{o}C/min to record the crystallization behavior upon cooling the melt. Finally, temperature was increased at the same rate to 200 ^{o}C to observe thermal response in a subsequent heating cycle. Figure 7.1 shows DSC thermograms where heat flow data obtained by applying this procedure were plotted versus temperature. Cooling and heating cycles are shown in Figure 7.1-a and Figure 7.1-b, respectively. Linear PLA did not reveal a crystallization peak in cooling which is expected from the very slow crystallization kinetics of PLA. Also, in the heating cycle, only a slight cold crystallization was observed at 140 ^{o}C followed by a small melting peak at 170 ^{o}C. Branched PLAs on the other hand showed a completely different crystallization behavior. In

cooling mode, all three branched structures showed a crystallization peak at about 102 ^{o}C. In addition, branched PLAs were further crystallized in a cold crystallization process during the subsequent heating cycle. Melting peaks were noticeable at about 172 ^{o}C, preceded by small exotherms that can be attributed to the transformation of less ordered α' crystals to more stable α crystals (Kawai et al., 2007; Zhang et al., 2008).

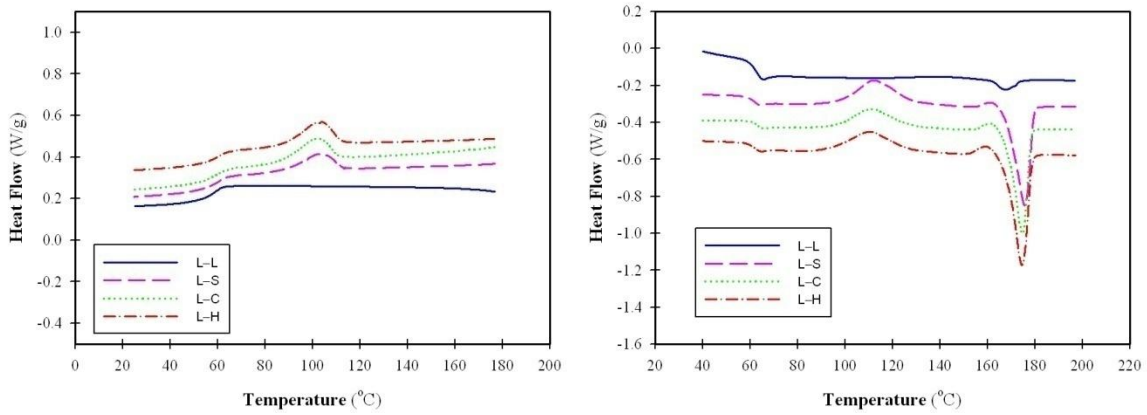

Figure 7.1. DSC thermograms of linear and branched PLAs in dynamic mode at 10 ^{o}C/min, cooling cycle (left), heating cycle (right), exotherm is upward

Thermal properties obtained from Figure 7.1 are summarized in Table 7.1. Crystallization peak temperature (T_c) was from 101.5 to 103.5 ^{o}C and crystallization enthalpy (ΔH_c) from 6.6 to 9.8 J/g, showing a moderate dependence on branch architecture. No significant change in glass transition temperature (T_g) by branching was observed which appeared at 59 to 61 ^{o}C. Cold crystallization peak temperature (T_{cc}) and enthalpy (ΔH_{cc}) were improved considerably by branching. T_{cc} of branched PLAs was decreased by almost 30 ^{o}C compared to linear PLA with enthalpies from 10 to 13.5 J/g. Melting enthalpy (ΔH_m) was almost equal to the sum of crystallization from the hot and cold crystallization enthalpies for all the samples and was about 20 J/g higher for branched polymers in comparison to the linear one. By assuming a melting enthalpy of 93 J/g for 100% crystalline PLA (Fischer et al., 1973), degree of crystallinity (X_c) was calculated for the four PLAs based on Equation (7.1):

$$X_c(\%) = 100 \times \frac{\Delta H_c}{\Delta H_{m,100\%}} \qquad \textbf{(7.1)}$$

It was the least for linear PLA equal to 2.5% while its highest value, observed for hyper branched structures, was equal to 25.7%. It should be noted that enthalpy of melting was used to calculate X_c since it is the total crystallinity obtained in cooling and heating cycles.

Table 7.1. Thermal properties of linear and branched PLAs in dynamic mode at 10 ^{o}C/min

Sample	T_c (^{o}C)	ΔH_c (J/g)	T_g (^{o}C)	T_{cc} (^{o}C)	ΔH_{cc} (J/g)	T_m (^{o}C)	ΔH_m (J/g)	X_c (%)
L-L	-	-	58.6	140.4	1.94	169.7	2.3	2.5
L-S	102.5	6.6	60.4	112.7	13.5	173.6	22.4	24.1
L-C	101.5	8.9	59.1	111.7	10.1	172.7	20.7	22.2
L-H	103.5	9.8	60.7	111.2	11.9	172.3	23.9	25.7

Based on the crystallinity values reported in Table 7.1, branched PLAs crystallized about ten times more than linear PLA. It is usually expected that branches cause less crystallinity as a result of disruption in crystallization by branched segments. However, the higher crystallinity achieved in the case of branched polymers can be attributed to their faster crystallization kinetics in a dynamic process. Crystallization is a combination of two phenomena, nucleation and growth. For linear PLA, nuclei do not form at a detectable rate during the cooling or may form but dissolve again as their radius is below a critical size. Therefore, before a considerable amount of crystalline phase is formed, viscosity is increased and growth is prohibited by lowering the temperature. On the other hand, due to the presence of less mobile chain segments of branched PLA, stable nuclei above critical size are inevitably present in the melt. These segments act as crystal nucleation sites at higher temperature where growth is not restricted and considerably promote the crystallization process. This is evidence by crystallization peaks upon cooling for branched polymers as well as a significant decrease in cold crystallization temperature. As a result of this faster crystallization, larger melting peaks were observed for branched PLAs. These peaks were also between 2 to 5 ^{o}C wider than for linear PLA. This is an indication of wider lamella thickness distribution due to irregularities in branched chains. Therefore, although crystallinity of linear PLA was much less than branched PLAs, lamella thickness was more uniform.

Effect of chain structure on crystallization was confirmed in non-isothermal optical microscopy observations as well in a non-isothermal procedure. As for DSC tests, thermal history

of thin films was removed by heating above the homocrystal melting temperature and the temperature was then reduced to 20 ^{o}C at a cooling rate of 10 ^{o}C/min. Images captured for all the structures at the temperature range of 130 to 100 ^{o}C are presented in Figure 7.2. Similarly to dynamic DSC tests, linear PLA did not crystallize, except for a few small crystallites which appeared between 110 and 100 ^{o}C. Meanwhile, crystallization was observed for branched PLAs from 120 ^{o}C and continued to lower temperatures with an increased number of small spherulites. By comparing the images obtained at 120 and 110 ^{o}C, hyper branched PLA was faster in crystallization followed by star shaped and comb like structures, respectively.

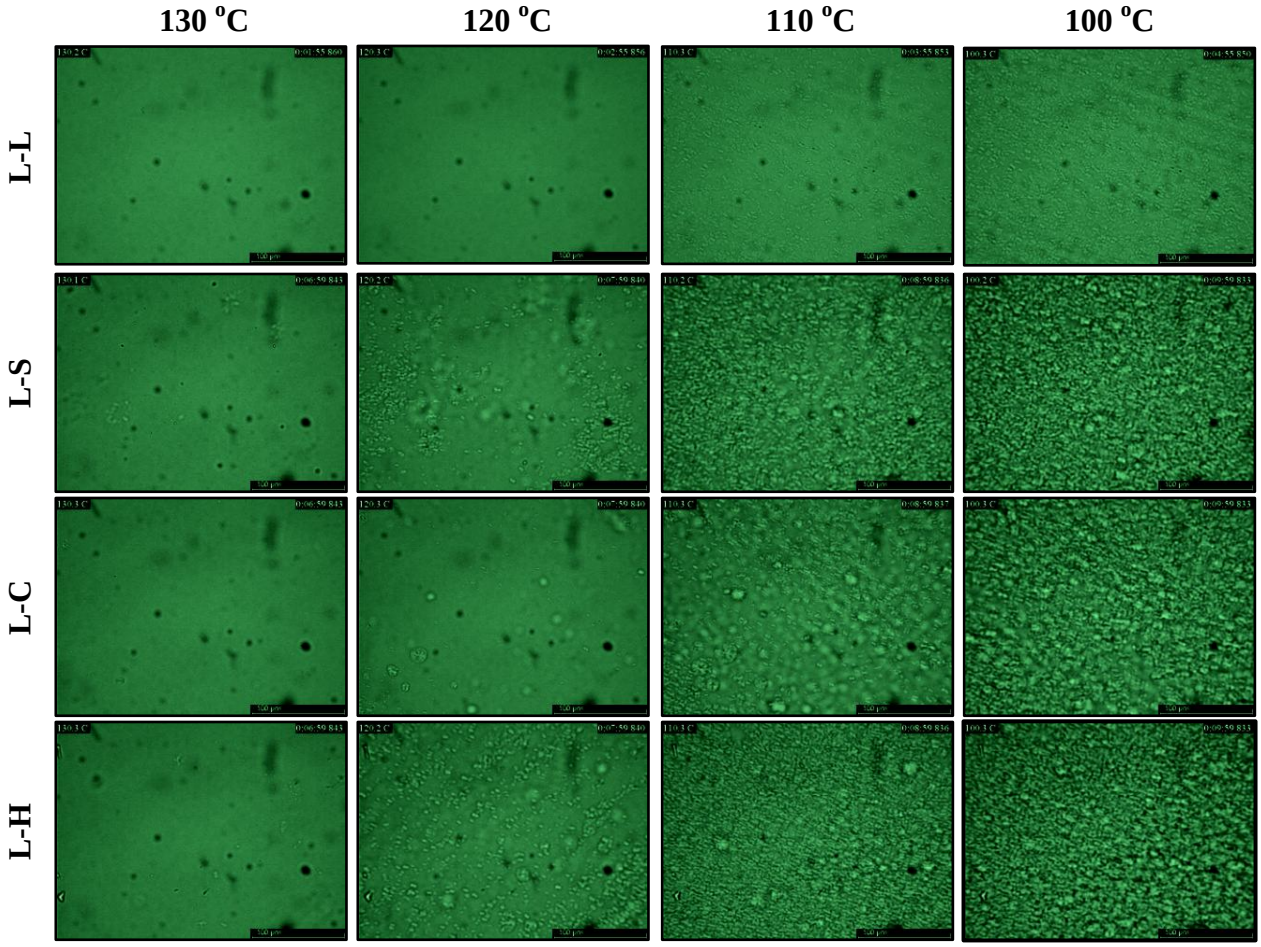

Figure 7.2. Optical microscopy images captured in a cooling cycle at a rate of 10 ^{o}C/min

Faster crystallization and higher spherulite density of hyper branched PLA at higher temperatures where linear PLA had not developed a significant amount of spherulites suggest that the branched structure improved the nucleation process. This was also observed for star and comb like architectures, but to a lower extent, in agreement with their reduced number of branching

points as compared to the hyper branched structure. These results confirm the findings from DSC tests regarding the nucleation function of branching points.

Since branched PLAs showed better crystallization behavior than linear one, it was interesting to see if branched/linear PLA blends have better crystallization than the linear PLA. For this purpose, hyper branched PLLA (L-H) was blended at 10, 20 and 30 wt.% with linear one and characterized in non-isothermal DSC tests. Samples were cooled at a rate of 10 ^{o}C/min from 200 ^{o}C to 20 ^{o}C and heated back at the same rate. DSC thermograms of the heating cycle are presented in Figure 7.3 and data are summarized in Table 7.2.

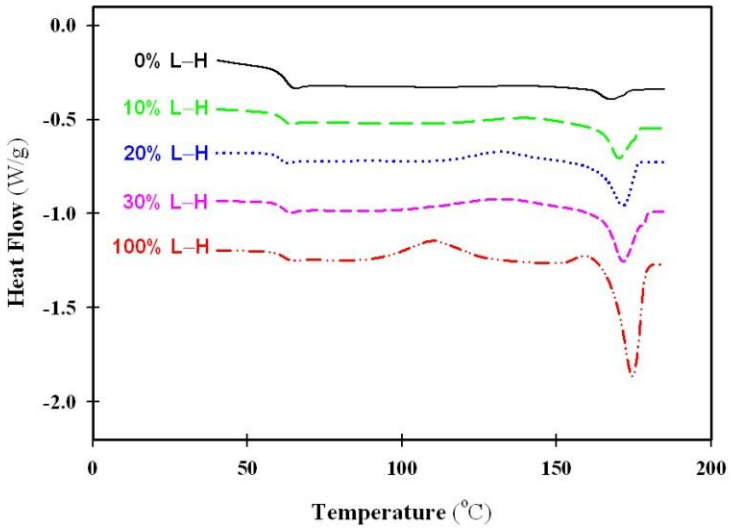

Figure 7.3. DSC heating cycle of samples with different L-H content at heating rate of 10 ^{o}C/min

From this figure and reported data in Table 7.2 it is clear that addition of L-H to L-L had positive effect on the crystallization behavior of the latter. 10% L-H increased crystallinity by about 5% and did not reduce cold crystallization temperature. However, increasing L-H content to 20 and 30% resulted in better crystallization. Total crystallinity was increased from 2.5% to 15.4% by replacing 30% L-L with L-H and cold crystallization peak was shifted by 10 ^{o}C to lower temperatures. Knowing that crystallization is a result of two distinct processes, i.e. primary nucleation and crystal growth, earlier cold crystallization is an indication of total crystallization improvement at a lower temperature. Growth rate versus temperature shows an optimum as a result of opposite trends for secondary nucleation and chain mobility; and for PLA this optimum is about 130 ^{o}C (Huang et al., 1998; Di Lorenzo, 2001; Kawai et al., 2007). However, enough

nucleation should be available for crystallization to happen at this temperature. Therefore, by increasing the L-H content, nucleation was increased and crystallization occurred closer to the optimum growth temperature. On the other hand, for 100% L-H, nucleation was much higher so that crystallization was completed below the optimum growth temperature. Similar effects have been reported for the addition of nucleating agents to PLA (Nam et al., 2006; Pan et al., 2009; Yu and Qiu, 2011).

Table 7.2. Thermal properties of the samples presented in Figure 7.3

[L-H] (%)	T_{cc} (^{o}C)	ΔH_{cc} (J/g)	ΔH_{m} (J/g)	X_c (%)
0	140.4	1.94	2.3	2.5
10	139.5	6.42	7.2	7.7
20	131.8	6.2	12.14	13.1
30	130.6	10.5	14.3	15.4
100	111.2	11.9	23.9	25.7

7.3.1.2 Isothermal crystallization

Effect of chain structure on PLA crystallization was further investigated by isothermal DSC tests between 90 to 120 ^{o}C. Isothermal crystallization temperature (T_{iso}) window was chosen based on the location of non-isothermal crystallization peaks for branched PLAs. Thermal history was removed similar to dynamic tests by keeping the samples at 200 ^{o}C for 3 min. Afterwards, they were cooled rapidly to T_{iso} and annealed at that temperature until crystallization peak was completed. In Figure 7.4, heat flow data versus time are plotted to display the crystallization peaks obtained at different isothermal crystallization temperatures for the four structures. For linear PLA, the wide crystallization peak at 90 ^{o}C was narrowed by increasing the temperature to 100 ^{o}C and widened again by increasing T_{iso} further to 110 and 120 ^{o}C, showing an optimum T_{iso} around 100 ^{o}C. In addition, crystallization induction time at 120 ^{o}C was longer than 90 ^{o}C, while the peak at 90 ^{o}C was tailed to longer crystallization times, showing that difficulty in nucleation for linear PLA at 120 ^{o}C was more significant, but at 90 ^{o}C chain mobility was the determining factor.

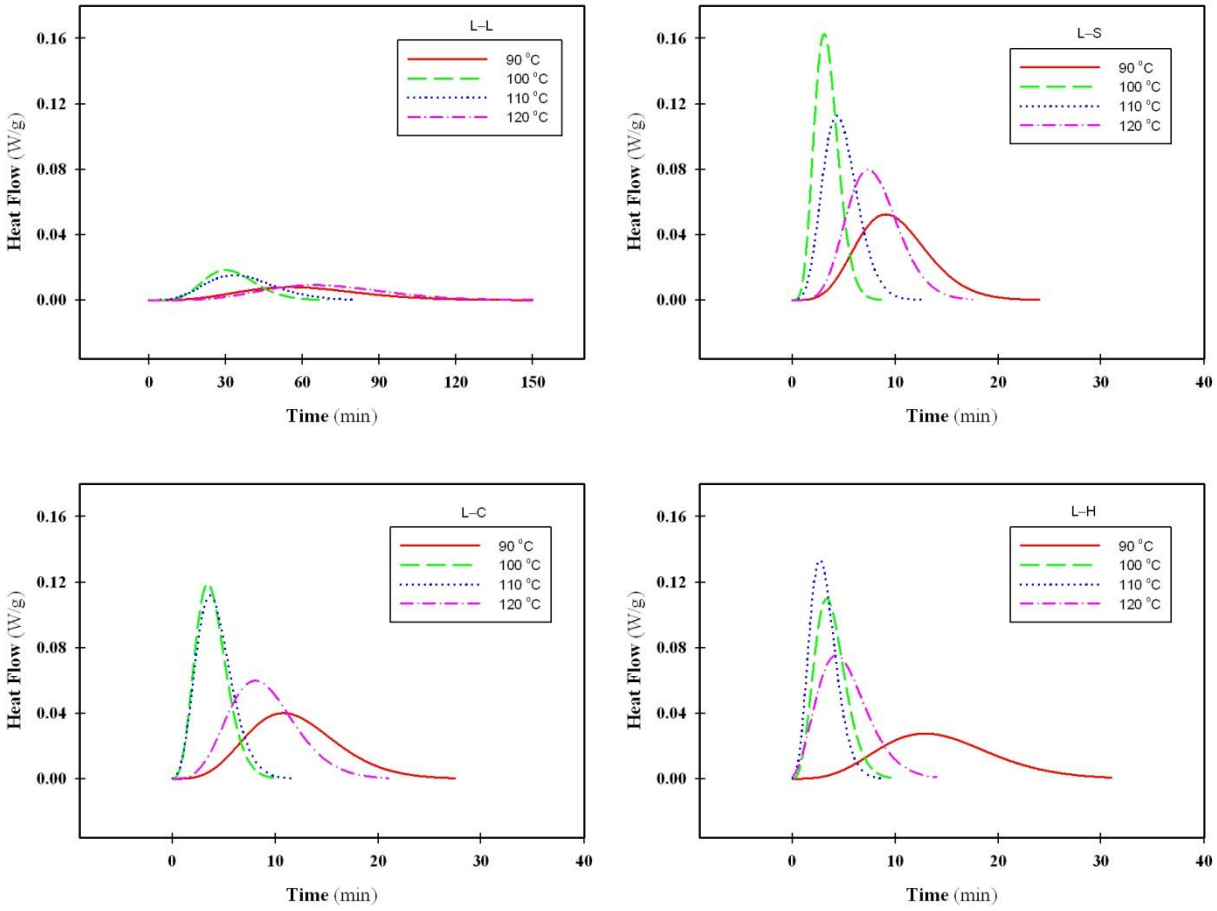

Figure 7.4. Crystallization peaks obtained by isothermally annealing the specimens at 90, 100, 110 and 120 °C

For star shaped PLA, much narrower peaks were obtained in relation to linear PLA, while a similar trend in crystallization peak narrowing and widening with temperature was observed; except that the peak for 120 °C was narrower in comparison with the peak for 90 °C. This suggests that presence of a branching point enhanced crystal nucleation at higher temperature. For comb like PLA, 100 and 110 °C peaks were almost similar, demonstrating a shift of optimum temperature to somewhere in the region between the two. Finally, for hyper branched PLA, crystallization was fastest at 110 °C, indicating an increase in optimum crystallization temperature with respect to chain architecture. Furthermore, crystallization peak obtained for T_{iso} of 90 °C was tailed at longer times as compared to star shaped and comb like PLAs, which is consistent with more restricted chain mobility at lower temperatures. On the other hand, in

comparison with linear PLA, faster crystallization of branched PLAs at this temperature suggests that better nucleation in branched PLAs prevailed better chain mobility of linear structure.

In Figure 7.5, crystallinity of samples after isothermal crystallization is plotted as a function of temperature for the linear and branched chain architectures. To calculate crystallinity values, total peak area which is equal to the enthalpy of crystallization, ΔH_c, was divided by the melting enthalpy for 100% crystalline PLA.

Based on this figure, achieved crystallinity in isothermal crystallization was a function of temperature and chain architecture. Increasing the crystallization temperature resulted in a higher crystallinity which can be associated to fewer defects found at crystal interface. Furthermore, linear chains resulted in higher crystallinity than branched ones, and hyper branched PLA with the highest level of chain branching resulted in the lowest crystallinity among branched PLAs. Therefore, branching was not in favor of total crystallinity by assuming branch points and chain ends as impurities in the system.

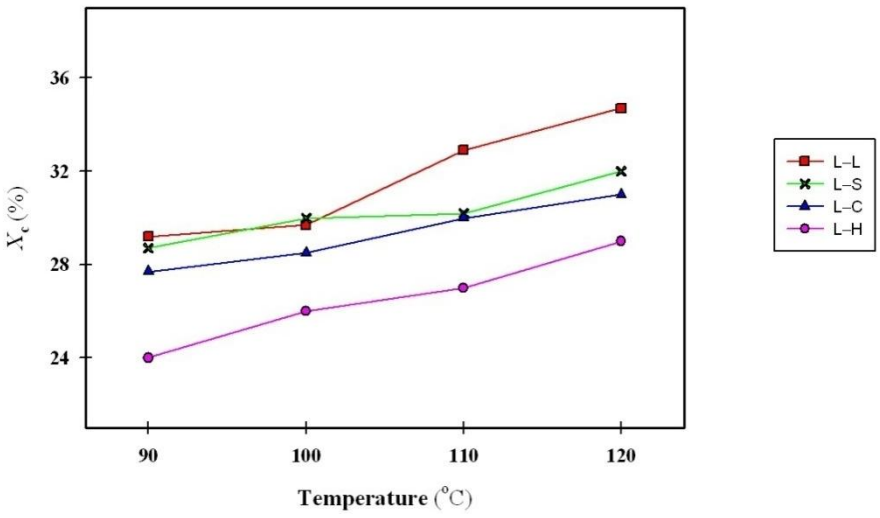

Figure 7.5. Crystallinity as a function of temperature and chain architecture for specimens isothermally crystallized between 90 to 120 °C

To better show the effect of chain architecture on isothermal crystallization kinetics, crystallization fraction was calculated as a function of time, $\alpha(t)$, by integrating the peaks at time t divided by the total peak area.

$$\alpha(t) = \frac{1}{\Delta H_c} \times \int_0^t \left(\frac{dH}{dt}\right) dt \qquad \textbf{(7.2)}$$

The resulting kinetic curves are shown in Figure 7.6. Generally, crystallization rate was slower at the two ends of temperature range and started after a longer elapsed time; for the hyper branched PLA there was a greater difference between the 90 and 120 ^{o}C curves. Also, linear PLA showed a much slower crystallization than branched PLAs.

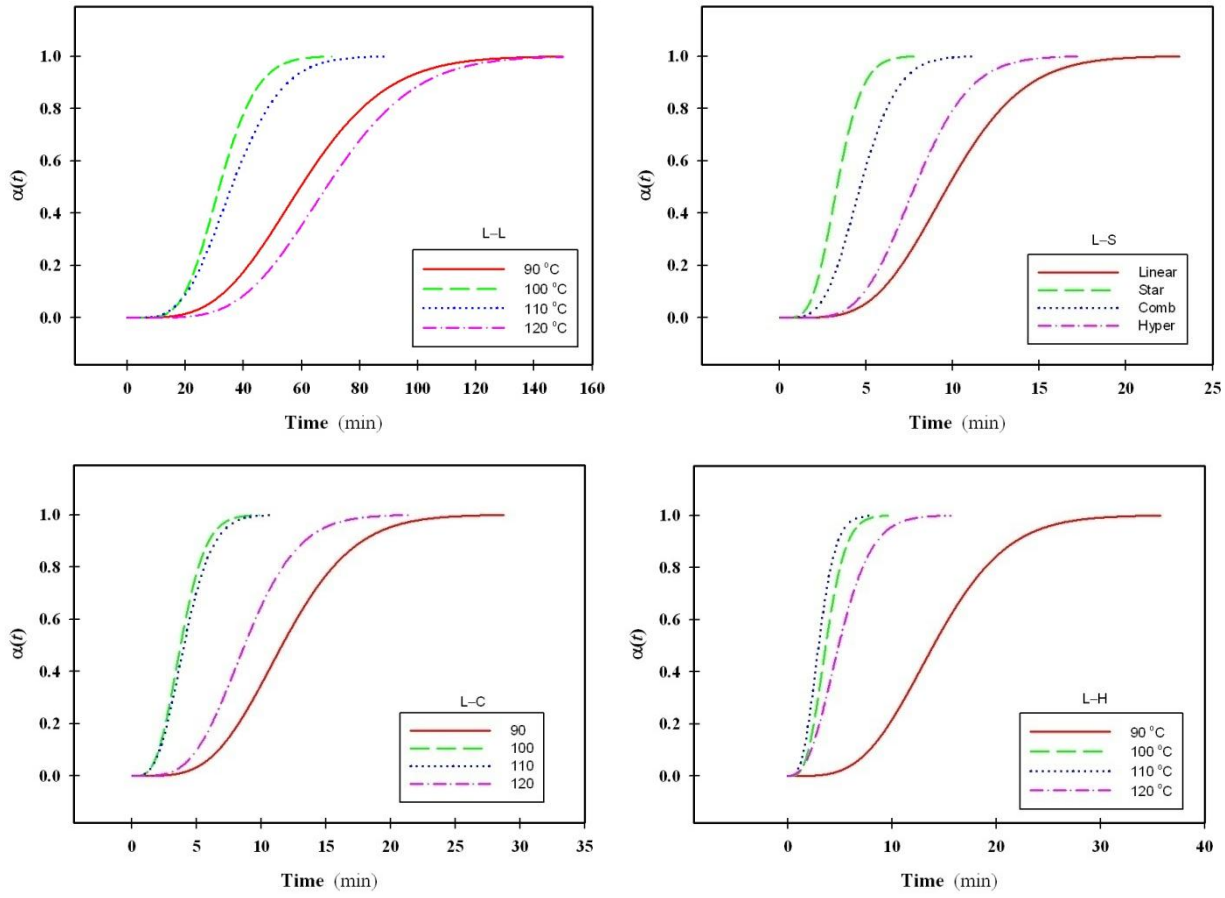

Figure 7.6. Crystallization fraction as a function of time for specimens isothermally crystallized at different temperatures

Crystallization half-time ($t_{1/2}$) is the time required to reach a relative crystallization degree of 50%. It is used commonly as an index for crystallization kinetics and can be obtained from isothermal crystallization data (Figure 7.6). Therefore, the time at which $\alpha(t)$ was equal to 0.5 was plotted as a function of crystallization temperature for different chain architectures in Figure 7.7.

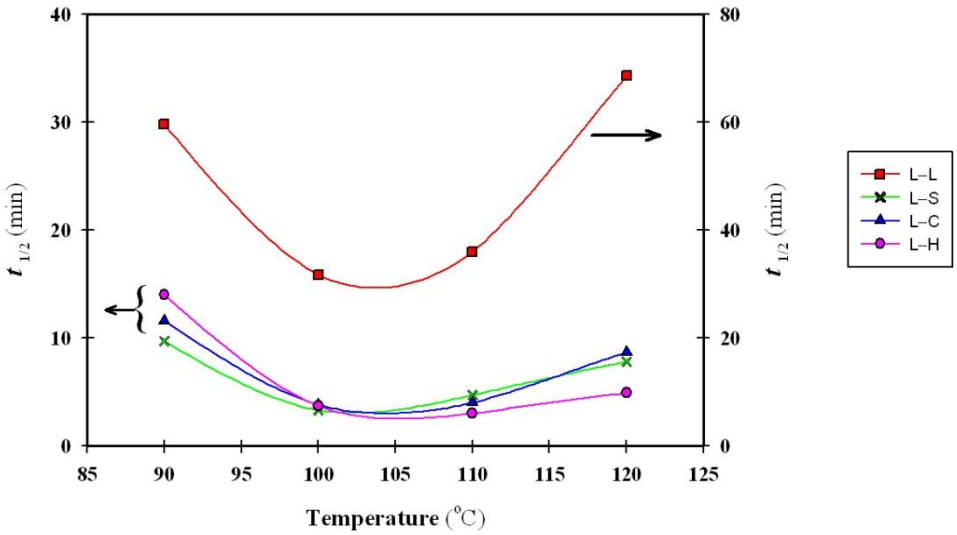

Figure 7.7. Crystallization half-time as a function of T_{iso} for PLAs with different chain architectures

$t_{1/2}$ for linear PLA decreased from 59.6 min at 90 °C to 31.7 min at 100 °C as a consequence of increased chain mobility, then it was increased to 35.9 and 68.6 min at 110 and 120 °C, respectively due to less nucleation at higher temperatures. On the other hand, $t_{1/2}$ for branched PLAs was highest at 90 °C than other investigated temperatures, ranging from 9.7 to 14 min, since crystallization is diffusion controlled at lower temperatures. By further increase of temperature to 100 °C, crystallization half-time for branched PLAs converged to 3.3-3.8 min as chain mobility was increased. At 110 °C, $t_{1/2}$ for star PLA increased from 3.3 to 4.7 min, for comb like PLA increased slightly from 3.8 to 4 min and for hyper branched PLA $t_{1/2}$ continued to decrease from 3.7 to 3 min. At 120 °C where nucleation became more important as compared to growth, hyper branched PLA had the lowest $t_{1/2}$, followed by star shaped and comb like PLA. Therefore, the temperature at which $t_{1/2}$ was minimum shifted to higher values by an increase in branching.

Avrami model is frequently used to describe the isothermal crystallization kinetics of polymers. It is expressed with the following equation:

$$\alpha(t) = 1 - \exp[-(kt)^n] \qquad \textbf{(7.3)}$$

where $\alpha(t)$ is the fraction of material transformed into crystal phase at time t as defined in Equation (7.2), n is the Avrami exponent and k is a rate constant. Equation (7.3) may also be written as:

$$\ln\left[-\ln\left[1-\alpha(t)\right]\right] = n\ln(t) + \ln k \qquad \textbf{(7.4)}$$

By plotting ln[-ln[1-$\alpha(t)$]] versus ln(t) a line is obtained with a slope equal to n and intercept with y axis equal to ln(k). This model was applied to the data presented in Figure 7.6 for $\alpha(t)$ between 0.2 and 0.8 (linear region) to obtain Avrami constants, as shown in Figure 7.8.

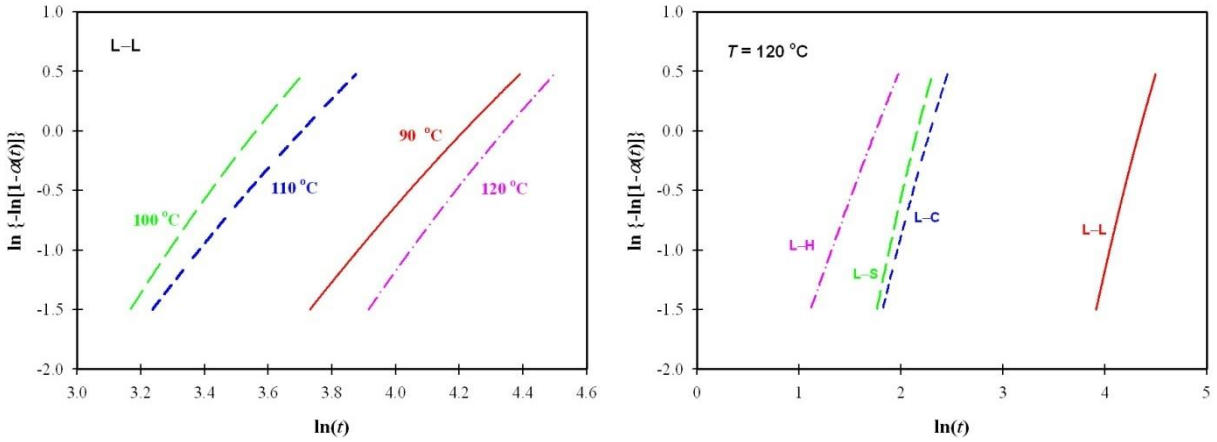

Figure 7.8. Avrami plots for a) linear PLA at different temperatures, b) different chain architectures at 120 °C

Crystallization half-times and Avrami constants are summarized in Table 7.3. n for linear and star shaped PLA was between 3 to 3.6 and for comb like and hyper branched PLA was reduced to 2.75-3.1 and 2.3-2.95, respectively. Avrami exponent depends on the mechanism of nucleation (predetermined or sporadic) and the form of crystal growth (fibrillar, discoid or spherulitic). This reduction in n with chain structure is an indication of a change in nucleation mechanism from sporadic to a combination of predetermined and spontaneous nucleation or more platelet than sphere crystals. k is also influenced by both nucleation and growth rate and is directly related to the overall crystallization rate according to Equation (7.5):

$$k = (t_{1/2}^{-1})^n \ln 2 \qquad \textbf{(7.5)}$$

Table 7.3. Avrami constants and crystallization half-times obtained from isothermal crystallization tests

	L-L			L-S			L-C			L-H		
T_{iso} (°C)	$t_{½}$ (min)	n	ln(k)	$t_{½}$ (min)	n	ln(k)	$t_{½}$ (min)	n	ln(k)	$t_{½}$ (min)	n	ln(k)
90	59.6	3.37	-14.62	9.7	3.26	-7.81	11.6	3.09	-7.96	14.0	2.95	-8.18
100	31.7	3.13	-11.59	3.3	3.3	-4.33	3.8	2.74	-4.20	3.7	2.81	-4.03
110	35.9	3.58	-12.75	4.7	3.19	-5.29	4.0	2.86	-4.16	3.0	2.67	-3.29
120	68.6	2.99	-12.56	7.8	3.6	-7.78	8.7	3.08	-7.06	4.9	2.29	-4.02

Hot stage optical microscopy was used to investigate the role of branch architecture on spherulite growth rate. For more accurate measurement, T_{iso} was set at 150 °C to have fewer spherulites that can grow to a larger size before impingement. Thin films were prepared to avoid the superposition of different crystal layers in optical microscopy images. Thermal history of the films was removed by keeping them at 200 °C for 3 min. At this temperature, only hyper branched PLA developed measurable spherulites during 15 min annealing as shown in Figure 7.9. Other structures had longer induction times and accurate measurement was not possible due to small spherulite size. Plot of spherulite radius versus time is also presented in Figure 7.9. From this plot it is clear that after an induction time and stable nuclei generation, spherulites grew at a constant rate. Spherulite growth rate was equal to 2.3 μm/min obtained from the slope of the trend line.

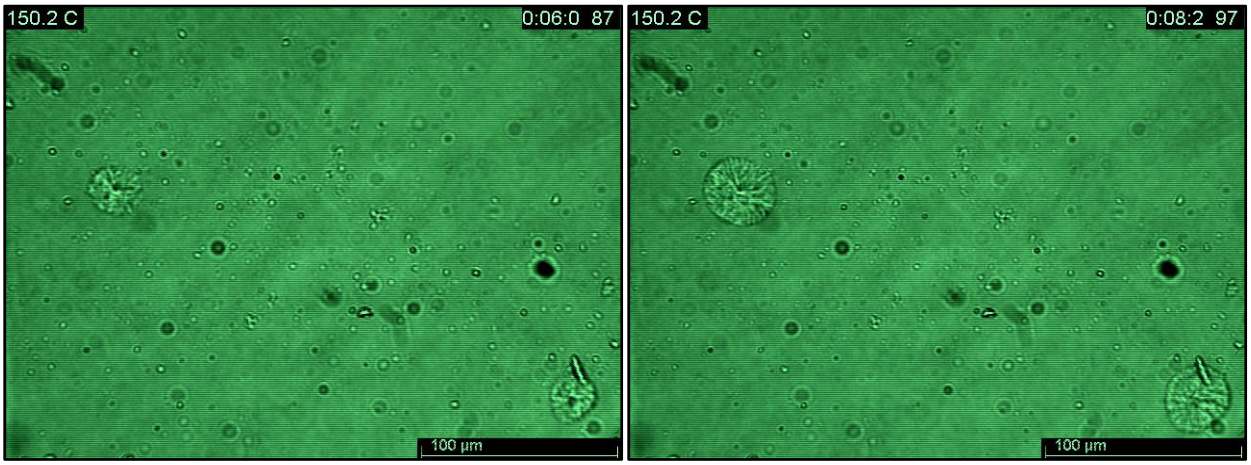

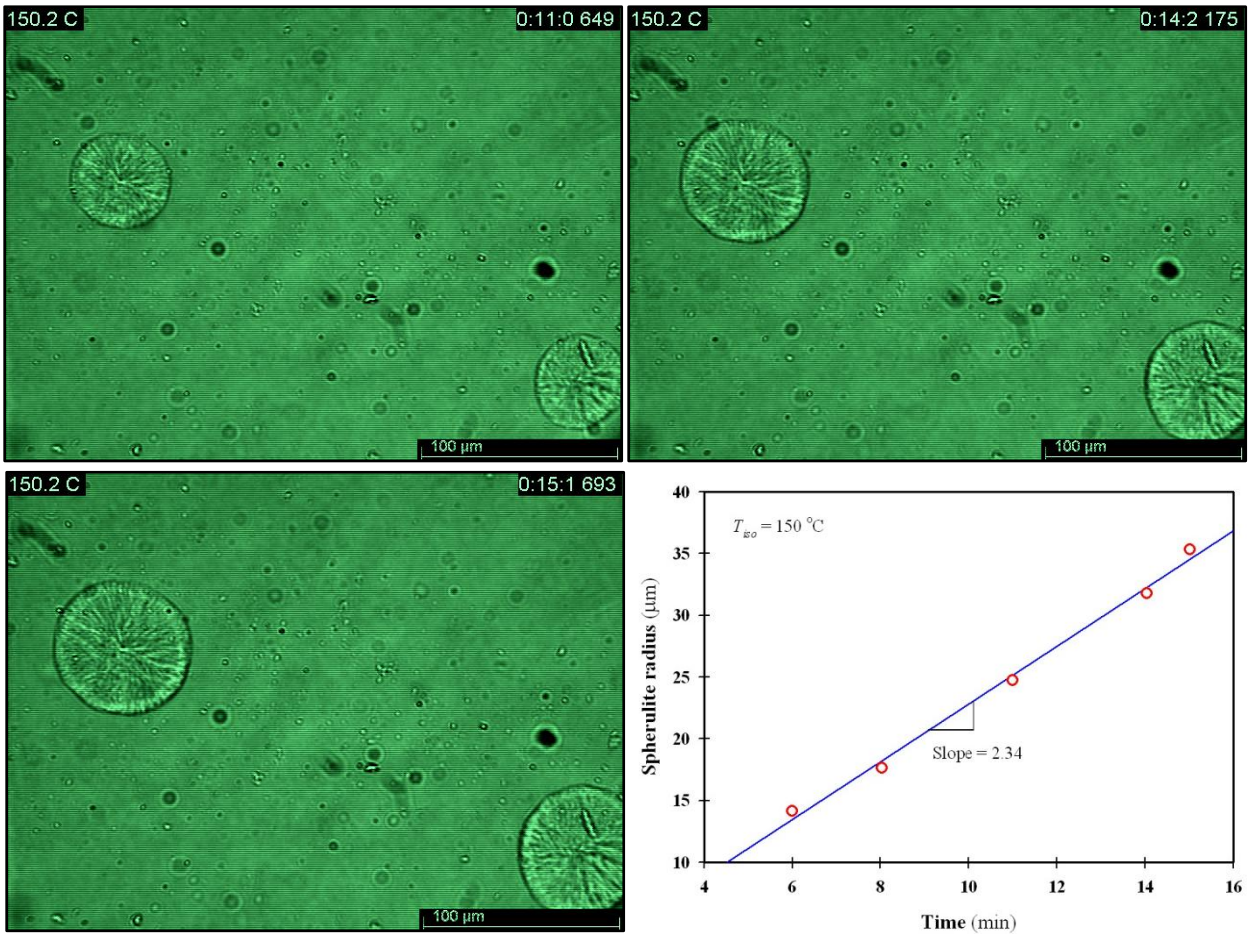

Figure 7.9. Optical microscopy images of hyper branched PLA isothermally crystallized at 150 ^{o}C and the corresponding spherulites radius vs. time plot

Isothermal crystallization temperature was reduced to 140 ^{o}C in another set of experiments to obtain measurable spherulites for other structures in the time frame of the experiment. Linear PLLA barely showed spherulites at this crystallization temperature which confirmed the lack of nucleation for this structure at high temperature. Images captured after 10 min crystallization at 140 ^{o}C as well as the plot of spherulite radius against time are presented in Figure 7.10. Each data point was based on the average of three spherulite radius at a given time. From the images it is clear that hyper branched PLA had higher spherulite density but spherulite size was smaller compared to other branched structures. Star shaped and comb like structures had almost similar crystal morphology at these conditions. Hyper branched PLA showed lowest growth rate equal to 5.7 µm/min while star and comb PLA revealed higher growth rates, equal to 6.4 and 7.3 µm/min, respectively. In addition, extrapolation of data to zero radius (intercept with time axis) confirms that crystallization started earlier for hyper branched PLA. These results are

due to an improved nucleation process, a restricted chain diffusion as well as an increased rejection of non-crystal forming parts at higher branch content.

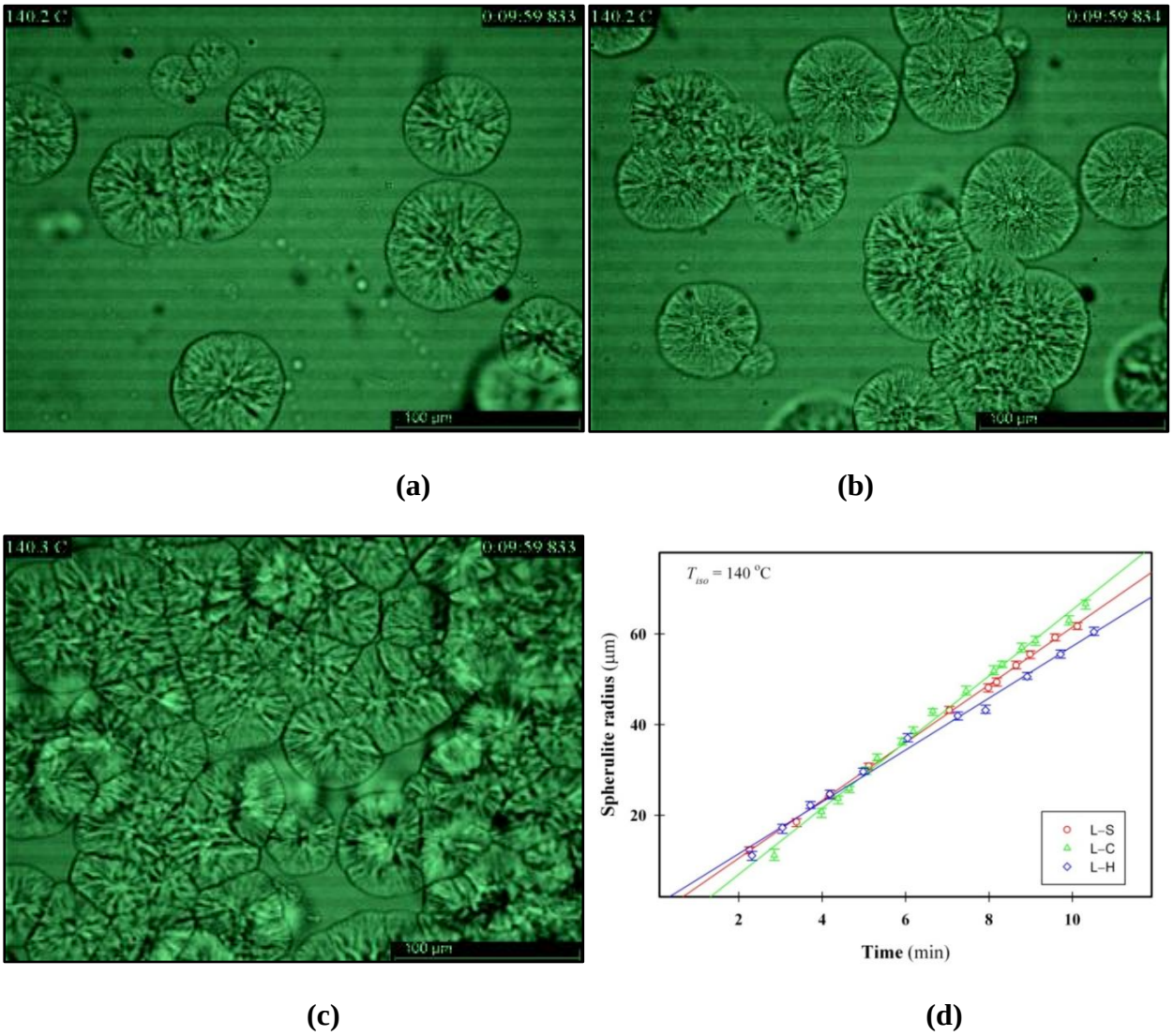

Figure 7.10. Optical microscopy images for isothermal crystallization at 140 °C after 10 min, a) L-S, b) L-C, c) L-H, d) spherulite radius vs. time for the same crystallization conditions

It is to be noted that spherulite growth rate of hyper branched PLA was increased by a factor of 2.5 when temperature was reduced from 150 to 140 °C. Thus, increased secondary nucleation explained by Lauritzen-Hoffman theory overcame reduced chain diffusion to growth front as temperature was decreased.

7.3.2 Stereocomplex crystallization

Another aspect of PLA crystallization is stereocomplex formation between stereochemically different chains. Effect of branch architecture on stereocomplex formation between branched PDLA and linear PLLA as well as the effect of stereocomplex crystals on PLLA homocrystallization were studied. Blends of linear PLLA with star shaped, comb like and hyper branched PDLA were prepared with PDLA concentrations of 5, 7 and 10 wt.%. Specimens were melted for 3 min at 240 ^{o}C and then they were cooled to 190 ^{o}C and isothermally crystallized. Stereocomplex melting peaks obtained by heating the samples to 240 ^{o}C are reported Figure 7.11.

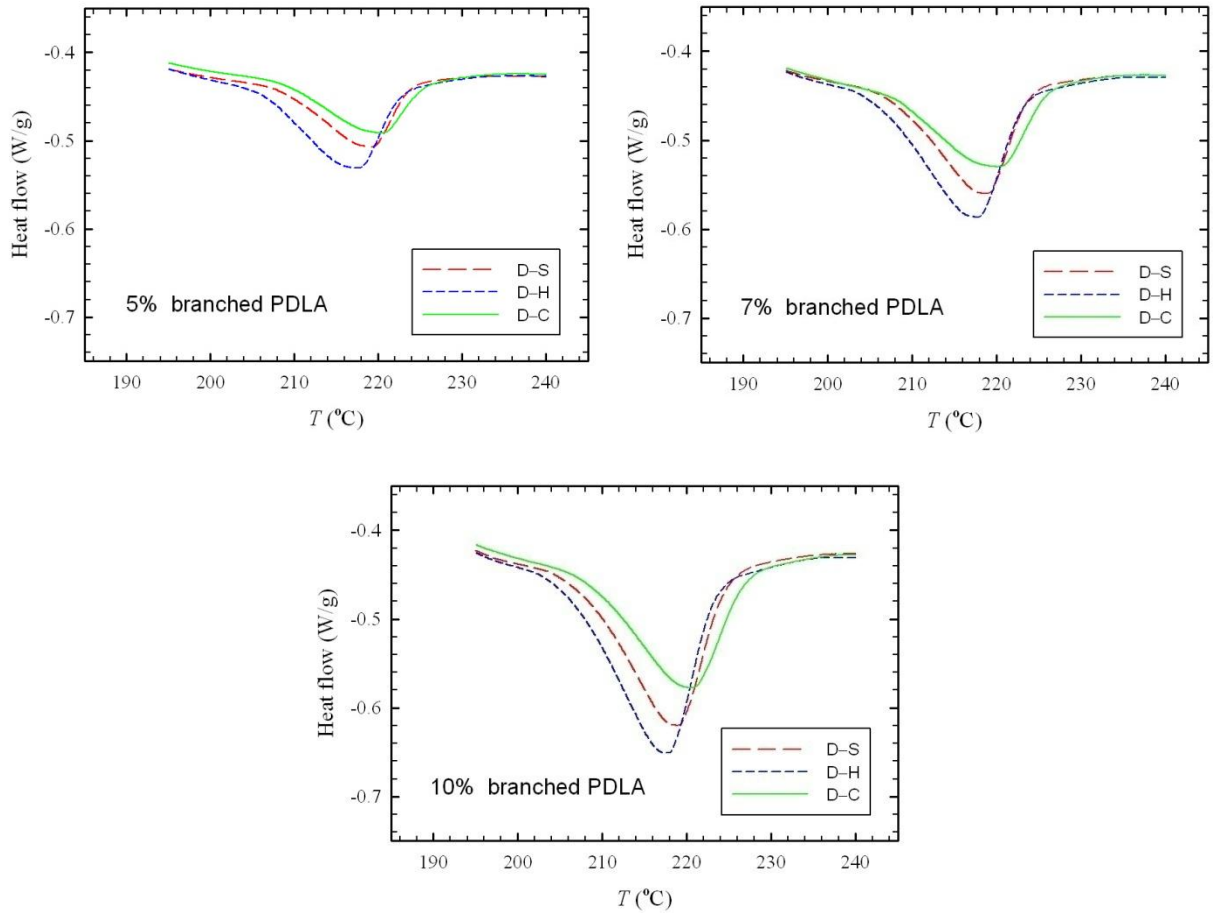

Figure 7.11. Stereocomplex melting peaks for blends of linear PLLA with branched PDLA at different branched PDLA concentrations

Thermal properties obtained from these plots are summarized in Table 7.4. Equations (7.6) and (7.7) were used to calculate the crystallinity in the form of stereocomplex and the yield of stereocomplex formation in relation to the co-crystalizable fraction, respectively:

$$X_{st}(\%) = \frac{\Delta H_{m,st}}{\Delta H_{100\%,st}} \times 100 \quad \textbf{(7.6)}$$

$$Y_{st}(\%) = \frac{\Delta H_{m,st}}{\Delta H_{100\%,st} \times 2 f_{PDLA}} \times 100 \quad \textbf{(7.7)}$$

where $\Delta H_{m,st}$ is the stereocomplex melting enthalpy, $\Delta H_{100\%,st}$ is the melting enthalpy of 100% crystalline PLA in the stereocomplex form equal to 146 J/g (Tsuji et al., 1992), and f_{PDLA} is the PDLA fraction in the system. The coefficient 2 in Equation (7.7) is to account for equal amounts of PLLA and PDLA chains that can participate in the stereocomplex formation process.

Table 7.4. Thermal properties of the samples presented in Figure 7.11

PDLA	f_{PDLA}	T_m (°C)	$\Delta H_{m,st}$ (J/g)	X_{st} (%)	Y_{st} (%)
D-S	0.05	219.1	6.9	4.7	47
	0.07	218.8	10.1	6.9	49.4
	0.1	218.9	14.8	10.1	50.7
D-C	0.05	220.4	6.6	4.5	45
	0.07	220.1	9.6	6.6	47
	0.1	220.6	13	8.9	44.5
D-H	0.05	217.5	8.6	5.9	59
	0.07	217.6	12.4	8.5	60.6
	0.1	217.6	16.9	11.6	57.9

For all the three branched structures, by increasing the PDLA content more stereocomplex was formed. Also at each PDLA concentration, stereocomplex crystallinity for star and comb PDLA was almost similar, but was higher for hyper branched PDLA with an average 10% higher yield. This is contrary to the relation between homocrystal content and branch structure observed in branched PLLA crystallization. Considering that at 190 °C, chain mobility is much higher than 90-120 °C, higher chain branching is in favor of stereocomplex formation by facilitating nucleation. On the other hand, stereocomplex melting point showed a different relationship with branch structure. T_m was lowest when PDLA had hyper branched structure and was highest for PDLA having comb like branch. For star shaped PDLA, T_m was in between the two, but closer to

that of comb like PDLA. Therefore, it is likely that hyper branched structure resulted in thinner and less perfect but more crystals while star shaped and comb like structures produced thicker and more perfect but less stereocomplex crystals.

Hyper branched PDLA was also employed to nucleate PLLA homocrystallization. 95 L-L/5 D-H blend was examined in two different procedures. In the first process, stereocomplex was initially formed in isothermal mode at 190 ^{o}C and consequently the specimen was cooled to 20 ^{o}C at a rate of 10 ^{o}C/min to observe homocrystallization in cooling. At the end, sample was heated back to 240 ^{o}C at a rate of 10 ^{o}C/min to observe cold crystallization, homocrystal melting and stereocomplex melting. Second procedure was similar except that instead of initial isothermal stereocomplex formation, stereocomplex was formed directly during the cooling cycle from the melt. DSC thermograms for these two thermal procedures are shown in Figure 7.12.

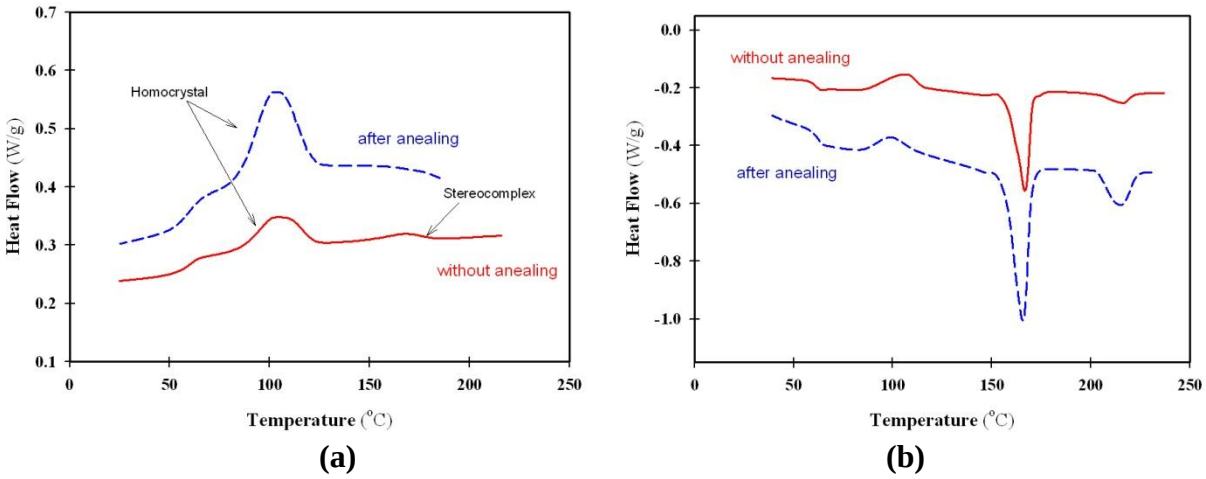

Figure 7.12. DSC thermograms of a) cooling and b) heating cycles of a L-L/D-H blend containing 5% PDLA

When stereocomplex was initially formed during isothermal crystallization step, a large crystallization peak in the cooling cycle with an enthalpy of 20.5 J/g and peak temperature of 102 ^{o}C was observed. On the other hand, when stereocomplex was not formed in an isothermal step, two peaks appeared in the cooling cycle. The smaller peak located at 165 ^{o}C can be attributed to stereocomplex formation during the cooling process. Stereocomplex crystals formed in this way nucleated PLLA homocrystallization. However, crystallization enthalpy was 7.2 J/g which is less than what was achieved in the first process. This is explained by less stereocomplex crystals that

were formed in a cooling cycle. In the heating cycle, both samples showed cold crystallization peaks which was expected due to the unfinished crystallization from the melt and nucleation role of stereocomplex crystals. Also for each sample, two melting peaks were observed, larger peaks at 169 ^{o}C which correspond to homocrystal melting and smaller peaks at 217 ^{o}C which are associated to stereocomplex melting. Homocrystal melting enthalpy for directly cooled sample was 15 J/g and for initially annealed one was 27.5 J/g. Also, annealed sample had a higher stereocomplex melting enthalpy since it was formed at isothermal crystallization step.

Nucleation role of stereocomplex crystals in 95 L-L/5 D-H blend was further investigated by optical microscopy observations. Blend was isothermally crystallized first to form stereocomplex and cooled at a rate of 10 ^{o}C/min. Captured images are shown in Figure 7.13. Figure 7.13-a is obtained after isothermal crystallization, clearly showing the stereocomplex crystals. Primarily formed stereocomplex crystals nucleated PLA homocrystallization at lower temperatures, as demonstrated in Figure 7.13-b. Surface of stereocomplex spherulites were covered with homocrystals while smaller homocrystal spherulites became visible. These smaller spherulites were probably nucleated by isolated stereocomplex crystallites since in the absence of PDLA, linear PLLA (L-L) did not form such structures as depicted in Figure 7.2 for 110 ^{o}C.

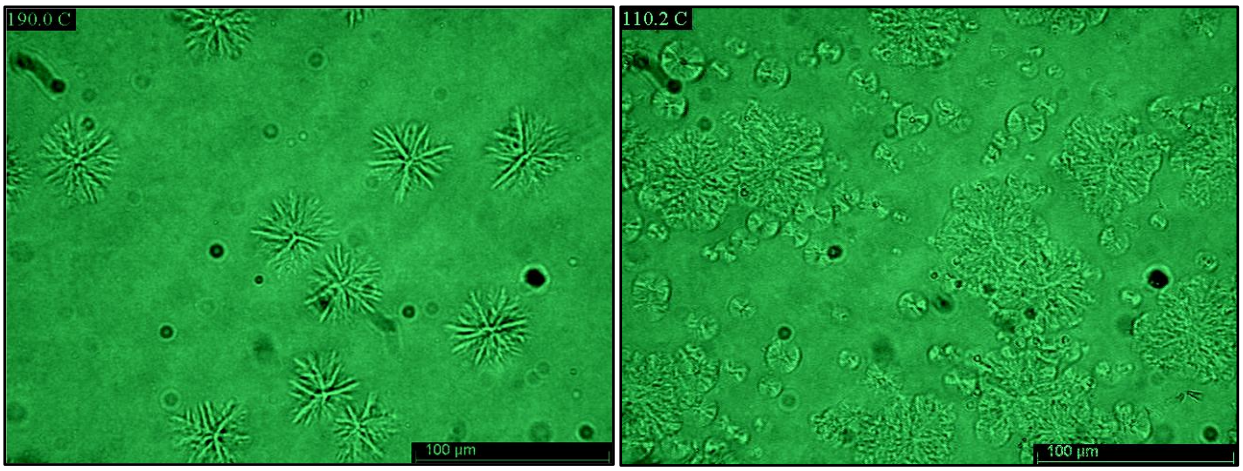

(a) **(b)**

Figure 7.13. Optical microscopy images of L-L/D-H blend containing 5% PDLA, a) annealing, b) cooling after annealing

An interesting observation to be noted is the clear difference in the internal morphology of stereocomplex and homocrystal spherulites. In Figure 7.14, two sets of optical microscopy images are presented which were captured at different spherulite growth stages of L-H (top) and

95 L-L/5 D-H blend (bottom) at 150 and 190 ^{o}C, respectively. As it is evident from these images, PLLA crystallization resulted in compact and dense spherulites with a constantly growing radius, while in the stereocomplex type initially few lamellae were formed in an open structure with irregular edges, then new lamellae were grown as side branches by fanning out and filling the amorphous space inside the spherulite. The difference in internal spherulite morphology may be the consequence of dissimilar crystallizable portions of the material in the two systems. For homocrystallization, only PLLA chains have to be transported from the amorphous to crystal phase while for stereocomplex crystals, lower PDLA concentration as well as the necessity for coupling of two components (L and D chains) make the crystallization process more difficult.

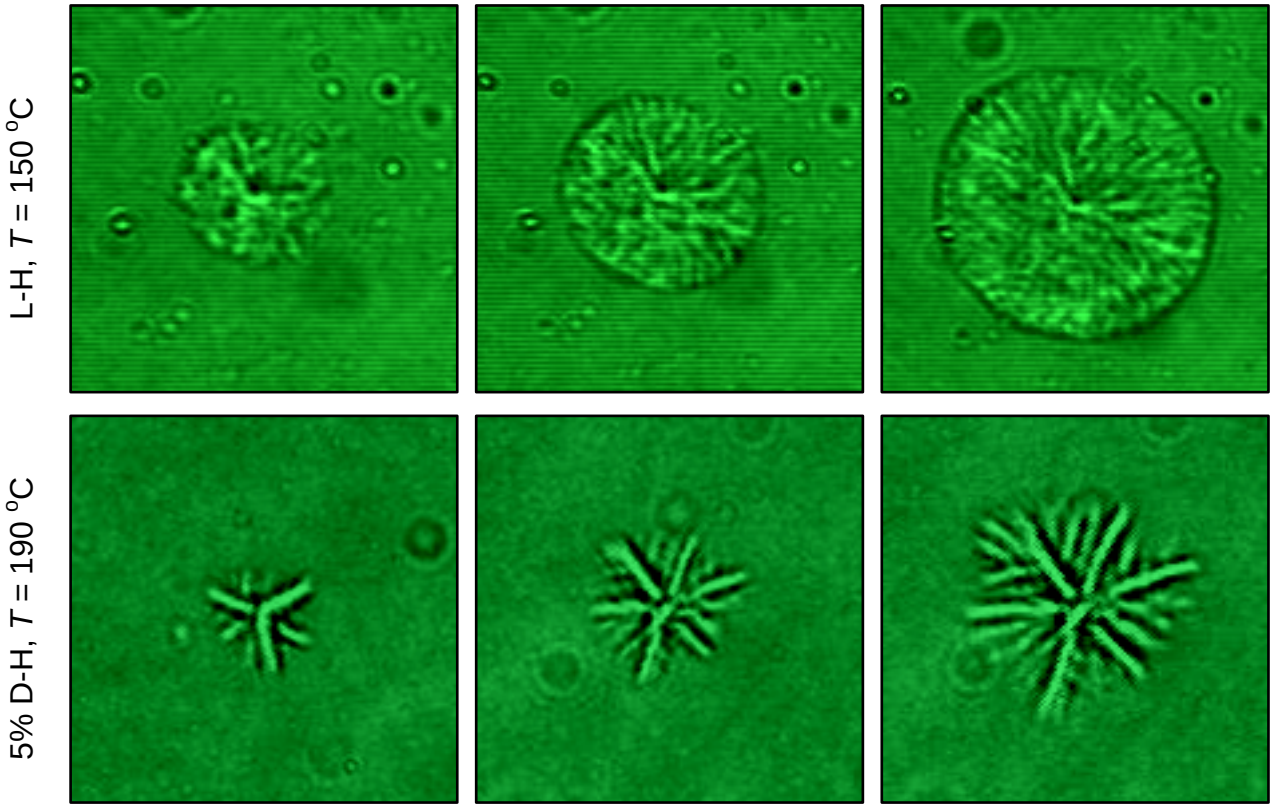

Figure 7.14. Spherulite shape at different growth stages for homocrystal (top) and stereocomplex (bottom)

7.4 Conclusions

Positive effect of chain branching on crystallization of PLA in the form of homocrystal and stereocomplex was shown in this study. Homocrystallization of branched PLLAs was enhanced in dynamic mode as evidenced by appearance of crystallization peak upon cooling and

intensified cold crystallization in heating cycle of DSC tests as well as increased spherulite density observed by optical microscopy. In addition blending branched PLLA with linear one improved the dynamic crystallization of the latter. Crystallinity was multiplied by a factor of 6 and cold crystallization peak showed a significant shift by 10 ^{o}C to lower temperatures in a blend containing 30% hyper branched PLLA. Isothermal DSC tests also confirmed the superior crystallization kinetics of branched PLAs in relation to linear one. $t_{1/2}$ was reduced between 4 to 14 folds depending on the branch architecture in the investigated range of crystallization temperature. Also, optimum T_{iso} shifted to higher values by increased branching showing a better nucleation process at higher temperatures. Meanwhile, higher branched content decreased total crystallinity by adding to the share of non-crystallizable parts in the bulk. By applying the Avrami model to isothermal data a reduction of Avrami exponent by increased branching was noticed which suggests the change of nucleation mechanism and deviation from three dimensional growth. Spherulite radius measurements from optical microscopy images revealed that higher branching was not in favor of growth rate which can be attributed to more restricted chain segments. From the investigation of stereocomplex formation between branched PDLAs and linear PLLA in isothermal mode it was found that contrary to homocrystallization, stereocomplex crystallinity was higher for more branched PDLA since at very high crystallization temperatures, nucleation is the dominant factor. Stereocomplex was used also to nucleate PLLA homocrystallization. Dynamic DSC tests and optical microscopy characterization both confirmed nucleation role of stereocomplex crystals for homocrystal formation. Besides, internal spherulite morphologies for stereocomplex and homocrystal were quite different with a compact spherulite for homocrystal and open branched morphology for stereocomplex.

CHAPTER 8. ARTICLE 4: ENHANCED FILM BLOWING OF POLYLACTIDE BY INCORPORATING BRANCHED CHAINS AND STEREOCOMPLEX CRYSTALS

Sahar Nouri, Charles Dubois, Pierre G. Lafleur

CREPEC, Chemical Engineering Department, Ecole Polytechnique, C.P. 6079, Succ. Centre ville, Montreal, QC, H3C 3A7 Canada

ABSTRACT Chain architecture is an influential parameter in melt processing of polymeric material. In this study effect of different chain structures on polylactide (PLA) film blowing process and on the final film properties was investigated. Blends of linear PLA with three branched poly(L-lactide)s with 4-arms star shaped, comb like and hyper branched structures were prepared by twin screw extruder. In another series of blending, poly(D-lactide) of these branched structures were used to obtain stereocomplex crystal. Operating window of blends were determined in a series of film blowing process experiments with different blow up and take up ratio and results were compared to linear PLA as a reference. Moreover, different characterization techniques were applied to determine the properties of produced films. It was found that addition of branched architecture and presence of stereocomplex in a linear PLA matrix result in a greater operating window for film blowing and improve mechanical and crystallization properties of blown films.

KEYWORDS Polylactide, branched, stereocomplex, film blowing

8.1 Introduction

PLA is a biopolymer that has been increasingly used in recent years as a sustainable packaging option. Especially thin films for flexible packaging applications are among the most popular forms of PLA products. Properties of thin films depend on polymer characteristics as well as processing conditions. PLA film properties are shown to depend on the level of molecular orientation achieved during the film production process (Ou and Cakmak, 2008; Stoclet et al., 2010; Wang et al., 2011; Stoclet et al., 2012; Tabatabaei and Ajji, 2012; Liu et al., 2014; Wang et

al., 2015). Film blowing is the most common way of producing thin plastic films. Compared to film casting process, better mechanical properties due to biaxial orientation, flexibility of producing different widths by a single die without trimming and annular shape of the product are among the advantages of this processing method. However, blown film processing of material with low melt strength and absence of strain hardening behavior, such as for PLA, is challenging. Based on the literature, commercial PLAs has a very narrow stable production window which is due to its linear chain structure and lack of strain hardening. To our knowledge, only few studies have dealt with improving stability and operating window of pure PLA film blowing process and most of the research work have focused on processing of PLA blends with other materials or enhancement of final film properties (Sirisinha and Somboon, 2012; Mallet et al., 2014) . Enhanced orientation in film blowing process was employed to increase barrier properties of PLA/layered silicate nanocomposite films. Orientated clay platelets in PLA films were shown to decrease oxygen and water vapor permeability up to 50% and CO_2 permeability up to 80% (Thellen et al., 2005; Zenkiewicz et al., 2010). Plasticizers such as adipate and citrate esters where used to prepare PLA/thermoplastic starch (TPS) biodegradable blown films (Shirai et al., 2013). Biodegradable agricultural mulch films have also been introduced recently based on the film blowing of PLA/poly(hydroxibutyrate) (PHB) blends compatibilized by maleic anhydride (MA). Biodegradation rate was increased by 45% compared to virgin PLA films (Jandas et al., 2013). Combination of polydiethylene glycol adipate as plasticizer and acrylic impact modifier was shown to effectively increase the elongation at break as well as the tear strength of PLA blown films (Zhang et al., 2014). Two main approaches to improve processability of PLA were internal cooling of the die mandrel (Tweed, 2006; Mallet et al., 2014) and using additives such as chain extender, plasticizer and nucleating agent (Mallet et al., 2014). However, processability enhancement of pure PLA through its chain structure modification for film blowing process has not been reported. In this study, homopolymer and stereocomplex PLAs with different chain architecture were used for the first time to enhance its film blowing processability.

8.2 Experimental

8.2.1 Materials

PLLA and PDLA with different branched architectures were synthesized by ring-opening polymerization of L-lactide and D-lactide (Purac Biochem, The Netherlands), respectively.

Pentaerythritol and Triglycerol (Sigma-Aldrich) were used as initiator to prepare star shaped and comb like polymers, while Glycidol (Sigma-Aldrich) was used as initiator-comonomer to produce hyper branched structure. Molecular weights of aproximately 125 kg/mol were obtained in all cases by adjusting the initiator's concentration based on the number of their hydroxyl groups. Polymerization procedure is explained in more details in a previous paper by this group (Nouri et al., 2015). In addition, a commercial linear PLLA (4032D from NatureWorks) with a molecular weight of 101 kg/mol was used in this study as a reference and for blending purpose.

8.2.2 Blending

Different blends of synthesized branched polymers with linear PLA were prepared by melt blending by a Leistritz ZSE 18mm co-rotating twin-screw extruder. Prior to the process, polymers were dried at 80 ^{o}C for 12 hours. Operating temperature of 190 ^{o}C and screw speed of 100 rpm was used to prepare the blends. In the case of linear/branched PLLA blends, branched PLLA concentration was set at 30%. For linear PLLA/branched PDLA, blends were prepared with 5 and 7% of branched PDLA. Theses concentrations were selected based on the extent of increase in viscosity of linear PLLA resulted from the addition of branched PLLA or PDLA (Nouri et al., 2015).

8.2.3 Film blowing

The films were prepared using a Labtech Engineering Extrusion Line having a single-screw extruder with 20 mm screw diameter and length/diameter ratio of 30. An annular die with a diameter of 50 mm and 1.5 mm die gap was connected to the extruder to form the tube. Different take-up ratios (TUR) and blow up ratios (BUR) were obtained by adjusting the winding speed and amount of air in the bubble, respectively. Temperature profile was selected starting from the end point of PLA melting peak for the feeding zone and increased for the next zones (see Table 8.1). For samples containing stereocomplex the temperature was increased by 10 ^{o}C in each zone.

Table 8.1: Temperature profile of film blowing extruder

Material	Feeding	Melting	Compression	Die
PLLA	180 ^{o}C	190 ^{o}C	190 ^{o}C	190 ^{o}C
PLLA+PDLA	190 ^{o}C	200 ^{o}C	200 ^{o}C	200 ^{o}C

8.2.4 Characterizations

Differential scanning calorimetry (DSC) by TA instrument DSC Q1000 was performed to study the post process crystallization of the films. Cold crystallization and melting of homocrystals and stereocomplex crystals were examined in dynamic heating mode. Samples were heated from 20 ^{o}C at a rate of 10 ^{o}C/min to 200 ^{o}C for PLLA and 240 ^{o}C for PLLA/PDLA blends. X-ray diffraction (XRD) measurements were performed using Bruker D8 Discover apparatus. The generator was set up at 40 kV and 40 mA and a copper CuKα radiation (λ=1.54056 A°) was selected. The samples were scanned in the 2θ range of 10 to 30 degree under scanning rate of 0.05 °/s to identify PLA crystalline structure. Afterward, at 2θ corresponding to observed peaks, φ scan at the rate of 1^{o}/s was performed to estimate crystal orientation. 2D-WAXD measurements were performed out using a Bruker Venture diffractometer equipped with a Photon 100 CMOS Detector, a Helios MX optics and a Kappa goniometer. The film - detector distance was 70 mm, and the data collection was carried out in 1024 x 1024 pixel mode with exposition of 300s. To compare optical properties of the produced films, haze measurement was performed by Perkin-Elmer Lambda 1050 High Performance Spectrometer in the wavelength range of 300 to 800 nm. This spectrometer has a 150 mm integrating sphere with a small port fraction (less than 5%). Light trap module was used to eliminate specular reflection and measure the transmitted light scattered more than 2.5° from the axis of the incident light. The tensile testing of films was carried out using INSTRON-3365 (USA). Young modulus, tensile strength and elongation at break were measured by extending rectangular specimens of 25 mm wide and 75 mm long at a speed of 5 mm/min.

8.3 Results and discussion

8.3.1 Film blowing process

First of all, to adjust the screw speed for obtaining the desired film thickness, it was necessary to determine the relationship between screw speed and material flow rate. Therefore, a series of extrusion tests were done using linear PLLA at different screw speeds, starting form 10 rpm and increasing to 145 rpm. Flow rate data were calculated by weighting the material exited from the die during 1 to 3 min (depending on screw speed). By plotting the flow rate versus screw speed as depicted in Figure 8.1, a linear relation between these parameters was obtained which is expressed by Equation (8.1):

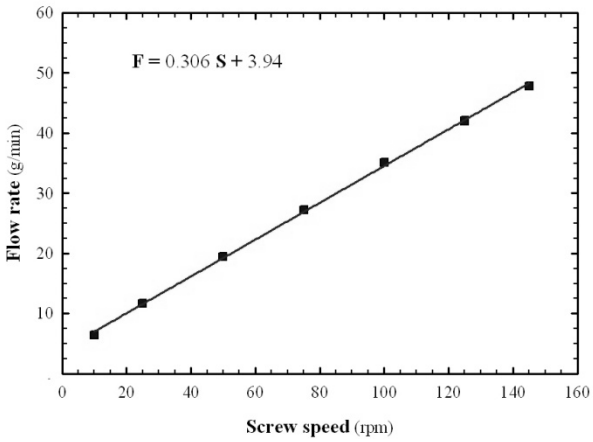

Figure 8.1 Flow rate verses screw speed in film blowing machine

$$F = 0.306S + 3.94 \quad \textbf{(8.1)}$$

where F is flow rate in g/min and S is screw speed in rpm. The material exiting the die per unit time is equal to the solid film passing the nip rolls. Therefore Equation (8.2) applies:

$$F = V_d s_d \rho_m = \pi D_b V_n T \rho_s = 2W_{lf} V_n T \rho_s \quad \textbf{(8.2)}$$

where V_d is the material speed at the die exit, s_d is the die gap area, ρ_m is melt density, D_b is bubble diameter, V_n is the nip roll speed, T is film thickness, ρ_s is solid density and W_{lf} is layflat width. Assuming that melt and solid densities are not very different, film thickness can be calculated from Equation (8.3):

$$T = \frac{F}{2W_{lf}V_n\rho} = \frac{0.306S + 3.94}{2W_{lf}V_n\rho} \quad \textbf{(8.3)}$$

This relation was used to keep the film thickness in a desired range to have comparable data for different operating conditions. It should be noted that flow rate and viscosity have an inverse relationship; therefore, for blends with different viscosities than linear PLLA, Equation (8.3) was used to estimate the starting conditions. Blow up ratio (BUR) and take up ratio (TUR) are two parameters commonly used to determine the operating window in film blowing process and are measures of extension and orientation in transverse and machine direction, respectively. BUR is the ratio of bubble diameter to die diameter and is obtained from Equation (8.4):

$$BUR = \frac{D_b}{D_d} = \frac{2W_{lf}}{\pi D_d} \quad \textbf{(8.4)}$$

TUR is the ratio of nip roll speed to material speed at die exit and can be calculated according to Equation (8.5):

$$TUR = \frac{die\ gap}{BUR \times T} \quad \textbf{(8.5)}$$

Reference PLA and modified blends were processed at different BUR and TUR to determine the stable region. Stability was primarily determined visually from bubble shape. Different types of bubble instability were observed as illustrated in Figure 8.2, including draw resonance, helical instability and frost line variation.

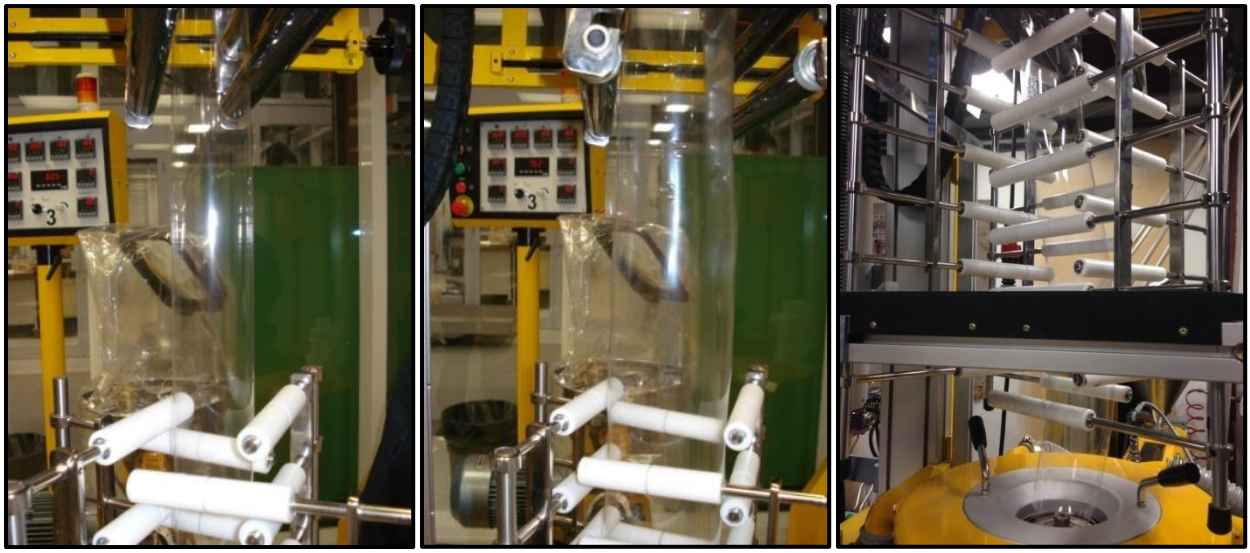

(a) (b) (c)

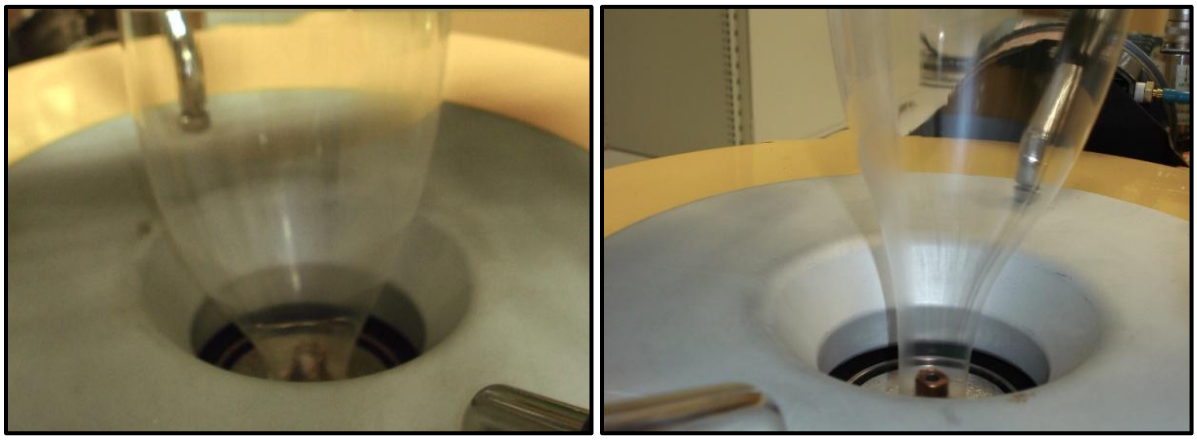

(e) (f)

Figure 8.2. a) Stable bubble, b) draw resonance, c) helical instability, d and e) frost line variation

In addition, in cases that unstable condition was not verified visually, bubble radius (from layflat width) and film thickness were measured at every 30 cm along the films to determine more accurately stable conditions. In Figure 8.3, typical graphs showing unstable conditions based on thickness and bubble radius variation along the film are presented. Boundaries for stable conditions were assumed 10 μm and 2.5 mm tolerance from the average for thickness and radius, respectively.

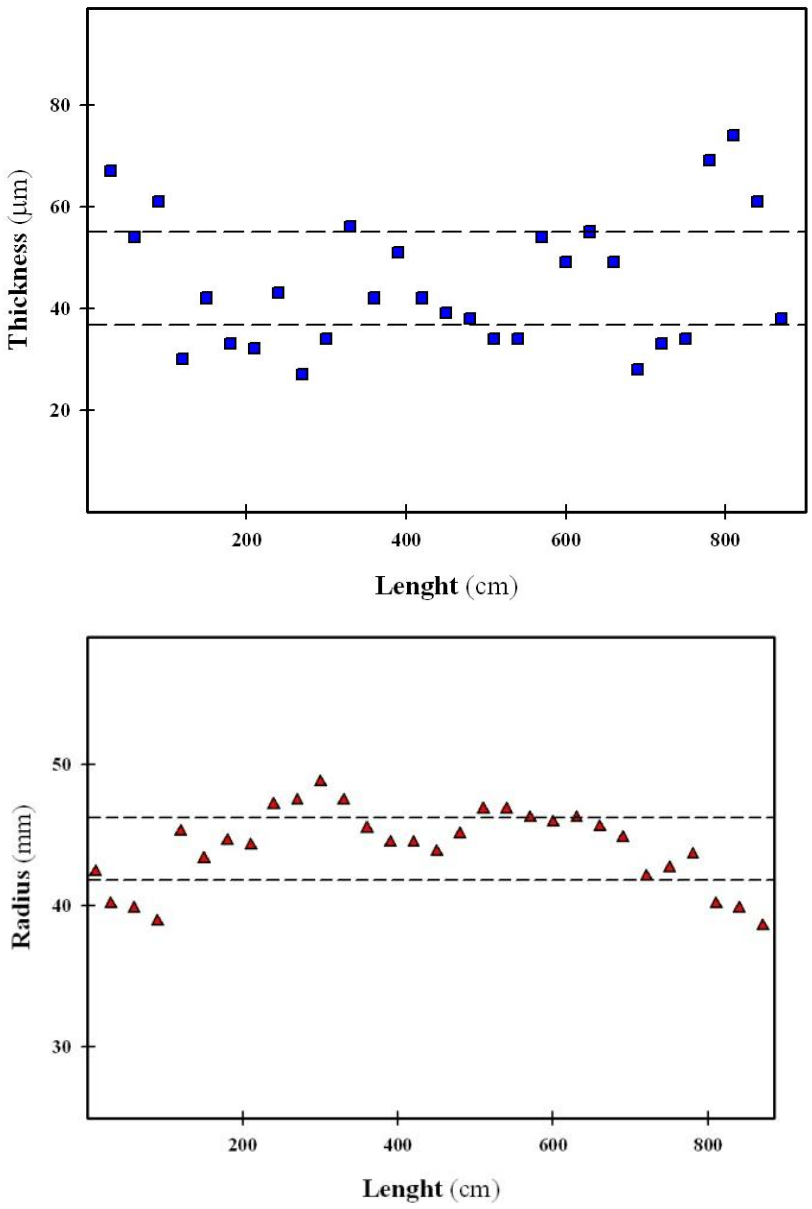

Figure 8.3. Examples of unstable process based on the variation of film thickness and bubble radius

According to the mentioned criteria, process stability maps were produced for each material by graphing the stable and unstable conditions in a BUR-TUR plot. Figure 8.4 shows the stability map obtained for neat linear PLA and its blends with 30% branched PLLA in different chain architectures.

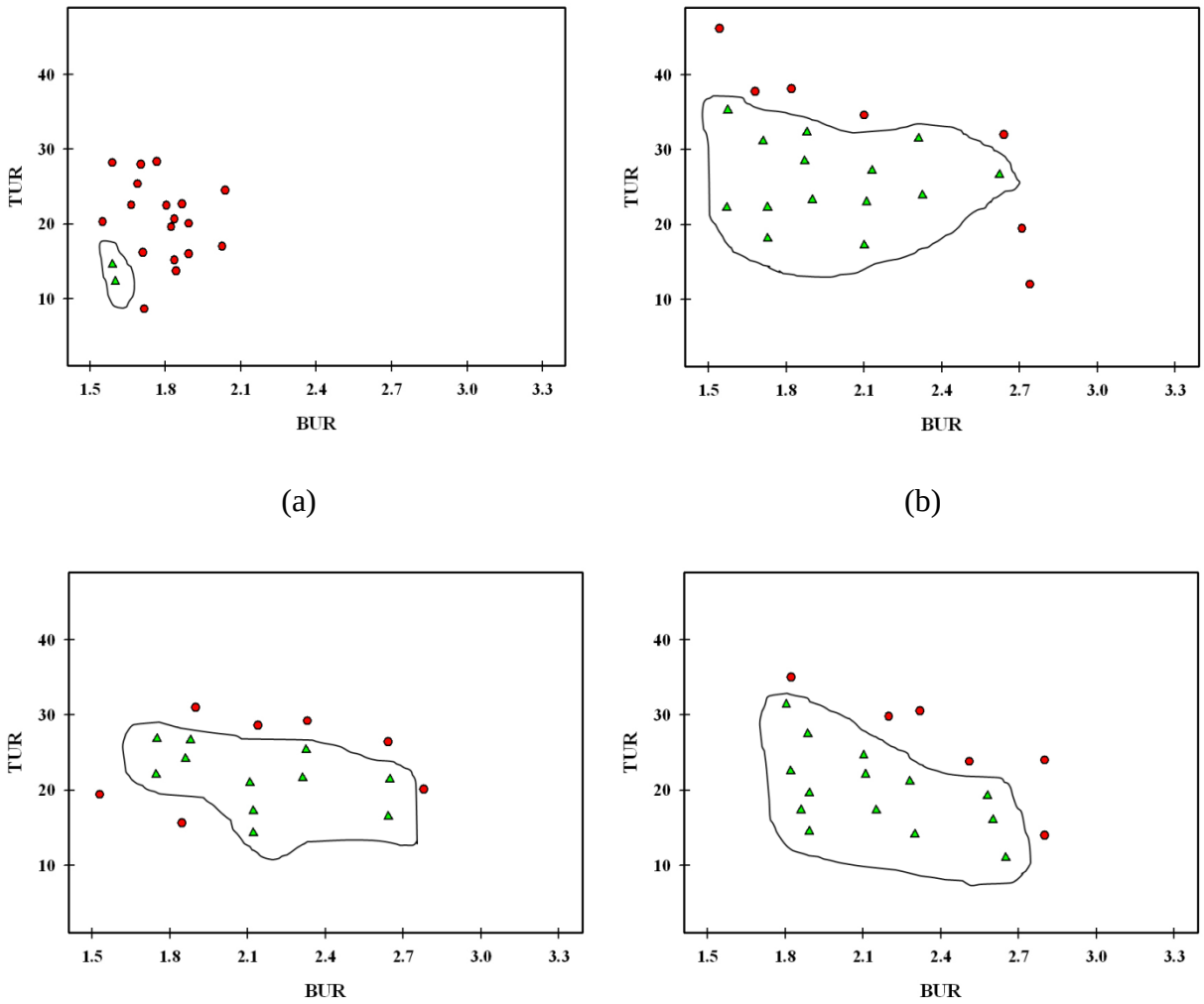

Figure 8.4. Stability map for (a) neat linear PLLA and its blends with 30% branched PLLA: (b) hyper branched, (c) comb like and (d) star shaped architectures, circles and triangles represent unstable and stable conditions, respectively

From this figure it is clear that linear PLA had a very narrow operating window which also corresponds to low blow up and take up ratios. At low BURs, process was unstable at low TURs, then became stable by increasing TUR to 12 – 15 and then unstable again by further increase of TUR. At high BURs, process was unstable for all tried TURs. Therefore, there is a very small window of operation for linear PLA. In order to increase film performance and production rate it is necessary to extend these conditions to higher values. The first modification strategy was blending synthesized branched PLLAs with linear PLLA as it showed some levels

of melt rheology enhancement in prior characterizations. Therefore, modified blends containing 30% branched PLLA were processed to evaluate the efficiency of this modification strategy on the expansion of stable processing region. Stability maps are illustrated in Figure 8.4.(b)-(d). In comparison to neat linear PLLA, more stable conditions were achieved and operating window was extended both for BUR and TUR. When branched PLLA was in hyper branched architecture, maximum BUR was 2.65 obtained at TUR of 11 and maximum TUR was 31.4 obtained at BUR of 1.8. However, simultaneous increase of BUR and TUR was not possible and process became unstable. For the blend containing 30% comb like chains, some instability was observed at low BUR and TUR region and increasing these parameters resulted in stabilization of the process. However, stable zone could not be extended beyond that achieved from hyper branched PLLA. Star shaped PLLA revealed a better performance in comparison to the other two branched architectures. For this structure, at BUR of 2.6 TUR could be increased to 26.6 while keeping the process stability. Also for a BUR of 2.3 stable conditions was achieved at TUR as high as 31.5. Therefore, blending branched PLLAs with linear PLLA was an effective strategy to expand processing window. This can be attributed to modified extensional viscosity of blends having branched structures, previously reported by this group (Nouri et al., 2015), especially for star structure with longer branches.

The other modification approach was blending branched PDLAs with linear PLLA to benefit from the branched structure of PDLA as well as stereocomplex formation between stereochemically different chains. Previous rheological studies showed that this strategy was very effective in increasing the melt strength and inducing strain hardening to linear PLA. Figure 8.5 shows the stability map for PDLA/PLLA blends containing 5 and 7% hyper branched PDLA. When 5% PDLA was incorporated into linear PLLA, a wider stable region was achieved in comparison to first modification strategy. TUR could be increased to 22 at a BUR of 3.15 or at a BUR of 2.8 TUR was increased up to 27.5. Further increase in BUR and TUR was not possible since small holes appeared in the bubble and air leaked out. Similar effect was observed at BUR of 2.9 – 3.1 for blends having 7% branched PDLA but at lower TURs. This was probably caused by pre-existing stereocomplex crystals which limited the extensibility of PLA.

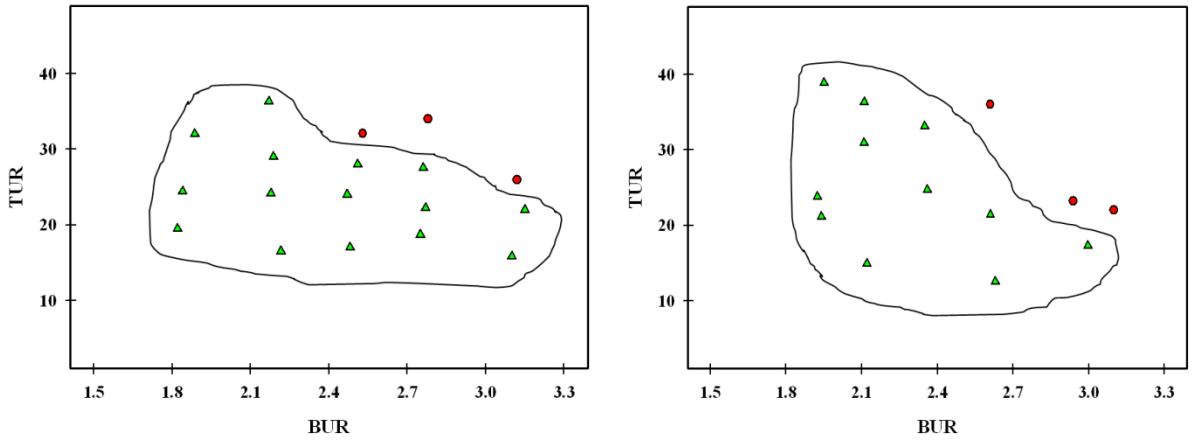

(a) (b)

Figure 8.5. Stability map for blends of linear PLLA with hyper branched PDLA: (a) 5% and (b) 7% branched PDLA, circles and triangles represent unstable and stable conditions, respectively

8.3.2 Properties of blown films

Mechanical properties: Tensile tests were performed on blown films to compare their mechanical properties. In Figure 8.6 stress-strain data are plotted for three types of films; i.e. linear PLLA, blend of linear PLLA with 30% hyper branched PLLA and blend of linear PLLA with 7% hyper branched PDLA. For each material, films obtained at two TURs were tested and their tensile properties are summarized in Table 8.2. At lower TUR conditions (presented in Figure 8.6 with open symbols), linear PLLA and its blend with 30% hyper branched PLLA showed almost similar behaviors except a slightly higher strain at break for linear PLLA. However, the blend of linear PLLA with 7% hyper branched PDLA showed a different response, tensile strength was increased from about 50 MPa to 63 MPa as a result of the presence of stereocomplex crystals. For films prepared at higher TUR (presented in Figure 8.6 with filled symbols), tensile modulus and tensile strength were higher and elongation at break was lower as compared to less drawn films. In addition, linear PLLA and its blend with 30% hyper branched PLLA did not reveal any yield behavior. The blend with 7% hyper branched PDLA drawn at TUR equal to 39 showed a remarkable increase in tensile modulus and strength as compared to linear PLLA films. Thus, both the presence of stereocomplex crystals and drawing improved the mechanical performance of blown films.

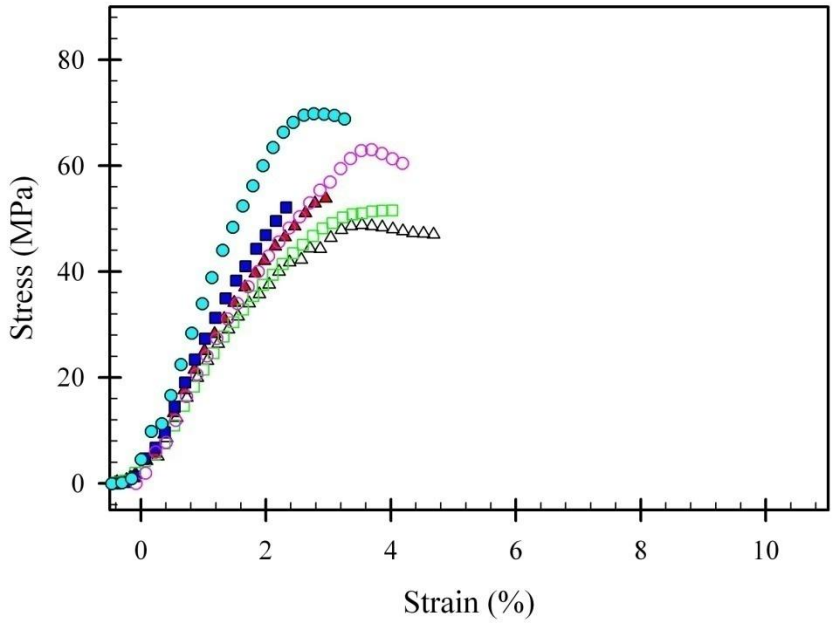

Figure 8.6. Tensile stress-strain dependencies for linear PLLA (triangle), 30% hyper branched PLLA blend (square) and 7% hyper branched PDLA blend (circle) at low TUR (open symbols) and high TUR (filled symbols) conditions

Table 8.2. Tensile properties of PLA films blown at different TURs

Material	TUR	Young modulus (GPa)	Tensile strength (MPa)	Strain at break (%)
Linear PLLA	8.7	2.1	48.8	4.7
	28	2.3	53.8	3
30% hyper branched PLLA	14	2.1	51.5	4
	35	2.4	52.1	2.3
7% hyper branched PDLA	15	2.3	63	4.2
	39	2.8	69.8	3.2

XRD analysis: Crystalline structure of blown films was examined using wide angle X-ray diffraction (WAXD) analysis. Figure 8.7 shows WAXD patterns for the 2θ range of 10 to 30 degree which covers the characteristic peaks for homocrystal and stereocomplex crystal. For linear PLLA (curve 1) and its blend with 30% hyper branched PLLA (curve 2) no homocrystal peak was observed, proving the amorphous state of the films after the process. Other branched structures resulted in amorphous film as well. This was expected since cooling in the film blowing process is much faster than PLA crystallization time scale. However, for blends of hyper branched PDLA with linear PLLA (curves 3 and 4), peaks at 2θ equal to 11.5, 20.5 and 23.7 were

observed which are associated to stereocomplex crystals. Since melting temperature of stereocomplex structure was higher than processing temperature, it did not melt and remained in the films. In addition, peak intensities were higher for 7% PDLA in comparison to 5% PDLA as the content of stereocomplex crystals was higher. Again for these films no homocrystal was detected from WAXD patterns, showing that even with nucleating effect of stereocomplex crystals and orientation of chains during the process homocrystallization was not possible at the very fast cooling rate.

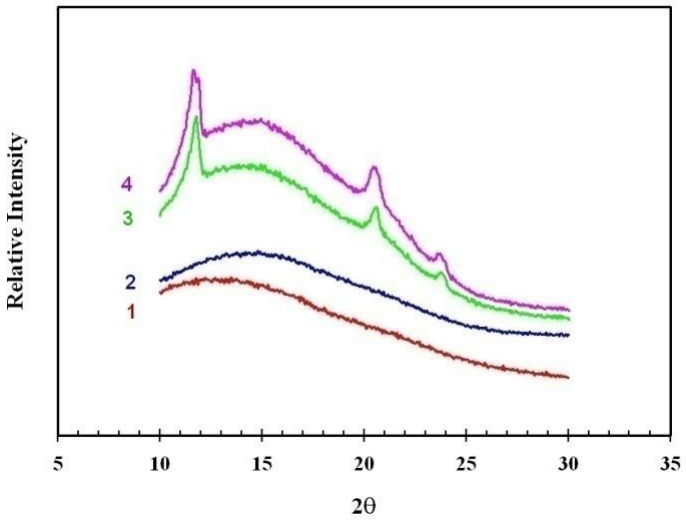

Figure 8.7. WAXD patterns of blown films: 1) linear PLLA, 2) 30% branched PLLA blend , 3) 5% hyper branched PDLA blend, 4) 7% hyper branched PDLA blend

To evaluate the orientation of stereocomplex crystals during the film blowing process, diffraction intensity was measured as a function of azimuth angle (φ). A constant intensity in a φ scan means that there is no orientation of crystal planes in any direction. On the other hand, if intensity shows a maximum at an azimuth angle, it means that crystal planes are oriented in that angle. Figure 8.8 shows the azimuth intensity profile for films having 7% PDLA and blown at different conditions. For both samples BUR was about 2 and TUR was 15 and 39.

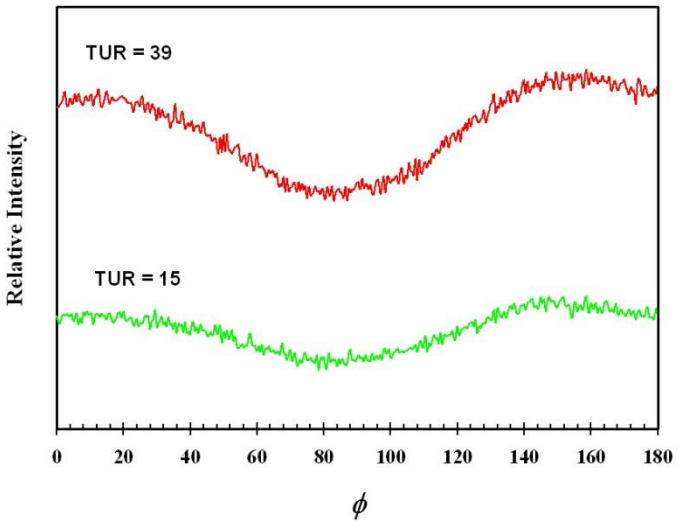

Figure 8.8. Azimuth intensity profile for films having 7% PDLA

Two maxima were observed at φ equal to 20^{o} and 160^{o}. Therefore, crystals were oriented more in machine direction (0 or 180^{o}), but they were not perfectly aligned in that direction as it will be expected at a BUR of 2. In addition, higher peak intensity at higher TUR confirmed that by increasing the take up ratio, more stereocomplex crystals were oriented in machine direction.

To investigate the structure of post process crystallized films, samples were annealed for 30 min at 120 ^{o}C and then characterized by XRD technique. Figure 8.9 shows XRD patterns obtained in θ scan for linear PLLA processed at TUR = 28 (curve 1) and its blends with 30% hyper branched PLLA processed at TUR = 35 (curve 2) and 7% hyper branched PDLA processed at TUR = 39 (curve 3). BUR was 1.6 to 1.9 for these films. Linear PLLA and its blend with 30% hyper branched PLLA only showed the peaks at 2θ equal to 14.7, 16.4 18.6 and 22 associated to homocrystal. In addition peaks for linear PLLA were wider with lower intensity compared to blends, implying less orientation of crystals in the film after annealing. Blend of linear PLLA with 7% PDLA revealed both stereocomplex and homocrystal peaks. Those peaks were also narrower with more intensity in comparison to linear PLLA film which suggests more alignment of crystals in the film.

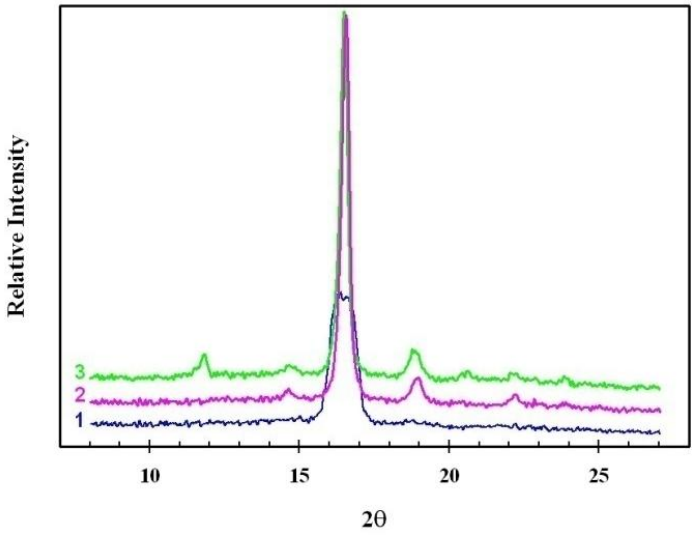

Figure 8.9. XRD patterns in θ scan for annealed films, 1) linear PLLA, 2) 30% hyper branched PLLA blend , 3) 7% hyper branched PDLA blend

Orientation of crystals was further studied by 2D-WAXD analysis of the films surface presented in Figure 8.10. Images at the top row are for linear PLLA, at the middle row for 30% hyper branched PLLA blend and at the bottom row for 7% hyper branched PDLA blend. Also three conditions are compared for each material. Patterns before annealing, after annealing for low TUR conditions and after annealing for high TUR conditions are shown on the left, middle and right columns, respectively. TUR values are similar to those reported in Table 8.2 for tensile tests. Before annealing, no clear Debye circle was observed for linear PLLA and 30% hyper branched PLLA blend, confirming their amorphous state. However, in the case of 7% hyper branched PDLA blend, rings at 2θ equal to 11.5, 20.5 and 23.7 which represent (110), (300)/(030) and (220) planes for stereocomplex crystals (Wen et al., 2013) were detectable before the annealing process. After the annealing, Debye circles at 2θ equal to 16.4 and 18.6 representing (200)/(110) and (203) reflections of homocrystal (Zhang et al., 2008) were observed for all the samples; however, their intensity distribution was not similar and was depended on the type of material and drawing conditions. Linear PLLA had uniform rings at low TUR condition, suggesting that drawing was insufficient to induce preferential crystallization in any direction. On the other hand, diffraction rings became more intense in the equatorial position for (110)/(200) planes and in the off-equatorial positions for (203) planes when TUR was increased, indicating the formation of oriented crystals after annealing. For blends containing 30% hyper branched

PLLA or 7% hyper branched PDLA, even at low TUR conditions oriented homocrystals were developed upon annealing. This clearly shows the difference between these materials and linear PLLA as chain orientation was preserved in the presence of branched structures.

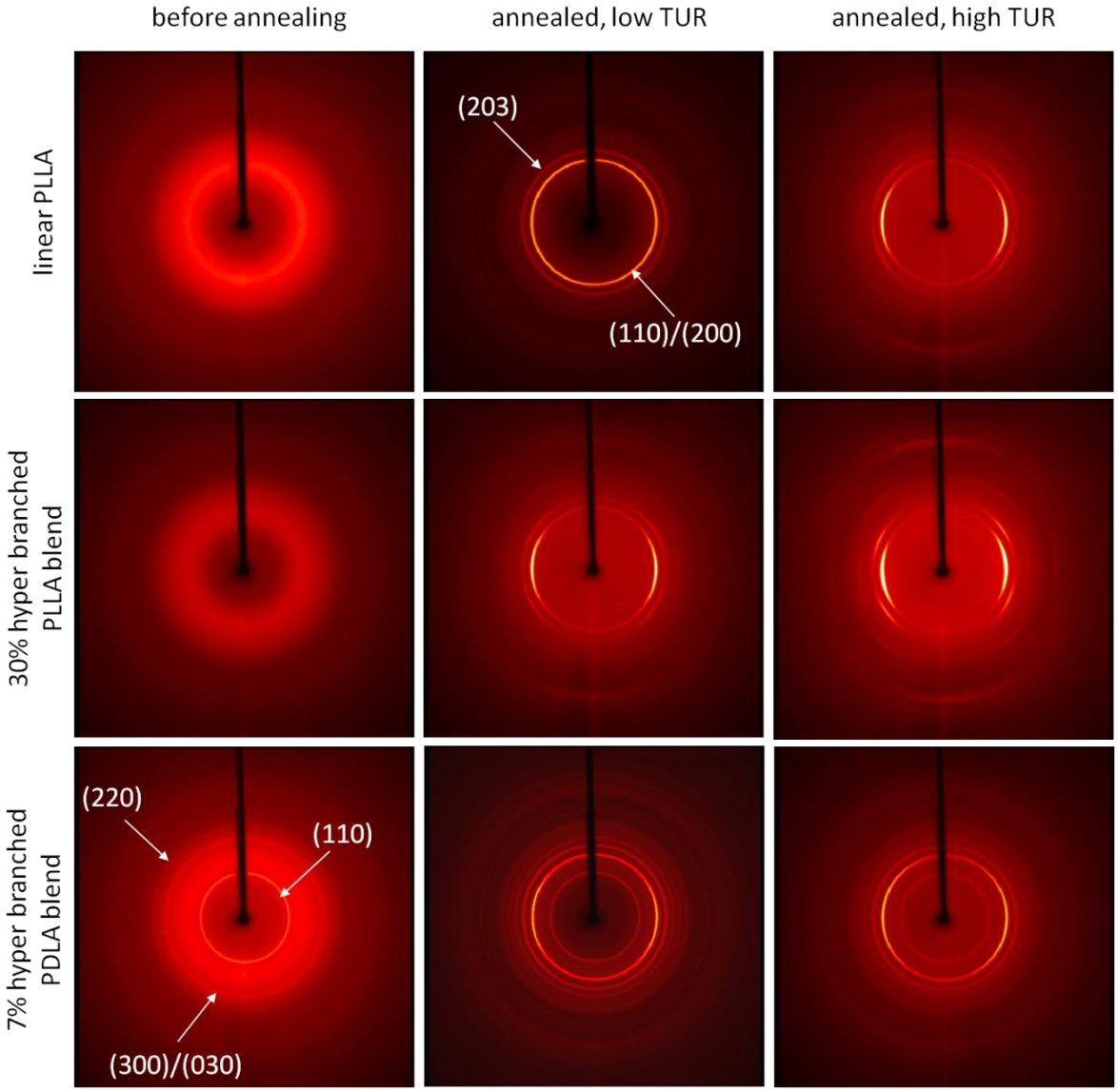

Figure 8.10. 2D-WAXD patterns of linear PLLA, 30% hyper branched PLLA blend and 7% hyper branched PDLA blend before and after annealing (Machine direction is vertical)

DSC analysis: Films were characterized in a heating scan to determine their crystallization and melting behavior after being processed. Specimens were heated from 20 ^{o}C at a rate of 10 ^{o}C/min to 200 or 240 ^{o}C, depending on the absence or presence of stereocomplex crystals. Recorded data are presented in Figure 8.11. Three types of films were tested; neat linear

PLLA and its blends with 30% hyper branched PLLA and 7% hyper branched PDLA, each being processed at low and high orientation conditions. BUR was between 1.6 and 2.1 for these films. It is clear from this figure that orientation and branching both had considerable impact on post process crystallization and melting of the films. Linear PLA had the highest cold crystallization temperature followed by its blends with 30% branched PLLA and 7% branched PDLA, respectively. In addition, for each material, cold crystallization temperature was lower for more oriented film in comparison to lower orientation condition.

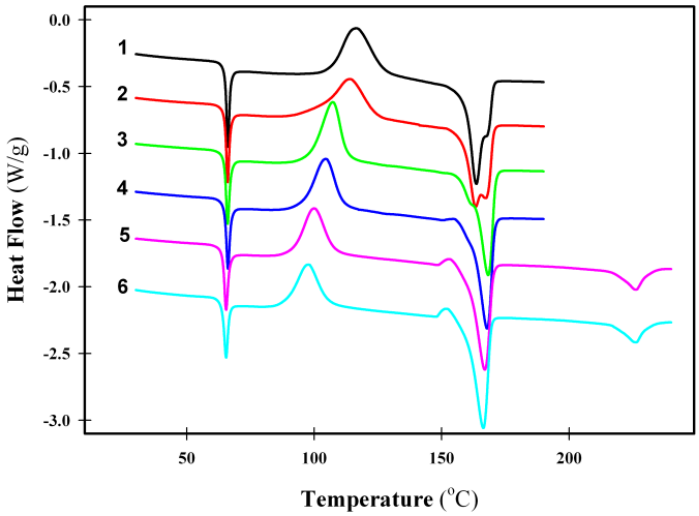

Figure 8.11. DSC thermograms of processed films heated at a rate of 10 °C/min, 1) neat PLLA TUR = 8.7, 2) neat PLLA TUR = 28, 3) 30% hyper branched PLLA blend TUR = 14, 4) 30% hyper branched PLLA blend TUR = 35, 5) 7% hyper branched PDLA blend TUR = 15, 6) 7% hyper branched PDLA blend TUR = 39

For linear PLLA, cold crystallization peak was located at 117 °C in low TUR and shifted to 114 °C for high TUR, showing a great difference with unprocessed PLA where only a slight cold crystallization peak was observed at 140 °C (Nouri et al., 2015). Blend of linear and branched PLLA cold crystallized at 105 and 100 °C which is a 9 to 7 °C reduction compared to neat PLLA, in agreement with a better crystallization in the presence of branched structure. Finally, blend of linear PLLA with 7% branched PDLA revealed the lowest cold crystallization peak temperatures at 100 and 97 °C, 17 °C less than neat PLLA. Therefore, combination of chain orientation and nucleation by stereocomplex crystals resulted in an early cold crystallization. Shape of the homocrystal melting peak, located between 155 and 170 °C, was also influenced by the type of material and operating conditions. A double melting peak was observed for

crystallized films at 163 and 168 ^{o}C with the ratio of the two peaks depending on the material and level of orientation. For linear PLLA at low TUR, lower temperature peak was larger, but when TUR was increased the two peaks became almost the same size. Therefore, increasing the orientation level resulted in thicker crystals. For blends containing 30% hyper branched PLLA or 7% hyper branched PDLA, lower temperature peak at 163 ^{o}C was like a shoulder on the larger peak at 168 ^{o}C and almost disappear at high TUR. Accordingly, similar to neat PLLA higher orientation resulted in thicker crystals. However, in contrast to linear PLLA, the homocrystal melting peak at 168 ^{o}C was the main one with a much larger size, suggesting that chains were oriented more in film blowing process compared to linear PLLA. This difference can be explained by more difficult chain relaxation in branched structures which permitted to preserve the applied orientation and to have a higher population of oriented chains in solidified films. In addition stereocomplex crystal melting peak was observed for the blend with 7% PDLA at 225 ^{o}C.

Optical properties: Processed films had different optical properties, especially in the presence and absence of stereocomplex crystals. In Figure 8.12, these two types of films are clearly demonstrated. Therefore, to quantify the effect of crystals on the appearance of films, their haze values were measured.

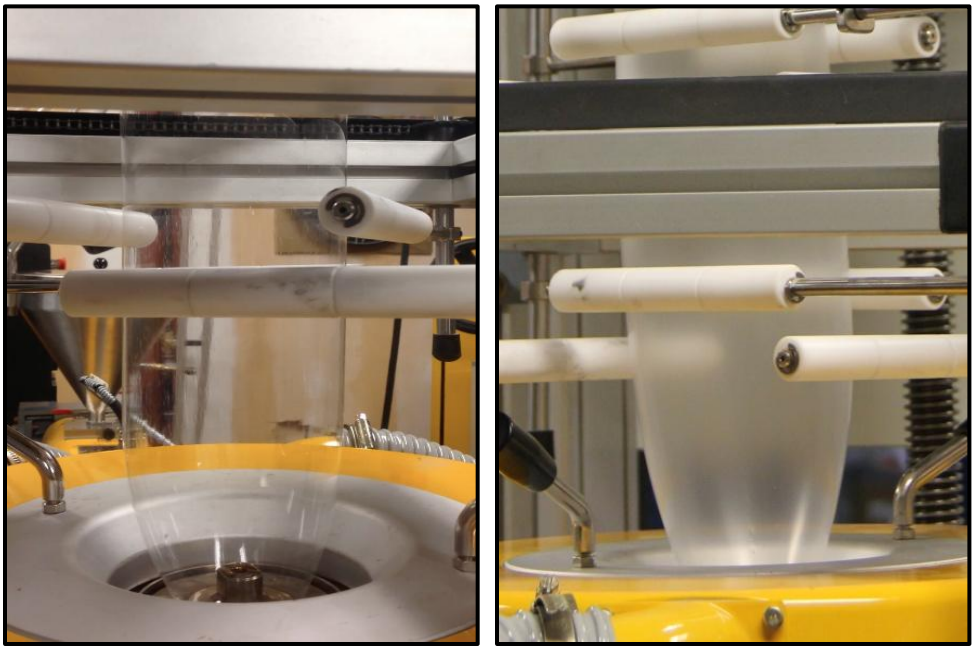

Figure 8.12. Transparent film (left) without stereocomplex crystals and translucent film (right) with stereocomplex crystals

Haze is defined as the percentage of transmitted light that deviates from the incident beam through forward scatter by more than 2.5°. In Figure 8.13, haze of different blown films is plotted versus wavelength in the visible light range. Linear PLLA films and blends containing 30% branched PLLA showed a haze close to zero, in agreement with their amorphous state. Meanwhile, films blown from the blends of linear PLLA and branched PDLA were translucent and revealed higher haze values depending on PDLA content. Films with 5 and 7% PDLA had a haze about 20 – 40 and 60 – 80%, respectively. Although process characteristic time is much shorter than the crystallization time for these blends, pre-existence of the stereocomplex crystals in the system which did not melt during the process and contributed to rheological modification of PLA caused higher haze in comparison to PLLA films. Also, it should be noted that for films with different crystalline content haze reduced as wavelength was increased. This decrease was more significant for higher crystalline content and haze values. The reason for such behavior is that as wavelength of light is increased, it surpasses the size of obstacles it encounters, therefore it is less scattered.

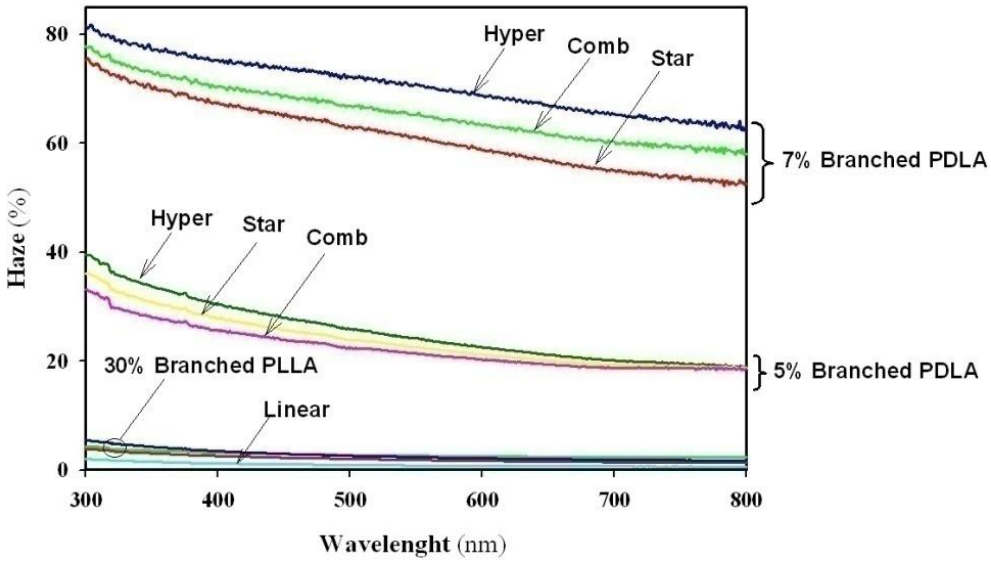

Figure 8.13. Haze at different wavelengths in visible light range for blown films

8.4 Conclusions

Branched PLLAs and PDLAs were employed to enhance film blowing processability of linear PLA. Bubble stability in different operating conditions (different BUR and TUR) was assessed

visually from the state of the bubble as well as by measuring the variation of film thickness and bubble radius. Stable region of operation for linear PLA was limited and located at small BUR and TUR value. Addition of branched structure to linear PLA greatly expanded the stable region boundaries to higher BUR and TUR conditions. Widest operating window was achieved in the presence of stereocomplex crystals, but bubble leakage occurred at very high BUR and TURs as a result of reduced extensibility. Tensile tests showed that both TUR and stereocomplex crystals increased tensile strength and modulus of the films but reduced their elongation at break. XRD analysis showed that blown films were amorphous except for those that already contained stereocomplex crystals. Also stereocomplex crystals were oriented almost in machine direction with a small deviation and the amount of oriented crystals was increased by increasing the take up ratio. By annealing the films, homocrystals were formed and showed different orientation levels depending on the precursor film. According to 2D-WAXD images, oriented crystals were formed in blend films even at low TUR but for linear PLLA only high TUR resulted in oriented homocrystals. DSC analysis also confirmed the enhanced cold crystallization due to chain alignment at high TURs. Films with stereocomplex crystals formed at high take up ratio revealed the lowest cold crystallization temperature at 97 ^{o}C. Finally, presence of stereocomplex crystals had a negative effect on film optical properties which resulted in translucent films with up to 80% haze value.

CHAPTER 9. GENERAL DISCUSSION

Utilization of bio-based polymers has expanded tremendously in the last decade as these materials provide unparalleled advantages in contrast to conventional petroleum based polymers. Reduced dependence on oil resources and environmental advantages are the main driving forces to employ biopolymers. Additionally, among biopolymers, biodegradable or compostable ones are more appealing from the waste management point of view. Polylactide is a bio-based and compostable polyester which is considered as a potential replacement for commodity polymers. However, it suffers from some deficiencies such as brittleness, low service temperature and slow crystallization. Also from the processing point of view, low melt strength is a major challenge for a number of melt processing methods. The common practice to cope with these problems is adding different modifiers to PLA. For example for faster crystallization, nucleating agents and plasticizers are added and for higher viscosity, peroxides and chain extenders are used. However, modification of PLA chain structure is less investigated. Changing PLA chain architecture from linear to branched can modify its rheological and crystallization properties. Therefore, this strategy was selected to enhance melt rheology and crystallization of PLA with the final goal to apply it in PLA film blowing process.

In the first step, among different branching methods, direct synthesis was selected as it gives high control over the final structure and eliminates the possibility of cross linking and gel formation. Three branched chain architectures were selected, i.e. star shaped, comb like and hyper branched chains and were synthesized using specific initiators. Branch length is an important parameter in determination of rheological and crystallization properties of polymers. From the rheology aspect, polymer properties are quite different if branch length is below or above the critical entanglement length. Short arms that cannot entangle reduce the effective chain length and contribute to a lower viscosity. On the other hand if branches are long enough to entangle, they increase the relaxation time of chain since the movement of branch is restricted to arm retraction in comparison with reptation in linear chains. This would increase viscosity and elasticity and may result in strain hardening effect if specific conditions are satisfied. Also concerning the crystallization of branched polymers, arm length is an important parameter. If branches are too short and cannot fold, they will not participate in crystallization process and reduce crystallinity, while long branches can fold and crystallize. Accordingly, molecular weight was chosen to obtain branched PLAs with arm lengths above the entanglement limit and long

enough for crystallization. The production of desired PLAs was confirmed by their characterization and their rheological and crystallization behavior were compared to a linear PLA. Better crystallization characteristics of branched PLAs than linear one and showing strain hardening proved the potential of synthesized polymers to overcome the aforementioned challenges to some extent. Therefore, their melt rheology and crystallization were investigated more deeply.

To enhance the processability of a polymer for film blowing process it is required to fulfill some criteria. Strain hardening behavior is an important feature that helps to have a stable and uninterrupted production and more uniform film thickness. Also, shear thinning helps to reduce viscosity and increase production rate with a lower power consumption. Therefore, the performance of branched PLAs was evaluated with respect to these requirements. Effect of branching on PLA melt rheology was investigated by adopting two different methods. The first method was chemical branching or the direct synthesis of branched structures. Detailed shear and extensional tests revealed that branched PLAs had better rheological characteristics as compared to linear PLA. Specifically, strain hardening, higher elasticity, higher extensional and zero-shear viscosities as well as intensified shear thinning showed that chemical branching was effective to improve the processability of PLA for a film blowing process. In addition, blending branched and linear PLAs ended in intermediate properties which depended on the amount of branched PLA in the system.

In the second approach, physical branching, stereocomplex formation between PLLA and PDLA chains was used to create the branched structure. Since the melting point of stereocomplex crystals is about 50 ^{o}C higher than PLA homocrystals, rheological characterization temperature (or process temperature) is located below stereocomplex melting and these crystals remain available in PLA melt. In addition, for stereocomplex formation, at least two different chains have to co-crystallize and the uncrystallized segments can be considered as branches on the counterpart chain. Thus, crystals function as branching points. Additionally, in this work branched PDLAs were used for this purpose to increase the level of branching, which was not tried before for PLA rheological modification. Evaluating the shear and extensional rheological response of physically branched PLAs revealed that this technique was more suitable in comparison to the first approach. Less branched PDLA was required than branched PLLA and higher viscosities and more pronounced strain hardening and shear thinning was resulted.

In addition to the melt processing requirements, final product properties are the matter of concern. Some of these properties are dictated by the processing conditions, some are inherent to polymer itself, and some are determined by both. Crystallization is an important aspect of polymers which directly influences other properties and therefore the overall performance of the product. It is in part related to the ability of the polymer to crystallize and in part to the processing conditions to allow or prevent crystallization. Chain architecture can influence crystallization directly by altering the ability of chains to crystallize and indirectly by influencing the melt processing conditions. Direct effects were studied for PLA crystallization at quiescent conditions. DSC tests and optical microscopy observations were conducted to study crystallization kinetics, crystallinity and crystalline morphology in relation to branch architecture. From the homocrystallization aspect, branched PLAs revealed higher ability to crystallize than linear PLA which was confirmed by several criteria. In non-isothermal tests, crystallization upon cooling from the melt, lower cold crystallization temperature and higher melting enthalpy are considered main outcomes achieved by branching. Observation of morphology suggested that this enhancement was in part due to better crystal nucleation which increased by branching. This was also in agreement with a lowered cold crystallization temperature and increased crystallinity when branched PLA was added to linear one, effects which are observed when nucleating agents are added to polymers. On the other hand, from isothermal crystallization tests it was revealed that total crystallinity decreased by increased branching. Although branches were long enough to crystallize, this is explained by increased chain ends and branching points which are considered non-crystallizable segments. However, based on crystallization half-time which was reduced by 4 to 14 folds, crystallization kinetics was highly affected by branching and branched architecture. Therefore, there is a trade-off between crystallinity and crystallization kinetics. From the isothermal tests and applying the Avrami kinetic model, reduced Avrami exponent was observed by branching that suggested a change in nucleation mechanism and crystal growth dimensionality. From spherulite growth measurements it was confirmed that growth rate reduced by increased branching. Despite that, total crystallization rate was increased. This implies that the role of increased nucleation by branching dominated the crystallization behavior.

Stereocomplex formation was also investigated as it was shown to be particularly advantageous in rheological studies. Contrary to homocrystallization, stereocomplex formation yield was shown to increase with branching. Since stereocomplex formation tests were performed

at much higher temperatures, this was attributed to the ability of branched chains to nucleate crystals in a region where chain mobility is not an issue. Nucleation role of stereocomplex crystals for PLA homocrystallization was also shown which depended primarily on the amount of stereocomplex in the system. This was demonstrated by comparing two procedures which resulted in different amount of setereocomplex crystals. Another interesting difference between homocrystal and stereocomplex was the internal spherulitic morphology. It was clearly shown that homocrystallization ended in compact spherulites while stereocomplex spherulites were open structures made of lamellae branched out of other lamellae with amorphous spaces in between. This difference was explained by different crystallizable portions of material and more difficult crystallization when PLLA and PDLA chains are required to associate.

Assessment of the processability of modified PLAs was the final step which was performed in a film blowing process. It is a popular film forming technique in packaging industry and at the same time challenging for PLA due to its low melt strength and absence of strain hardening behavior. In this process, the two important parameters that determine the operating window are blow up ratio (BUR) and take up ratio (TUR). Having higher BUR and TUR means wider films and higher production rate. They are also very important from the final properties perspective since higher BUR and TUR values equal to higher film orientation in transverse and machine direction. However, increasing these parameters will increase production instability and the limits are dictated by polymer properties. Commercial PLA was tested and a very small stable production window was achieved. On the other hand, modified blends based on the two adopted strategies showed significant widening of the operating window. Best results were obtained from the physical branching method (using stereocomplex crystals) which was shown to be more efficient in rheological studies. However, lower PDLA concentration was preferred since at higher stereocomplex content, melt extensibility was reduced. In addition films with higher stereocomplex content were hazier. Orientation of chains with increasing TUR and the presence of stereocomplex crystals also helped to improve the mechanical and crystallization properties of blown films.

CHAPTER 10. CONCLUSIONS AND RECOMMENDATIONS

10.1 Conclusions

In this thesis, effect of branched chain architecture on PLA rheological and crystallization properties and final application in film blowing process was investigated. In the first step, ring-opening polymerization was used to synthesize star shaped and comb like PLAs by multifunctional initiators and hyper branched one using a comonomer-initiator molecule. Synthesized branched PLAs had high molecular weights and narrow molecular weight distributions with branch length above the critical entanglement length. During this project, a commercial linear PLA was also used as a reference to compare the properties of branched and linear PLAs as well as to improve its properties and processability through blending with branched structures. While linear PLA did not crystallize considerably, appearance of crystallization peak in a DSC cooling cycle for branched PLAs, as well as higher spherulite density in isothermal and dynamic mode from optical microscopy observations showed superior crystallization of branched PLAs compare to linear one, with the highest effect for hyper branched PLA. Furthermore, in extensional rheometry tests, while linear PLA failed after a viscosity plateau, synthesized branched PLAs revealed strain hardening. These noticeable changes showed that branching is a viable method to improve melt rheology and crystallization of PLA.

Based on the primary results, rheological properties of branched PLAs were the center of the second phase. In this step, two branching strategies were explored. First method was chemical branching or direct synthesis of branched architectures. From oscillatory shear tests it was found that branched PLAs had higher viscosity and elastic modulus compared to linear PLA and shear thinning was intensified by branching. These parameters were highest for star shaped PLA which was associated to higher branch length. An increase in viscosity was observed when 10% star shaped PLA was blended with linear one and continued to increase when branched PLA content was increased to 20 and 30%. Also from uniaxial extensional viscosity measurements it was found that blending branched structures with linear PLA had an improving effect on the extensional response of linear structure by appearing strain hardening. The observed strain hardening was more evident at lower applied Hencky strain rates and increasing strain rate to 5 s^{-1} resulted in premature rupture of the samples before extensional viscosity increase.

Physical branching based on stereocomplex formation between stereochemically different polymer chains was the second strategy. It was a double branching method since synthesized PDLAs were prepared in branched structure themselves. Blends of linear PLLA and branched PDLA containing 5, 7 and 10% branched PDLA showed remarkable viscosity increase which was in direct relation with PDLA content. Also, no viscosity plateau was observed and shear thinning behavior was more pronounced than chemical branching approach. From the chain architecture aspect, hyper branched PDLA resulted in higher viscosity increase. It was confirmed by DSC tests that more stereocomplex was formed by this structure which was the result of shorter branches and higher nucleation effect of branching points. Extensional viscosity measurements of physically branched blends showed a continuous viscosity increase without a plateau with a strong strain hardening at the end. Comparing the rheological properties of linear/branched PLLA blends with linear PLLA/branched PDLA blends showed that physical branching is more helpful to modify linear PLLA. This is because of the simultaneous increase of branching and apparent molecular weight by physically connecting chains together.

Effect of chain branching on PLLA homocrystallization and PLLA/PDLA co-crystallization was explored in the third phase. From dynamic DSC and optical microscopy tests, lower cold crystallization temperature and higher spherulite density were observed, proving the nucleation role of branched architectures. This was used to enhance linear PLLA crystallization by adding up to 30% branched PLLA to it. At 30% branched PLLA content, melting enthalpy was 6 times more than linear PLLA and cold crystallization temperature was 10 ^{o}C lower. Therefore blending branched with linear PLLA contributed positively to PLA crystallization acceleration. Isothermal DSC tests showed a more clear image of the difference in crystallization kinetics of branched and linear polymers and between branched architectures. Crystallization half-time for branched PLAs was between 4 to 14 times less than linear one, depending on branch type and crystallization temperature. A shift of optimum crystallization temperature to higher values was also observed as the branch content increased, confirming a better nucleation process in the presence of branches. From the application of Avrami kinetic model a decrease in Avrami exponent was observed by increased branching, implying a change in crystal nucleation mechanism and crystal growth from three to two dimensional. The downside of branching was lower overall crystallinity which was caused by increased amount of non-crystallizable segments such as chain ends and branching points. Effect of branching on growth rate and nucleation was

also assessed from isothermal optical microscopy characterizations. Spherulite radius growth rate was lower for hyper branched structure due to higher chain restriction. At the same time, this structure resulted in considerably higher spherulite density which ended in higher overall crystallization rates at higher temperatures.

On the subject of co-crystallization in branched PDLA/linear PLLA blends it was found that stereocomplex yield was increased by branching opposite to the case of homocrystallization. Considering that isothermal crystallization temperature was 70 to 100 ^{o}C higher, nucleation became a controlling parameter. In addition, a clear difference between the internal spherulite morphology for homocrystal and stereocomplex was demonstrated and it was suggested that lower crystallizable portion of material and necessity for coupling of stereochemically different chains for stereocomplex formation were the origins of less packed spherulites. Furthermore, nucleation role of stereocomplex crystals for PLA homocrystallization was shown both by DSC and optical microscopy tests. From DSC results it was concluded that nucleation effect depends on the thermal history and stereocomplex content in the system. Also by comparing the optical microscopy images for neat linear PLLA and its blend with branched PDLA it was revealed that homocrystal were formed in blends on the surface of stereocomplex spherulites and in randomly scattered spaces implying the nucleation of new spherulites by very small isolated stereocomplex crystallites.

In the last phase of the project, film blowing of linear PLA and its modified blends based on the two modification approaches was performed to determine the effect of these modifications on widening of operating window leading to stable film production, especially at high blow up and take up ratios. Linear PLLA had a very narrow stable region which was also located at low BUR and TUR values. Meanwhile blends containing 30% branched PLLA or 5-7% branched PDLA expanded the stable region to higher BUR and TUR values. Blends containing stereocomplex crystals showed better performance in film blowing process, in agreement with higher melt strength from rheological studies. However, lower PDLA concentration was more favorable since high stereocomplex content reduced melt extensibility and resulted in hazier films. In addition, orientation of chains at high take up ratios and stereocomplex crystals resulted in better mechanical properties and post process crystallization. Lowest cold crystallization temperature and highest tensile strength were obtained for films having stereocomplex crystals and processed at high TUR.

10.2 Recommendations

In this thesis work, rheological and crystallization properties as well as film blowing of branched PLAs with defined structures was covered. Promising results were achieved regarding PLA melt rheology and crystallization kinetics which led to improved blown film processability and final properties. Accordingly, the following subjects are suggested for the continuation of this work and future studies in the field:

1. Molecular weight and its distribution are parameters which were not dealt with in this project. Therefore, it is suggested to synthesize the chosen branched architectures in different molecular weights to have a better view of the optimum polymer characteristics depending on the concerned properties.
2. Film blowing of the branched PLAs was done basically to investigate the effect of branching on the processability of PLA. However, another objective could be to maximize the performance of the final film. As a result, more operating conditions and subsequent characterizations are needed to be done.
3. Since rheological and crystallization properties are important aspects of other melt processing techniques and products, it is proposed to test the processing of modified PLAs in other processes to assess their influence on other types of materials. For example the enhanced crystallization could be useful to achieve higher crystallinity or shorter cycle time for injected parts. Rheologically modified materials also can be tested for processes such as thermoforming, extrusion foaming, etc.
4. In this work, synthesized branched PLAs were blended with linear PLA to improve its properties as branched ones demonstrated better characteristics. This resulted in blends with better properties than neat PLLA but not as good as neat branched PLAs. The limit to use branched PLAs alone was their produced quantities. It is therefore suggested to produce branched PLAs in larger quantities and try their melt processing without blending with linear PLA.
5. Employment of stereocomplex structure was shown to be very effective to expand the operating window in film blowing process. However, due to the size of crystals, hazy films were obtained. Since optical clarity is a major advantage for packaging

applications, it is suggested to investigate further this issue to obtain transparent or less hazy films while using stereocomplex crystals to have a better processability. For example using nucleating agents to reduce crystal size may be explored.

REFERENCES

Adeli, M. and R. Haag (2006). "Multiarm star nanocarriers containing a poly(ethylene imine) core and polylactide arms." Journal of Polymer Science, Part A: Polymer Chemistry 44(19): 5740-5749.

Ahmed, J. and S. K. Varshney (2011). "Polylactides-chemistry, properties and green packaging technology: A review." International Journal of Food Properties 14(Compendex): 37-58.

Ahmed, J., S. K. Varshney and F. Janvier (2014). "Rheological and thermal properties of stereocomplexed polylactide films." Journal of Thermal Analysis and Calorimetry 115(3): 2053-2061.

Ajioka, M., K. Enomoto, K. Suzuki and A. Yamaguchi (1995). "Basic properties of poly(lactic acid) produced by the direct condensation polymerization of lactic acid." Journal of Environmental Polymer Degradation 3(4): 225-225.

Ajji, A., P. Sammut and M. A. Huneault (2003). "Elongational rheology of LLDPE/LDPE blends." Journal of Applied Polymer Science 88(14): 3070-3077.

Al-Itry, R., K. Lamnawar and A. Maazouz (2012). Improvement of thermal stability, rheological and mechanical properties of PLA, PBAT and their blends by reactive extrusion with functionalized epoxy, Langford Lane, Kidlington, Oxford, OX5 1GB, United Kingdom, Elsevier Ltd.

Andreopoulos, A. G., E. Hatzi and M. Doxastakis (1999). "Synthesis and properties of poly(lactic acid)." Journal of Materials Science: Materials in Medicine 10(1): 29-33.

Androsch, R. and M. L. Di Lorenzo (2013). "Crystal nucleation in glassy poly(l -lactic acid)." Macromolecules 46(15): 6048-6056.

Atkinson, J. L. and S. Vyazovkin (2012). "Thermal properties and degradation behavior of linear and branched poly(L-lactide)s and poly(L-lactide-co-glycolide)s." Macromolecular Chemistry and Physics 213(9): 924-936.

Biela, T., A. Duda, H. Pasch and K. Rode (2005). "Star-shaped poly(L-lactide)s with variable numbers of hydroxyl groups at polyester arms chain-ends and directly attached to the star-shaped core - Controlled synthesis and characterization." Journal of Polymer Science, Part A: Polymer Chemistry 43(23): 6116-6133.

Bigg, D. M. (1996). "Effect of copolymer ratio on the crystallinity and properties of polylactic acid copolymers." Journal of Engineering and Applied Science 2: 2028-2039.

Bigg, D. M. (2005). "Polylactide copolymers: Effect of copolymer ratio and end capping on their properties." Advances in Polymer Technology 24(Compendex): 69-82.

Blomqvist, J. (2001). "RIS Metropolis Monte Carlo studies of poly(L-lactic), poly(L,D-lactic) and polyglycolic acids." Polymer 42(8): 3515-3521.

Boufarguine, M., A. Guinault, G. Miquelard-Garnier and C. Sollogoub (2013). "PLA/PHBV films with improved mechanical and gas barrier properties." Macromolecular Materials and Engineering 298(10): 1065-1073.

Cailloux, J., O. O. Santana, E. Franco-Urquiza, J. J. Bou, F. Carrasco and M. L. Maspoch (2014). "Sheets of branched poly(lactic acid) obtained by one-step reactive extrusion-calendering process: Physical aging and fracture behavior." Journal of Materials Science 49(11): 4093-4107.

Carlson, D., P. Dubois, L. Nie and R. Narayan (1998). "Free radical branching of polylactide by reactive extrusion." Polymer Engineering and Science 38(2): 311-321.

Carus, M., W. Baltus, D. Carrez, H. Kaeb, J. Ravenstijn and S. Zepnik (2013). "Market study on bio-based polymers in the world." Bioplastics Magazine-NOVA Institute.

Chellamuthu, M., D. Arora, H. H. Winter and J. P. Rothstein (2011). "Extensional flow-induced crystallization of isotactic poly-1-butene using a filament stretching rheometer." Journal of Rheology 55(4): 901-920.

Cicero, J. A., J. R. Dorgan, J. Garrett, J. Runt and J. S. Lin (2002). "Effects of molecular architecture on two-step, melt-spun poly(lactic acid) fibers." Journal of Applied Polymer Science 86(11): 2839-2846.

Contreras, J., J. Pestana, F. Lopez-Carrasquero and C. Torres (2014). "Synthesis of -caprolactone-b-l-lactide block copolymers by mean sequential polymerization, using diphenylzinc as initiator." Polymer Bulletin 71(7): 1661-1674.

Cooper-White, J. J. and M. E. Mackay (1999). "Rheological properties of poly(lactides). Effect of molecular weight and temperature on the viscoelasticity of poly(l-lactic acid)." Journal of Polymer Science, Part B: Polymer Physics 37(15): 1803-1814.

Corre, Y.-M., A. Maazouz, J. Duchet and J. Reignier (2011). "Batch foaming of chain extended PLA with supercritical CO2: Influence of the rheological properties and the process parameters on the cellular structure." Journal of Supercritical Fluids 58(1): 177-188.

Dalmoro, A., A. A. Barba, M. Lamberti, M. Mazzeo, V. Venditto and G. Lamberti (2014). "Random l-lactide/-caprolactone copolymers as drug delivery materials." Journal of Materials Science 49(17): 5986-5996.

Darensbourg, D. J. and O. Karroonnirun (2010). "Ring-opening polymerization of l-lactide and -caprolactone utilizing biocompatible zinc catalysts. random copolymerization of l-lactide and -caprolactone." Macromolecules 43(21): 8880-8886.

Dean, K. M., E. Petinakis, S. Meure, L. Yu and A. Chryss (2012). "Melt Strength and Rheological Properties of Biodegradable Poly(Lactic Aacid) Modified via Alkyl Radical-Based Reactive Extrusion Processes." Journal of Polymers and the Environment 20(3): 741-747.

Dechy-Cabaret, O., B. Martin-Vaca and D. Bourissou (2004). "Controlled ring-opening polymerization of lactide and glycolide." Chemical Reviews 104(Compendex): 6147-6176.

Di Lorenzo, M. L. (2001). "Determination of spherulite growth rates of poly(L-lactic acid) using combined isothermal and non-isothermal procedures." Polymer 42(Compendex): 9441-9446.

Di, Y., S. Iannace, E. Di Maio and L. Nicolais (2005). "Reactively modified poly (lactic acid): Properties and foam processing." Macromolecular Materials and Engineering 290(11): 1083-1090.

Dorgan, J. R., J. Janzen, M. P. Clayton, S. B. Hait and D. M. Knauss (2005-a). "Melt rheology of variable L-content poly(lactic acid)." Journal of Rheology 49(3): 607-619.

Dorgan, J. R., J. Janzen, D. M. Knauss, S. B. Hait, B. R. Limoges and M. H. Hutchinson (2005-b). "Fundamental solution and single-chain properties of polylactides." Journal of Polymer Science, Part B: Polymer Physics 43(21): 3100-3111.

Dorgan, J. R., H. Lehermeier and M. Mang (2000). "Thermal and rheological properties of commercial-grade poly(lactic acid)s." Journal of Polymers and the Environment 8(1): 1-9.

Dorgan, J. R., J. S. Williams and D. N. Lewis (1999). "Melt rheology of poly(lactic acid): Entanglement and chain architecture effects." Journal of Rheology 43(5): 1141-1155.

Dutkiewicz, S., D. Grochowska-Lapienis and W. Tomaszewski (2003). "Synthesis of poly(L(+) lactic acid) by polycondensation method in solution." Fibres & Textiles in Eastern Europe 11(4): 66-70.

Eenink, M. J. D., J. Feijen, J. Olijslager, J. H. M. Albers, J. C. Rieke and P. J. Greidanus (1987). "Biodegradable hollow fibres for the controlled release of hormones." Journal of Controlled Release 6(1): 225-247.

Enomoto, K. K., JP), Ajioka, Masanobu (Kanagawa, JP), Yamaguchi, Akihiro (Kanagawa, JP) (1994). Polyhydroxycarboxylic acid and preparation process thereof. United States, Mitsui Toatsu Chemicals, Incorporated (Tokyo, JP).

Eslami, H. and M. R. Kamal (2013). "Effect of a chain extender on the rheological and mechanical properties of biodegradable poly(lactic acid)/poly[(butylene succinate)-co-adipate] blends." Journal of Applied Polymer Science 129(5): 2418-2428.

Fang, H., Y. Zhang, J. Bai and Z. Wang (2013). "Shear-induced nucleation and morphological evolution for bimodal long chain branched polylactide." Macromolecules 46(16): 6555-6565.

Ferry, J. D. (1961). Viscoelastic properties of polymers. New York, John Wiley and Sons.

Fetters, L. J., D. J. Lohse and W. W. Graessley (1999). "Chain dimensions and entanglement spacings in dense macromolecular systems." Journal of Polymer Science, Part B: Polymer Physics 37(10): 1023-1033.

Fischer, E. W., H. J. Sterzel and G. Wegner (1973). "Investigation of the structure of solution grown crystals of lactide copolymers by means of chemical reactions." Colloid & Polymer Science 251(11): 980-990.

Fraschini, C., M. Jalabert and R. E. Prud'homme (2005). "Physical Characterization of Blends of Poly(d-lactide) and LHRH (A Leuprolide Decapeptide Analog)." Biomacromolecules 6(6): 3112-3118.

Garlotta, D. (2001). "A literature review of poly(lactic acid)." Journal of Polymers and the Environment 9(2): 63-84.

George, K. A., F. Schue, T. V. Chirila and E. Wentrup-Byrne (2009). "Synthesis of four-arm star poly(L-Lactide) oligomers using an in situ-generated calcium-based initiator." Journal of Polymer Science, Part A: Polymer Chemistry 47(18): 4736-4748.

Gerard, T. and T. Budtova (2012). "Morphology and molten-state rheology of polylactide and polyhydroxyalkanoate blends." European Polymer Journal 48(6): 1110-1117.

Gilding, D. K. and A. M. Reed (1979). "Biodegradable polymers for use in surgery--polyglycolic/poly(actic acid) homo- and copolymers: 1." Polymer 20(12): 1459-1464.

Gottschalk, C. and H. Frey (2006). "Hyperbranched polylactide copolymers." Macromolecules 39(5): 1719-1723.

Gottschalk, C., F. Wolf and H. Frey (2007). "Multi-arm star poly(L-lactide) with hyperbranched polyglycerol core." Macromolecular Chemistry and Physics 208(15): 1657-1665.

Grijpma, D. W., J. P. Penning and A. J. Pennings (1994). "Chain entanglement, mechanical properties and drawability of poly(lactide)." Colloid and Polymer Science 272(Compendex): 1068-1081.

Gu, S. Y., M. Yang, T. Yu, T. B. Ren and J. Ren (2008). "Synthesis and characterization of biodegradable lactic acid-based polymers by chain extension." Polymer International 57(8): 982-986.

Gui, Z.-Y., H.-R. Wang, Y. Gao, C. Lu and S.-J. Cheng (2012). "Morphology and melt rheology of biodegradable poly(lactic acid)/poly(butylene succinate adipate) blends: Effect of blend compositions." Iranian Polymer Journal (English Edition) 21(2): 81-89.

Gupta, B., N. Revagade and J. Hilborn (2007). "Poly(lactic acid) fiber: An overview." Progress in Polymer Science (Oxford) 32(Compendex): 455-482.

Hadinata, C., D. Boos, C. Gabriel, E. Wassner, M. Rullmann, N. Kao and M. Laun (2007). "Elongation-induced crystallization of a high molecular weight isotactic polybutene-1 melt compared to shear-induced crystallization." Journal of Rheology 51(2): 195-215.

Hao, Q., F. Li, Q. Li, Y. Li, L. Jia, J. Yang, Q. Fang and A. Cao (2005). "Preparation and crystallization kinetics of new structurally well-defined star-shaped biodegradable poly(L-lactide)s initiated with diverse natural sugar alcohols." Biomacromolecules 6(4): 2236-2247.

Hartmann, M. (1998). High molecular weight polylactic acid polymers. Biopolymers from renewable resources. D. Kaplan. Berlin/Heidelberg, Springer-Verlag: 367–411.

Henton, D., P. Gruber, J. Lunt and J. Randall (2005). Polylactic Acid Technology. Natural Fibers, Biopolymers, and Biocomposites, CRC Press. null.

Huang, J., M. S. Lisowski, J. Runt, E. S. Hall, R. T. Kean, N. Buehler and J. S. Lin (1998). "Crystallization and microstructure of poly(L-lactide-co-meso-lactide) copolymers." Macromolecules 31(Compendex): 2593-2599.

Huneault, M. A. and H. Li (2007). "Morphology and properties of compatibilized polylactide/thermoplastic starch blends." Polymer 48(1): 270-280.

Hyon, S.-H., K. Jamshidi and Y. Ikada (1997). "Synthesis of polylactides with different molecular weights." Biomaterials 18(22): 1503-1508.

Idage, B. B., S. B. Idage, A. S. Kasegaonkar and R. V. Jadhav (2010). "Ring opening polymerization of dilactide using salen complex as catalyst." Materials Science and Engineering: B 168(1-3): 193-198.

Ikada, Y., K. Jamshidi, H. Tsuji and S. H. Hyon (1987). "Stereocomplex formation between enantiomeric poly(lactides)." Macromolecules 20(4): 904-906.

Jabbarzadeh, A., J. D. Atkinson and R. I. Tanner (2003). "Effect of molecular shape on rheological properties in molecular dynamics simulation of star, H, comb, and linear polymer melts." Macromolecules 36(Compendex): 5020-5031.

Jamshidi, K., S. H. Hyon and Y. Ikada (1988). "Thermal characterization of polylactides." Polymer 29(Compendex): 2229-2234.

Jandas, P. J., S. Mohanty and S. K. Nayak (2013). "Sustainability, compostability, and specific microbial activity on agricultural mulch films prepared from poly(lactic acid)." Industrial and Engineering Chemistry Research 52(50): 17714-17724.

Janzen, J. and R. H. Colby (1999). "Diagnosing long-chain branching in polyethylenes." Journal of Molecular Structure 485-486: 569-584.

Jiang, L., M. P. Wolcott and J. Zhang (2006). "Study of biodegradable polylactide/poly(butylene adipate-co-terephthalate) blends." Biomacromolecules 7(1): 199-207.

Jiao, M., K. Yang, J. Cao, H. Liu, W. Pan and P. Gao (2014). "Designing and characterization of poly(L-Lactide)/poly(-Caprolactone) multiblock copolymers." Journal of Macromolecular Science, Part B: Physics 53(2): 191-204.

Joziasse, C. A. P., H. Veenstra, D. W. Grijpma and A. J. Pennings (1996). "On the chain stiffness of poly(lactide)s." Macromolecular Chemistry and Physics 197(7): 2219-2229.

Jung, Y., S.-H. Lee, S.-H. Kim, J. C. Lim and S. H. Kim (2013). "Synthesis and characterization of the biodegradable and elastic terpolymer poly(glycolide-co-L-lactide-co--caprolactone) for mechano-active tissue engineering." Journal of Biomaterials Science, Polymer Edition 24(4): 386-397.

Kakuta, M., M. Hirata and Y. Kimura (2009). "Stereoblock polylactides as high-performance bio-based polymers." Polymer Reviews 49(Compendex): 107-140.

Kasehagen, L. J. and C. W. Macosko (1998). "Nonlinear shear and extensional rheology of long-chain randomly branched polybutadiene." Journal of Rheology 42(6): 1303-1327.

Kawai, T., N. Rahman, G. Matsuba, K. Nishida, T. Kanaya, M. Nakano, H. Okamoto, J. Kawada, A. Usuki, N. Honma, K. Nakajima and M. Matsuda (2007). "Crystallization and Melting Behavior of Poly (l-lactic Acid)." Macromolecules 40(26): 9463-9469.

Kawamoto, N., A. Sakai, T. Horikoshi, T. Urushihara and E. Tobita (2007). "Nucleating agent for poly(L-lactic acid) - An optimization of chemical structure of hydrazide compound for advanced nucleation ability." Journal of Applied Polymer Science 103(Compendex): 198-203.

Kim, E., E. Shin, I.-K. Yoo, J. Chung, Y. Hong and Y. Kim (2009). "Ring-opening polymerization ofl-lactide with silica supported titanium alkoxide catalysts." Macromolecular Research 17(5): 346-351.

Kolstad, J. J. (1996). "Crystallization kinetics of poly(L-lactide-co-meso-lactide)." Journal of Applied Polymer Science 62(7): 1079-1091.

Korhonen, H., A. Helminen and J. V. Seppala (2001). "Synthesis of polylactides in the presence of co-initiators with different numbers of hydroxyl groups." Polymer 42(18): 7541-7549.

Kowalski, A., A. Duda and S. Penczek (2000). "Kinetics and mechanism of cyclic esters polymerization initiated with Tin(II) Octoate. 3.â€ polymerization of l,l-dilactide." Macromolecules 33(20): 7359-7370.

Kricheldorf, H. R., I. Kreiser-Saunders and C. Boettcher (1995). "Polylactones. 31. Sn(II)octoate-initiated polymerization of l-lactide. A mechanistic study." Polymer 36(6): 1253-1253.

Kricheldorf, H. R., I. Kreiser-Saunders and A. Stricker (2000). "Polylactones 48. SnOct2-initiated polymerizations of lactide: a mechanistic study." Macromolecules 33(3): 702-709.

Kulinski, Z. and E. Piorkowska (2005). "Crystallization, structure and properties of plasticized poly(L-lactide)." Polymer 46(23): 10290-10300.

Kylma, J., J. Tuominen, A. Helminen and J. Seppala (2001). "Chain extending of lactic acid oligomers. Effect of 2,2-bis(2-oxazoline) on 1,6-hexamethylene diisocyanate linking reaction." Polymer 42(8): 3333-3343.

La Mantia, F. P. and D. Acierno (1985). "Rheological behaviour of HDPE/LDPE blends: III. Melt strength and extensibility." Plastics and Rubber Processing and Applications 5(2): 183-185.

Larson, R. G. (2001). "Combinatorial rheology of branched polymer melts." Macromolecules 34(13): 4556-4571.

Lehermeier, H. J. and J. R. Dorgan (2001). "Melt rheology of poly(lactic acid): Consequences of blending chain architectures." Polymer Engineering and Science 41(12): 2172-2184.

Li, H. and M. A. Huneault (2007). "Effect of nucleation and plasticization on the crystallization of poly(lactic acid)." Polymer 48(23): 6855-6866.

Li, H. and M. A. Huneault (2011). "Effect of chain extension on the properties of PLA/TPS blends." Journal of Applied Polymer Science 122(1): 134-141.

Li, K., J. Peng, L.-S. Turng and H.-X. Huang (2011). "Dynamic rheological behavior and morphology of polylactide/poly(butylenes adipate-co-terephthalate) blends with various composition ratios." Advances in Polymer Technology 30(2): 150-157.

Lim, L. T., R. Auras and M. Rubino (2008). "Processing technologies for poly(lactic acid)." Progress in Polymer Science 33(8): 820-852.

Ling, F., Q. Rongrong, L. Linbo, J. Gongwen and H. Suangwu (2009). Synthesis of Poly(L-lactide) via Solvothermal Method, Hindawi Publishing Corporation.

Liu, J., S. Zhang, L. Zhang, L. Liu and Y. Bai (2014). "Uniaxial stretching of polylactide with different initial crystalline morphologies and temperature effect." European Polymer Journal 61(0): 83-92.

Loomis, G. L., J. R. Murdoch and K. H. Gardner (1990). Polylactide stereocomplexes. Papers presented at the Washington, DC Meeting 1990 of the ACS, Division of Polymer Chemistry, August 26, 1990 - August 31, 1990, Washington, DC, USA, Publ by ACS.

Lu, D. D., L. Q. Yang, X. L. Shi, Y. Chang, H. Zhang and Z. Q. Lei (2012). "Synthesis and characterization of amphiphilic biodegradable hyperbranched-linear-hyperbranched copolymers based on PEG, PLA, and BHP." International Journal of Polymeric Materials 61(5): 384-394.

Lunt, J. (1998). "Large-scale production, properties and commercial applications of polylactic acid polymers." Polymer Degradation and Stability 59(1-3): 145-152.

Ma, P., A. B. Spoelstra, P. Schmit and P. J. Lemstra (2013). "Toughening of poly (lactic acid) by poly (-hydroxybutyrate-co-- hydroxyvalerate) with high -hydroxyvalerate content." European Polymer Journal 49(6): 1523-1531.

Malberg, S., D. Basalp, A. Finne-Wistrand and A.-C. Albertsson (2010). "Bio-safe synthesis of linear and branched PLLA." Journal of Polymer Science, Part A: Polymer Chemistry 48(5): 1214-1219.

Mallet, B., K. Lamnawar and A. Maazouz (2014). "Improvement of blown film extrusion of poly(Lactic Acid): Structure–Processing–Properties relationships." Polymer Engineering & Science 54(4): 840-857.

Marques, D. A. S., S. Jarmelo, C. M. S. G. Baptista and M. H. Gil (2010). "Poly(lactic acid) synthesis in solution polymerization." Macromolecular Symposia 296: 63-71.

Mazumdar, S., J. M. Clomburg and R. Gonzalez (2010). "Escherichia coli strains engineered for homofermentative production of D-lactic acid from glycerol." Applied and Environmental Microbiology 76(13): 4327-4336.

Mehta, R., V. Kumar, H. Bhunia and S. N. Upadhyay (2005). "Synthesis of poly(lactic acid): A review." Journal of Macromolecular Science - Polymer Reviews 45: 325-349.

Mehta, R., V. Kumar, H. Bhunia and S. N. Upadhyay (2005). "Synthesis of poly(lactic acid): A review." Journal of Macromolecular Science, Part C: Polymer Reviews 45(4): 325 - 349.

Meng, Q., M.-C. Heuzey and P. J. Carreau (2012). Control of thermal degradation of polylactide/clay nanocomposites during melt processing by chain extension reaction, Langford Lane, Kidlington, Oxford, OX5 1GB, United Kingdom, Elsevier Ltd.

Mihai, M., M. A. Huneault and B. D. Favis (2009). Extrusion-foaming in the presence of carbon dioxide of branched polylactide: Relationship composition - Rheological behavior - Crystallization. 7th International Conference on Foam Processing and Technology, FOAMS 2009, September 16, 2009 - September 17, 2009, Iselin, NJ, United states, Society of Plastics Engineers.

Mihai, M., M. A. Huneault and B. D. Favis (2010). "Rheology and extrusion foaming of chain-branched poly(lactic acid)." Polymer Engineering and Science 50(3): 629-642.

Mihai, M., M. A. Huneault, B. D. Favis and H. Li (2007). "Extrusion foaming of semi-crystalline PLA and PLA/thermoplastic starch blends." Macromolecular Bioscience 7(7): 907-920.

Miyata, T. and T. Masuko (1998). "Crystallization behaviour of poly(L-lactide)." Polymer 39(Compendex): 5515-5521.

Moon, S. I., C. W. Lee, M. Miyamoto and Y. Kimura (2000). "Melt polycondensation of L-lactic acid with Sn(II) catalysts activated by various proton acids: A direct manufacturing route to high

molecular weight poly(L-lactic acid)." Journal of Polymer Science, Part A: Polymer Chemistry 38(9): 1673-1679.

Moravek, S. J., J. M. Messman and R. F. Storey (2009). "Polymerization kinetics of rac-lactide initiated with alcohol/stannous octoate using in situ attenuated total reflectance-fourier transform infrared spectroscopy: An initiator study." Journal of Polymer Science, Part A: Polymer Chemistry 47(3): 797-803.

Nam, J. Y., M. Okamoto, H. Okamoto, M. Nakano, A. Usuki and M. Matsuda (2006). "Morphology and crystallization kinetics in a mixture of low-molecular weight aliphatic amide and polylactide." Polymer 47(Compendex): 1340-1347.

Nofar, M., W. Zhu, C. B. Park and J. Randall (2011). "Crystallization kinetics of linear and long-chain-branched polylactide." Industrial and Engineering Chemistry Research 50(24): 13789-13798.

Nouri, S., C. Dubois and P. Lafleur (2015). "Effect of chemical and physical branching on rheological behavior of polylactide " Journal of Rheology Submitted.

Nouri, S., C. Dubois and P. Lafleur (2015). "Homocrystal and stereocomplex formation behavior of polylactides with different branched structures." Polymer Submitted.

Nouri, S., C. Dubois and P. G. Lafleur (2015). " Synthesis and characterization of polylactides with different branched architectues." Journal of Polymer Science Part b-Polymer Physics 53(7): 522-531.

Ojijo, V., T. Malwela, S. Sinha Ray and R. Sadiku (2012). "Unique isothermal crystallization phenomenon in the ternary blends of biopolymers polylactide and poly[(butylene succinate)-co-adipate] and nano-clay." Polymer 53(2): 505-518.

Okihara, T., M. Tsuji, A. Kawaguchi, K.-i. Katayama, H. Tsuji, S.-H. Hyon and Y. Ikada (1991). "Crystal structure of stereocomplex of poly(L-lactide) and poly(D-lactide)." Journal of Macromolecular Science - Physics B30(Compendex): 119-140.

Othman, N., A. Acosta-Ramirez, P. Mehrkhodavandi, J. R. Dorgan and S. G. Hatzikiriakos (2011). "Solution and melt viscoelastic properties of controlled microstructure poly(lactide)." Journal of Rheology 55(5): 987-1005.

Otto G. Piringer , A. L. B. E. (2008). Plastic Packaging: Interactions with Food and Pharmaceuticals, 2nd, Completely Revised Edition, Wiley.

Ou, X. and M. Cakmak (2008). "Influence of biaxial stretching mode on the crystalline texture in polylactic acid films." Polymer 49(24): 5344-5352.

Ouchi, T., S. Ichimura and Y. Ohya (2006). "Synthesis of branched poly(lactide) using polyglycidol and thermal, mechanical properties of its solution-cast film." Polymer 47(1): 429-434.

Palade, L.-I., H. J. Lehermeier and J. R. Dorgan (2001). "Melt rheology of high l-content poly(lactic acid)." Macromolecules 34(5): 1384-1390.

Pan, P., Z. Liang, A. Cao and Y. Inoue (2009). "Layered Metal Phosphonate Reinforced Poly(l-lactide) Composites with a Highly Enhanced Crystallization Rate." ACS Applied Materials & Interfaces 1(2): 402-411.

Penco, M., G. Spagnoli, I. Peroni, M. A. Rahman, M. Frediani, W. Oberhauser and A. Lazzeri (2011). Effect of nucleating agents on the molar mass distribution and its correlation with the isothermal crystallization behavior of poly(L -lactic acid). Contributions from the 5th International Conference on Times of Polymers (TOP) and Composites, Ischia, Italy, June 20-23, 2010., P.O.Box 18667, Newark, NJ 07191-8667, United States, John Wiley and Sons Inc.

Perry, M. R. and M. P. Shaver (2011). "Flexible and rigid core molecules in the synthesis of poly(lactic acid) star polymers." Canadian Journal of Chemistry 89(4): 499-505.

Phuphuak, Y. and S. Chirachanchai (2013). "Simple preparation of multi-branched poly(l-lactic acid) and its role as nucleating agent for poly(lactic acid)." Polymer (United Kingdom) 54(2): 572-582.

Pilla, S., S. G. Kim, G. K. Auer, S. Gong and C. B. Park (2009). "Microcellular extrusion-foaming of polylactide with chain-extender." Polymer Engineering and Science 49(8): 1653-1660.

Pitet, L. M., S. B. Hait, T. J. Lanyk and D. M. Knauss (2007). "Linear and branched architectures from the polymerization of lactide with glycidol." Macromolecules 40(7): 2327-2334.

Plastemart (2010). "Foaming and stability of PLA blown film improve with chain extenders."

Podzimek, S. (2011). Light Scattering. Light Scattering, Size Exclusion Chromatography and Asymmetric Flow Field Flow Fractionation, John Wiley & Sons, Inc.: 37-98.

Rahaman, M. H. and H. Tsuji (2013). "Isothermal crystallization and spherulite growth behavior of stereo multiblock poly(lactic acid)s: Effects of block length." Journal of Applied Polymer Science.

Rahman, N., T. Kawai, K. N. Go Matsuba, T. Kanaya, H. Watanabe, H. Okamoto, M. Kato, A. Usuki, M. Matsuda, K. Nakajima and N. Honma (2009). "Effect of polylactide stereocomplex on the crystallization behavior of poly(L-lactic acid)." Macromolecules 42(Compendex): 4739-4745.

Ravari, F., A. Mashak, M. Nekoomanesh and H. Mobedi (2013). "Non-isothermal cold crystallization behavior and kinetics of poly(l-lactide): effect of l-lactide dimer." Polymer Bulletin 70: 2569–2586.

Ren, J., Q.-F. Wang, S.-Y. Gu, N.-W. Zhang and T.-B. Ren (2006). "Chain-linked lactic acid polymers by benzene diisocyanate." Journal of Applied Polymer Science 99(3): 1045-1049.

Ren, J., Z. Zhang, Y. Feng, J. Li and W. Yuan (2010). "Synthesis of star-shaped poly(-caprolactone)-b-poly(L-lactide) copolymers: From star architectures to crystalline morphologies." Journal of Applied Polymer Science 118(5): 2650-2658.

Ren, Q., J. Wang, W. Zhai and S. Su (2013). "Solid state foaming of poly(lactic acid) blown with compressed CO 2: Influences of long chain branching and induced crystallization on foam expansion and cell morphology." Industrial and Engineering Chemistry Research 52(37): 13411-13421.

Saeidlou, S., M. A. Huneault, H. Li and C. B. Park (2012). "Poly(lactic acid) crystallization." Progress in Polymer Science 37(12): 1657-1677.

Saeidlou, S., M. A. Huneault, H. Li and C. B. Park (2014). "Poly(lactic acid) stereocomplex formation: Application to PLA rheological property modification." Journal of Applied Polymer Science 131(22).

Sakamoto, Y. and H. Tsuji (2013). "Crystallization behavior and physical properties of linear 2-arm and branched 4-arm poly(l-lactide)s: Effects of branching." Polymer (United Kingdom) 54(9): 2422-2434.

Sakamoto, Y. and H. Tsuji (2013). "Stereocomplex crystallization behavior and physical properties of linear 1-Arm, 2-Arm, and branched 4-arm poly(L-lactide)/poly(D-lactide) blends: Effects of chain directional change and branching." Macromolecular Chemistry and Physics 214(7): 776-786.

Sarazin, P., G. Li, W. J. Orts and B. D. Favis (2008). "Binary and ternary blends of polylactide, polycaprolactone and thermoplastic starch." Polymer 49(2): 599-609.

Schmidt, S. C. and M. A. Hillmyer (2001). "Polylactide Stereocomplex Crystallites as Nucleating Agents for Isotactic Polylactide." Journal of Polymer Science, Part B: Polymer Physics 39(3): 300-313.

Schneider, A. K. (1955). Polymers of high melting lactide. United States, Pont DU.

Sentmanat, M., O. Delgadillo-Vel√°zquez and S. Hatzikiriakos (2010). "Crystallization of an ethylene-based butene plastomer: the effect of uniaxial extension." Rheologica Acta 49(9): 931-939.

Shin, B. Y., D. H. Han and R. Narayan (2010). "Rheological and Thermal Properties of the PLA Modified by Electron Beam Irradiation in the Presence of Functional Monomer." Journal of Polymers and the Environment 18(4): 558-566.

Shirai, M. A., M. V. E. Grossmann, S. Mali, F. Yamashita, P. S. Garcia and C. M. O. Muller (2013). "Development of biodegradable flexible films of starch and poly(lactic acid) plasticized with adipate or citrate esters." Carbohydrate Polymers 92(1): 19-22.

Sinha Ray, S. and M. Okamoto (2003). "New Polylactide/Layered Silicate Nanocomposites, 6." Macromolecular Materials and Engineering 288(12): 936-944.

Sirisinha, K. and W. Somboon (2012). "Melt characteristics, mechanical, and thermal properties of blown film from modified blends of poly(butylene adipate-co-terephthalate) and poly(lactide)." Journal of Applied Polymer Science 124(6): 4986-4992.

Sodergard, A. and J. H. Nasman (1994). "Stabilization of poly(L-lactide) in the melt." Polymer Degradation and Stability 46(Compendex): 25-30.

Sodergard, A., M. Niemi, J.-F. Selin and J. H. Nasman (1995). "Changes in peroxide melt-modified poly(L-lactide)." Industrial and Engineering Chemistry Research 34(4): 1203-1207.

Stoclet, G., R. Seguela, J. M. Lefebvre, S. Elkoun and C. Vanmansart (2010). "Strain-Induced Molecular Ordering in Polylactide upon Uniaxial Stretching." Macromolecules 43(3): 1488-1498.

Stoclet, G., R. Seguela, C. Vanmansart, C. Rochas and J. M. Lefebvre (2012). "WAXS study of the structural reorganization of semi-crystalline polylactide under tensile drawing." Polymer 53(2): 519-528.

Storey, R. F. and J. W. Sherman (2002). "Kinetics and mechanism of the stannous octoate-catalyzed bulk polymerization of -caprolactone." Macromolecules 35(5): 1504-1512.

Stridsberg, K., M. Ryner and A.-C. Albertsson (2002). Controlled Ring-Opening Polymerization: Polymers with designed Macromolecular Architecture. Degradable Aliphatic Polyesters, Springer Berlin Heidelberg. 157: 41-65.

Sungsanit, K., N. Kao and S. N. Bhattacharya (2012). "Properties of linear poly(lactic acid)/polyethylene glycol blends." Polymer Engineering and Science 52(1): 108-116.

Tabatabaei, S. H. and A. Ajji (2012). "Crystal structure and orientation of uniaxially and biaxially oriented PLA and PP nanoclay composite films." Journal of Applied Polymer Science 124(6): 4854-4863.

Tabatabaei, S. H., P. J. Carreau and A. Ajji (2009). "Rheological and thermal properties of blends of a long-chain branched polypropylene and different linear polypropylenes." Chemical Engineering Science 64(22): 4719-4731.

Takamura, M., T. Nakamura, T. Takahashi and K. Koyama (2008). "Effect of type of peroxide on cross-linking of poly(l-lactide)." Polymer Degradation and Stability 93(10): 1909-1916.

Takamura, M., M. Sugimoto, S. Kawaguchi, T. Takahashi and K. Koyama (2012). "Influence of extrusion temperature on molecular architecture and crystallization behavior of peroxide-induced slightly crosslinked poly(L -lactide) by reactive extrusion." Journal of Applied Polymer Science 123(3): 1468-1478.

Tashiro, Y., W. Kaneko, Y. Sun, K. Shibata, K. Inokuma, T. Zendo and K. Sonomoto (2011). "Continuous D-lactic acid production by a novelthermotolerant Lactobacillus delbrueckii subsp. lactis QU 41." Applied Microbiology and Biotechnology 89(6): 1741-1750.

Thellen, C., C. Orroth, D. Froio, D. Ziegler, J. Lucciarini, R. Farrell, N. A. D'Souza and J. A. Ratto (2005). "Influence of montmorillonite layered silicate on plasticized poly(l-lactide) blown films." Polymer 46(25): 11716-11727.

Thongchul, N. (2013). Production of Lactic Acid and Polylactic Acid for Industrial Applications. Bioprocessing Technologies in Biorefinery for Sustainable Production of Fuels, Chemicals, and Polymers, John Wiley & Sons, Inc.: 293-316.

Tsuji, H., F. Horii, S.-H. Hyon and Y. Ikada (1991). "Stereocomplex formation between enantiomeric poly(lactic acid)s. 2. Stereocomplex formation in concentrated solutions." Macromolecules 24(Compendex): 2719-2724.

Tsuji, H., F. Horii, M. Nakagawa, Y. Ikada, H. Odani and R. Kitamaru (1992). "Stereocomplex formation between enantiomeric poly(lactic acid)s. 7. Phase structure of the stereocomplex crystallized from a dilute acetonitrile solution as studied by high-resolution solid-state carbon-13 NMR spectroscopy." Macromolecules 25(16): 4114-4118.

Tsuji, H. and Y. Ikada (1996). "Crystallization from the melt of poly(lactide)s with different optical purities and their blends." Macromolecular Chemistry and Physics 197(10): 3483-3499.

Tsuji, H. and Y. Ikada (1999). "Stereocomplex formation between enantiomeric poly(lactic acid)s. XI. Mechanical properties and morphology of solution-cast films." Polymer 40(Compendex): 6699-6708.

Tsuji, H., T. Miyase, Y. Tezuka and S. K. Saha (2005). "Physical properties, crystallization, and spherulite growth of linear and 3-arm poly(L-lactide)s." Biomacromolecules 6(Compendex): 244-254.

Tsuji, H., H. Takai, N. Fukuda and H. Takikawa (2006). "Non-isothermal crystallization behavior of poly(L-lactic acid) in the presence of various additives." Macromolecular Materials and Engineering 291(Compendex): 325-335.

Tsuji, H., H. Takai and S. K. Saha (2006). "Isothermal and non-isothermal crystallization behavior of poly(l-lactic acid): Effects of stereocomplex as nucleating agent." Polymer 47(11): 3826-3837.

Tsuji, H., T. Wada, Y. Sakamoto and Y. Sugiura (2010). "Stereocomplex crystallization and spherulite growth behavior of poly(l-lactide)-b-poly(d-lactide) stereodiblock copolymers." Polymer 51(Compendex): 4937-4947.

Tuominen, J., J. Kylma and J. Seppala (2002). "Chain extending of lactic acid oligomers. 2. Increase of molecular weight with 1,6-hexamethylene diisocyanate and 2,2-bis(2-oxazoline)." Polymer 43(1): 3-10.

Tweed, E. C. G., OH, US), Stephens, Henry Mike (Reynoldsburg, OH, US), Riegert, Theodore Emil (Pataskala, OH, US) (2006). Polylactic acid blown film and method of manufacturing same. United States, PLASTIC SUPPLIERS, INC. (Columbus, OH, US).

Ulery, B. D., L. S. Nair and C. T. Laurencin (2011). "Biomedical applications of biodegradable polymers." Journal of Polymer Science, Part B: Polymer Physics 49(12): 832-864.

Utracki, L. A., Ed. (2002). Polymer blends handbook, Kluwer Academic Publishers.

Wagner, M. H., H. Bastian, P. Hachmann, J. Meissner, S. Kurzbeck, H. Münstedt and F. Langouche (2000). "The strain-hardening behaviour of linear and long-chain-branched polyolefin melts in extensional flows." Rheologica Acta 39(2): 97-109.

Wang, B., X. Zhao and L. Wang (2013). "Isothermal Crystallization and Melting Behaviors of Biodegradable Poly(lactic acid)/Poly(Butylene Adipate-co-terephthalate) Blends Compatibilized by Transesterification." Polymer - Plastics Technology and Engineering 52(7): 718-726.

Wang, L., X. Jing, H. Cheng, X. Hu, L. Yang and Y. Huang (2012). "Blends of linear and long-chain branched poly(l -lactide)s with high melt strength and fast crystallization rate." Industrial and Engineering Chemistry Research 51(30): 10088-10099.

Wang, L., X. Jing, H. Cheng, X. Hu, L. Yang and Y. Huang (2012). "Rheology and crystallization of long-chain branched poly(l-lactide)s with controlled branch length." Industrial and Engineering Chemistry Research 51(33): 10731-10741.

Wang, L. U. and C.-M. Dong (2006). "Synthesis, crystallization kinetics, and spherulitic growth of linear and star-shaped poly(L-lactide)s with different numbers of arms." Journal of Polymer Science, Part A: Polymer Chemistry 44(7): 2226-2236.

Wang, Q. and Y. Wang (2011). "Synthesis of novel amphiphilic graft copolymers composed of poly(ethylene oxide) as backbone and polylactide as side chains." Journal of Polymer Research 18: 385-391.

Wang, Y., M. Li and C. Shen (2011). "Effect of constrained annealing on the microstructures of extrusion cast polylactic acid films." Materials Letters 65(23–24): 3525-3528.

Wang, Y., L. Yang, Y. Niu, Z. Wang, J. Zhang, F. Yu and H. Zhang (2011). "Rheological and topological characterizations of electron beam irradiation prepared long-chain branched polylactic acid." Journal of Applied Polymer Science 122(3): 1857-1865.

Wang, Y., H. Zhang, M. Li, W. Cao, C. Liu and C. Shen (2015). "Orientation and structural development of semicrystalline poly(lactic acid) under uniaxial drawing assessed by infrared spectroscopy and X-ray diffraction." Polymer Testing 41(0): 163-171.

Wen, L. and Z. Xin (2010). "Effect of a novel nucleating agent on isothermal crystallization of poly(L-lactic acid)." Chinese Journal of Chemical Engineering 18(Compendex): 899-904.

Wen, T., Z. Xiong, G. Liu, X. Zhang, S. de Vos, R. Wang, C. A. P. Joziasse, F. Wang and D. Wang (2013). "The inexistence of epitaxial relationship between stereocomplex and α crystal of poly(lactic acid): Direct experimental evidence." Polymer 54(7): 1923-1929.

Witzke, D. R. (1997). Introduction to properties, engineering, and prospects of polylactide polymers. United States -- Michigan, Michigan State University: 389.

Wolf, F. K. and H. Frey (2009). "Inimer-Promoted synthesis of branched and hyperbranched polylactide copolymers." Macromolecules 42(24): 9443-9456.

Wood-Adams, P. M. (2001). "Effect of long chain branches on the shear flow behavior of polyethylene." Journal of Rheology 45(Compendex): 203-210.

Xiao, H., W. Lu and J.-T. Yeh (2009). "Effect of plasticizer on the crystallization behavior of poly(lactic acid)." Journal of Applied Polymer Science 113(Compendex): 112-121.

Xiao, H. W., P. Li, X. Ren, T. Jiang and J.-T. Yeh (2010). "Isothermal crystallization kinetics and crystal structure of poly(lactic acid): Effect of triphenyl phosphate and talc." Journal of Applied Polymer Science 118(Compendex): 3558-3569.

Xu, H., H. Fang, J. Bai, Y. Zhang and Z. Wang (2014). "Preparation and characterization of high-melt-strength polylactide with long-chain branched structure through -radiation-induced chemical reactions." Industrial and Engineering Chemistry Research 53(3): 1150-1159.

Yamane, H., K. Sasai, M. Takano and M. Takahashi (2004). "Poly(D-lactic acid) as a rheological modifier of poly(L-lactic acid): Shear and biaxial extensional flow behavior." Journal of Rheology 48(3): 599-609.

Yasuniwa, M., S. Tsubakihara, K. Iura, Y. Ono, Y. Dan and K. Takahashi (2006). "Crystallization behavior of poly(l-lactic acid)." Polymer 47(Compendex): 7554-7563.

You, J., L. Lou, W. Yu and C. Zhou (2013). "The preparation and crystallization of long chain branching polylactide made by melt radicals reaction." Journal of Applied Polymer Science 129(4): 1959-1970.

Yu, J. and Z. Qiu (2011). "Preparation and properties of biodegradable poly(L-lactide)/octamethyl- polyhedral oligomeric silsesquioxanes nanocomposites with enhanced crystallization rate via simple melt compounding." ACS Applied Materials and Interfaces 3(Compendex): 890-897.

Yu, Y., G. Storti and M. Morbidelli (2009). "Ring-opening polymerization of L,L-lactide: Kinetic and modeling study." Macromolecules 42(21): 8187-8197.

Yu, Y., G. Storti and M. Morbidelli (2011). "Kinetics of ring-opening polymerization of l, l - lactide." Industrial and Engineering Chemistry Research 50(13): 7927-7940.

Yuan, F., H. Pan, F. Cheng, Y. Chen and S.-C. Jiang (2012). "One-pot synthesis of comb-like copolymer bearing side chains composed of branched and linear polylactides." Polymer 53(11): 2175-2182.

Zenkiewicz, M., J. Richert and A. Rozanski (2010). "Effect of blow moulding ratio on barrier properties of polylactide nanocomposite films." Polymer Testing 29(2): 251-257.

Zhang, C.-X., B. Wang, Y. Chen, F. Cheng and S.-C. Jiang (2012). "Amphiphilic multiarm star polylactide with hyperbranched polyethylenimine as core: A systematic reinvestigation." Polymer (United Kingdom) 53(18): 3900-3909.

Zhang, H., H. Liang, J. Bian, Y. Hao, L. Han, X. Wang, G. Zhang, S. Liu and L. Dong (2014). "Influence of acrylic impact modifier on plasticized polylactide blown films." Polymer International 63(6): 1076-1084.

Zhang, J., K. Tashiro, H. Tsuji and A. J. Domb (2008). "Disorder-to-order phase transition and multiple melting behavior of poly(L-lactide) investigated by simultaneous measurements of WAXD and DSC." Macromolecules 41(4): 1352-1357.

Zhang, X. C., D. A. Macdonald, M. F. A. Goosen and K. B. McAuley (1994). "Mechanism of lactide polymerization in the presence of stannous octoate - the effect of hydroxy and carboxylic-acid substances." Journal of Polymer Science Part a-Polymer Chemistry 32(15): 2965-2970.

Zhang, Y., X. Yuan, Q. Liu and A. Hrymak (2012). "The Effect of Polymeric Chain Extenders on Physical Properties of Thermoplastic Starch and Polylactic Acid Blends." Journal of Polymers and the Environment 20(2): 315-325.

Zhao, R.-X., L. Li, B. Wang, W.-W. Yang, Y. Chen, X.-H. He, F. Cheng and S.-C. Jiang (2012). "Aliphatic tertiary amine mediated synthesis of highly branched polylactide copolymers." Polymer 53(3): 719-727.

Zhao, W., D. Cui, X. Liu and X. Chen (2010). "Facile synthesis of hydroxyl-ended, highly stereoregular, star-shaped poly(lactide) from immortal ROP of rac-lactide and kinetics study." Macromolecules 43(16): 6678-6684.

Zhao, Y.-L., Q. Cai, J. Jiang, X.-T. Shuai, J.-Z. Bei, C.-F. Chen and F. Xi (2002). "Synthesis and thermal properties of novel star-shaped poly(L-lactide)s with starburst PAMAM-OH dendrimer macroinitiator." Polymer 43(22): 5819-5825.